Title
Development of Adaptive Signal Control (ASC) Based on Automatic Vehicle Location (AVL) System and Its Applications

Author
Wu, Guoyuan

Publication Date
2010

Peer reviewed|Thesis/dissertation

Development of Adaptive Signal Control (ASC) based on Automatic Vehicle Location (AVL) System and Its Applications

by

Guoyuan Wu

A dissertation submitted in partial satisfaction of the

requirements for the degree of

Doctor of Philosophy

in

Engineering – Mechanical Engineering

in the

Graduate Division

of the

University of California, Berkeley

Committee in charge:

Professor Masayoshi Tomizuka, Chair
Professor Alexander Skabardonis
Professor Karl Hedrick

Fall 2010

Development of Adaptive Signal Control (ASC) based on Automatic Vehicle Location (AVL) System and Its Applications

by

Guoyuan Wu

Abstract

Development of Adaptive Signal Control (ASC) based on Automatic Vehicle Location (AVL) System and Its Applications

by

Guoyuan Wu

Doctor of Philosophy in Engineering – Mechanical Engineering

University of California, Berkeley

Professor Masayoshi Tomizuka, Chair

With the growth of population and increase of travelling requirements in metropolitan areas, public transit has been recognized as a promising remedy and is playing an ever more important role in sustainable transportation systems. However, the development of the public transit system has not received enough attention until the recent emergence of Bus Rapid Transit **(**BRT**)**. In the conventional public transit system, little to no communication passes between transit vehicles and the roadside infrastructure, such as traffic signals and loop detectors. But now, thanks to advancements in automatic vehicle location (AVL) systems and wireless communication, real-time and high-resolution information of the movement of transit vehicles has become available, which may potentially facilitate the development of more advanced traffic control and management systems.

This dissertation introduces a novel adaptive traffic signal control system, which utilizes the real-time location information of transit vehicles. By predicting the movement of the transit vehicle based on continuous detection of the vehicle motion by the on-board AVL system and estimating the measures of effectiveness (MOE) of other motor vehicles based on the surveillance of traffic conditions, optimal signal timings can be obtained by solving the proposed traffic signal optimization models. Both numerical analysis and simulation tests demonstrate that the proposed system improves a transit vehicle's operation as well as minimizes its negative impacts on other motor vehicles in the traffic system. In summary, there are three major contributions of this dissertation: a) development of a novel AVL-based adaptive traffic signal control system; b) modeling of the associated traffic signal timing optimization problem, which is the key component of the proposed system; c) applications of the proposed system to two real world cases.

After presenting background knowledge on two major types of transit operations, i.e., preemption and priority, traffic signal control and AVL systems, the architecture of the proposed adaptive signal control system and the associated algorithm are presented. The proposed system includes a data-base, fleet equipped with surveillance system, traffic signal controllers, a transit movement predictor, a traffic signal timing optimizer and a request server. The mixed integer quadratic programming (MIQP) and nonlinear programming (NP) are used to formulate signal timing optimization problems. Then the proposed system and algorithm are applied to two real-world case studies. The first case study concerns the SPRINTER rail transit service. The proposed adaptive signal control (ASC) system is developed to relieve the traffic congestion and to clear the accumulated vehicle queues at the isolated signal around the grade crossing, based on the location information on SPRINTER from PATH-developed cellular GPS trackers. The second case study involves the San Diego trolley system. With the information provided by the AVL system, the proposed ASC system predicts the arrival times of the instrumented trolley at signals and provides the corresponding optimal signal timings to improve the schedule adherence, thus reducing the delays at intersections and enhancing the trip reliability for the trolley travelling along a signalized corridor in the downtown area under the priority operation. The negative impact (e.g., delay increase) on other traffic is minimized simultaneously. Both numerical analysis and simulation tests in the microscopic environment are conducted using the PARAMICS software to validate the proposed system for the aforementioned applications. The results present a promising future for further field operational testing.

Table of Contents

List of Tables

List of Figures

Acknowledgements

I do feel honored to obtain so many supports and helps from those who make this dissertation possible.

I owe my sincerest gratitude to my advisor, Professor Tomizuka, from whom I have learned a lot in the pursuit of my Ph. D degree. I am so lucky to be not only cultivated by his invaluable suggestions and insightful guidance on my research, but also inspired by his work spirits and attitudes. I am so grateful for his supports and cares on my study.

I would like to also express my deepest appreciation to my supervisor at California PATH, UC Berkeley, Mr. Wei-Bin Zhang. With his continuing supports, I can complete my Ph. D study. I do appreciate his suggestions and helps not only on my study and dissertation, but also my daily life and my family.

It is a great pleasure to thank all my doctoral committee members, Professor Karl Hedrick, Professor Alexander Skabardonis, Professor Kameshwar Poolla, Professor Haiyan Huang and Professor Zuo-jun Shen. They provided significant suggestions and comments on my research, my presentation and my dissertation. I am really grateful for their patience and helps on improving my Ph. D work.

This dissertation would not be completed without the supports from my family, particularly my parents Xirong Wu and Jinghua Zhou, my wife Qingming Zeng, my daughter Yihan Wu, my brother Guosen Wu, my sister-in-law Zhenzi Wang and my niece Yiyun Wu. Their continuing supports and expectations helped me overcome all obstacles along the way to achieve my Ph. D degree. They are the major source of power which keeps me moving forward along my career path without stops.

I am greatly indebted to my colleagues at California PATH, UC Berkeley, particularly Dr. Ching-Yao Chan, Dr. Meng Li, Dr. Kun Zhou, Dr. Liping Zhang, Dr. Jing-Quan Li, Dr. Fanping Bu and Dr. Yue Li. I am thankful for their helps on both my work and daily life during the completion of my Ph. D degree.

At last, I would like to offer my regards and blessings to all those who ever helped and supported me in any aspect along my Ph. D. study.

Chapter 1

1. Introduction

1.1 Background

With the uninterrupted trend in the growth of world population [1] and ever increasing needs in traveling [2] (see Figure 1.1), the burdens on existing traffic systems are becoming increasingly heavy. More vehicles are swarming into the streets, highways and freeways, particularly in the metropolitan areas, resulting in congestion throughout the traffic network and even paralysis of traffic operation.

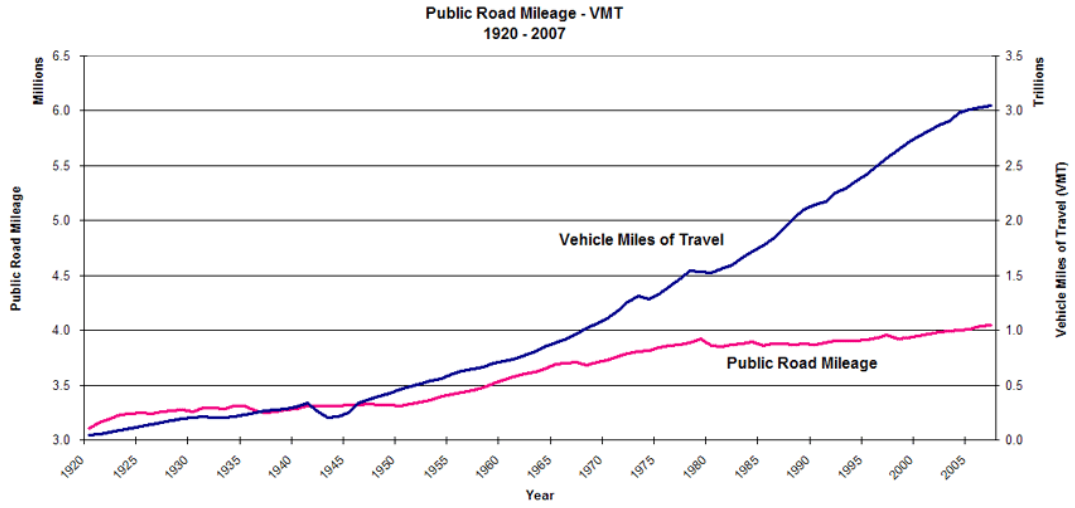

Figure 1.1: Public road mileage and vehicle mile of travel chart throughout U. S.

Despite the ever increasing demand, the capacities of road infrastructures in most urban areas, especially in the metropolitan areas, have already reached their limits to accommodate more traffic volume. It is almost impossible and extremely costly to redesign or expand the existing road infrastructures for such developed areas. Therefore, the continuous rise in traveling demands cannot be satisfied by the present capabilities of these road infrastructures.

Furthermore, the ceaseless increases in the population and the number of vehicles are accompanied by the ever-serious rise of consumption of liquid fuel, which causes

concerns about energy shortage. In the United States, automobile gasoline consumption has been estimated to be as much as 140 billion gallons in 2005 [3]. It is reported that gasoline used by passenger cars and light trucks accounts for approximately 44% of U.S. oil consumption and around 10% of world oil consumption [4].

The growth in consumption of petroleum also causes a substantial increase in greenhouse gas (GHG) emissions, which contribute to global climate change. The U.S. *Environmental Protection Agency* (EPA) reported that in 2006 approximately 29% of the total U.S. GHG emissions come from the transportation sector [5]. Reducing fuel consumption and associated GHG emissions, particularly carbon dioxide (CO_2), from motor vehicles has been one of the important tasks for a variety of sustainable transportation programs.

A promising solution to the problem mentioned above is to develop a multi-modal transportation system, e.g., a public transit service, which has been widely recognized as the key to future sustainable transportation systems. A well-operated public transit system can efficiently utilize the limited capacity of road infrastructure, lessen our dependence on fossil fuels, and reduce the emission of pollutants, while satisfying people's needs to travel around.

Bus and light rail transit (LRT) have been playing increasingly important roles in the transportation systems of major cities throughout the world. The dependence of people's daily lives on such public transit has been apparent for years. For example, a report from the American Public Transit Association (APTA) [6] showed that "National ridership levels reached a record 10.7 billion passenger trips during 2008—the highest level in 52 years and a 4.0 percent increase from 2007." However, the development of public transit systems has not received enough attention until the recent efforts on Bus Rapid Transit (BRT), which is an enhanced transit system utilizing "a combination of advanced technologies, infrastructure and operational investments that provide significantly better service than traditional transit service" [7]. Advanced traffic signal control is one of the BRT-related technologies that can improve the operation of the traditional transit system and benefit other traffic simultaneously. The Automatic Vehicle Location (AVL) based adaptive signal control strategy proposed in this thesis is one remedy designed to enhance both transit service, such as shortening trip travel time and improving schedule adherence, and the operation of other traffic (e.g., reducing overall delays).

Because applications of the proposed signal control strategy presented in Chapter 3 and Chapter 4 are closely related to public transit, in particular rail transit, some background knowledge on the operation of rail transit and traffic signal control at intersections will be described briefly in the following sections.

1.2 Preemption and Priority

As mentioned before, the rail transit service, e.g., light rail transit (LRT), is an effective solution to mitigate traffic congestion along major urban corridors. However, frequent operation of the light rail vehicle (LRV) may interrupt traffic flows, thus resulting in significant delays and potential safety concerns to both motor vehicles and pedestrians at the intersections at or around highway-rail grade crossings (HRGC).

Preemption and priority are two major types of traffic signal operations that are employed at or around HRGC. Both preemption and priority refer modes of operation where preferential treatment is given to transit vehicles at traffic signals over other traffic to reduce transit delays.

The preemption signal operation (see Figure 1.2) is intended to deliver an immediate response to prevent collisions of transit vehicles and other motor vehicles. Briefly speaking, when a light rail vehicle (LRV) is approaching the HRGC, a warning signal will be provided continuously for a certain time interval (called the queue clearance time, or QCT), during which the queue of traffic along the cross street is cleared out of track. Then the gate descents and keeps down to guarantee the LRV passing through the HRGC without disruption. After the LRV clears the HRGC, the gate rises and the overall traffic system goes back to the normal operation.

On the other hand, the priority signal operation is intended to consider signal performance in addition to safety before granting preference to transit vehicles. Basically speaking, the green interval along the LRV direction is longer than the cross street such that the LRV is apt to pass through signals without stops. Figure 1.3 illustrates the priority of a two-phased signal and its operation will be elaborated in Chapter 4.

Both preemption and priority are widely used all around the world. Table 1.1 presents some examples of signal preemption and priority applications for light rail transit (LRT) throughout the United States and Canada [8].

More information on preemption and priority signal operations related to the proposed adaptive signal control strategy will be elaborated in Chapter 3 and Chapter 4 of this thesis, along with two real-world applications.

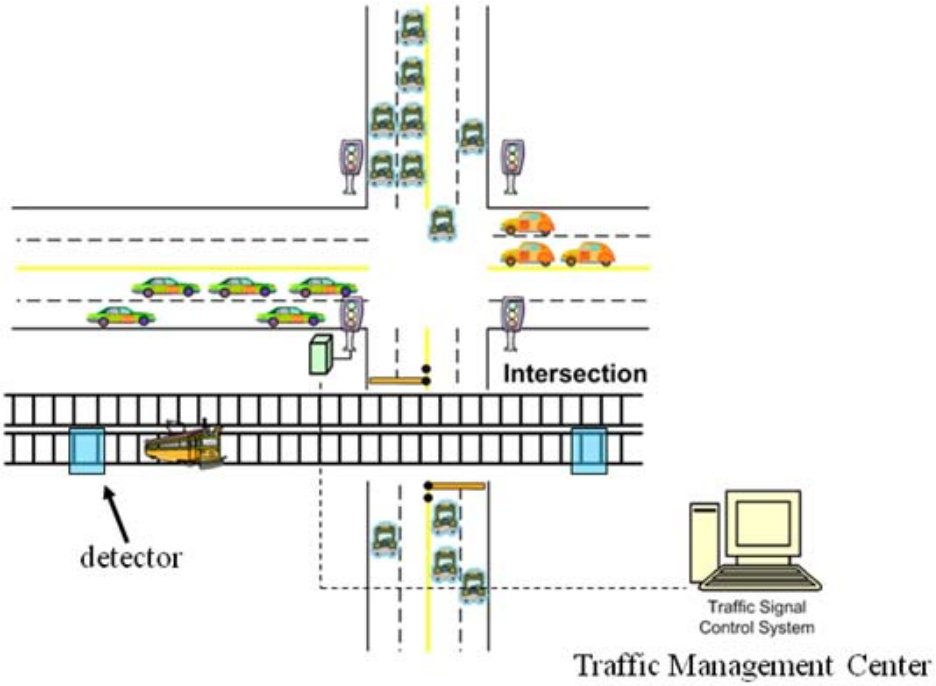

Figure 1.2: Illustration of preemption

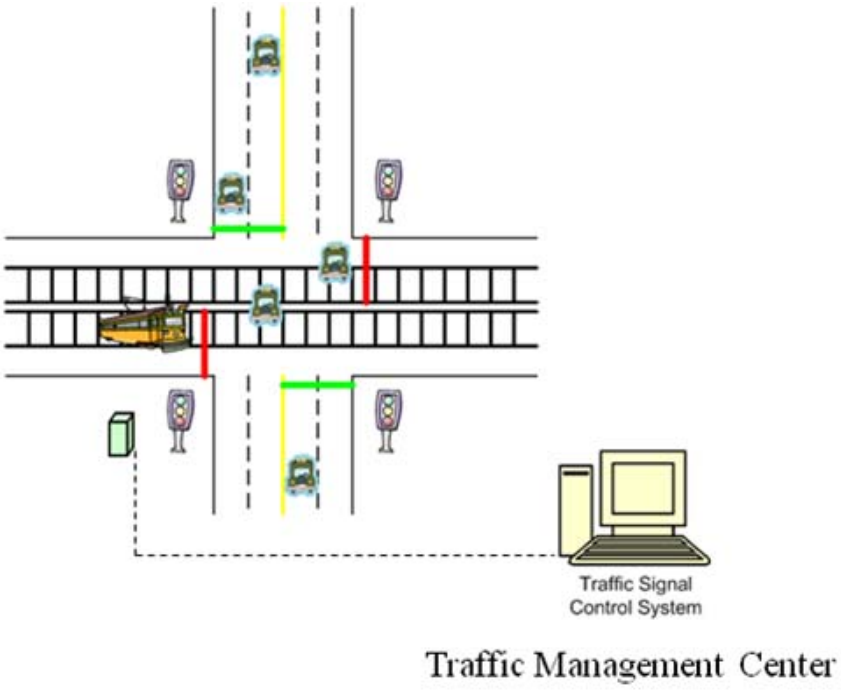

Figure 1.3: Illustration of priority for a two-phased signal

1.3 Traffic Signal

As mentioned in Section 1.1, an improved traffic signal control strategy, which serves as one of the components in BRT-related technologies, can benefit both public transit vehicles and other traffic. Since the introduction of traffic signals, a special importance has always been attached to traffic signal control. The core purpose of this thesis is to develop an advanced traffic signal control system and apply it to real world cases. Therefore, it is necessary to present some background knowledge on traffic signal operation and control first.

Table 1.1: Examples on LRT Preemption and Priority Applications

City	LRT Operations
San Diego, CA	LRV has passive priority. Train operators need to wait for green light at stations [9].
Los Angeles, CA	The system uses custom designed software in the controller which allows full, partial, or total preemption [10].
Boston, MA	The automatic vehicle identification (AVI) system and voice communication between trains and the operation control center (OCC). No signal priority for LRVs, but LRT operations include four types of control actions: holding a train, short-turning, expressing, and deadheading [11].
Buffalo, NY	LRV preemption requested by the train operator.
Calgary, Canada	No preemption, fixed signal progression timed to the LRT schedule using TRANSYT-7F [12].
Melbourne, Australia	SCATS provides dynamic active priority phasing.
Portland, OR	Signal progression favoring LRVs in downtown loops. Some cabs are operated full preemption with "decision point" markers on tracks [13].
Sacramento, CA	Signalized intersections redesigned to accommodate the LRV movements.
San Francisco, CA	Among total 108 at-grade crossings, 20 controlled by traffic signals, 5 with LRV priority.
San Jose, CA	The National Electrical Manufacturers Association (NEMA) controllers have been designed to permit any degree of LRV priority, from none to full. Roadway crossings generally have signal priority [14].

1.3.1 Traffic Signal Operations

Traffic signals were originally installed at intersections to guarantee the safe crossing maneuvers among conflicting approaches of vehicles and pedestrians and are a major element of urban transportation management networks. Before the traffic signal operation is elaborated, basic definitions [15, 16, 17] are put forth in the following:

- **Cycle**: A complete sequence of intervals.
- **Cycle length**: The time it takes to complete one cycle.
- **Phase**: The part of the cycle assigned to a fixed set of traffic movements; when any of these movements changes, the phase changes.
- **Green time**: The duration of the green indication for a given phase with the right-of-way at a signalized intersection.
- **Maximum green**: The maximum length of time that a phase can be green in the presence of a conflicting call.
- **Minimum green**: The first timed portion of a green interval, which may be set in consideration of driver expectancy and the storage of vehicles between the detectors and the stop line when volume density or presence detection is not used.
- **Yellow interval**: The interval in which yellow indications tell drivers in the phase with the right-of-way that their movement is about to lose its right-of-way.
- **Red clearance interval**: The interval, when all of the indications are red, that serves as a safety measure designed to give the oncoming traffic enough time to clear the intersection before the next phase begins.
- **Ring**: A set of phases that operate in sequence.
- **Barrier**: A separation of intersecting movements in separate rings to prevent operating conflicting phases at the same time.

Figure 1.4 illustrates a typical intersection layout with the *National Electrical Manufacturers Association* (NEMA) phase labels. This is a four way intersection with through lanes and separate left turn lanes in which each number corresponds to one movement. The assignment of these numbers to movements actually follows a certain set of rules regulated by NEMA. For example, even numbers are assigned for through movements while odd ones for left-turn movements. The setting of these rules is out of the scope of this study; the reader may refer to [18] for details.

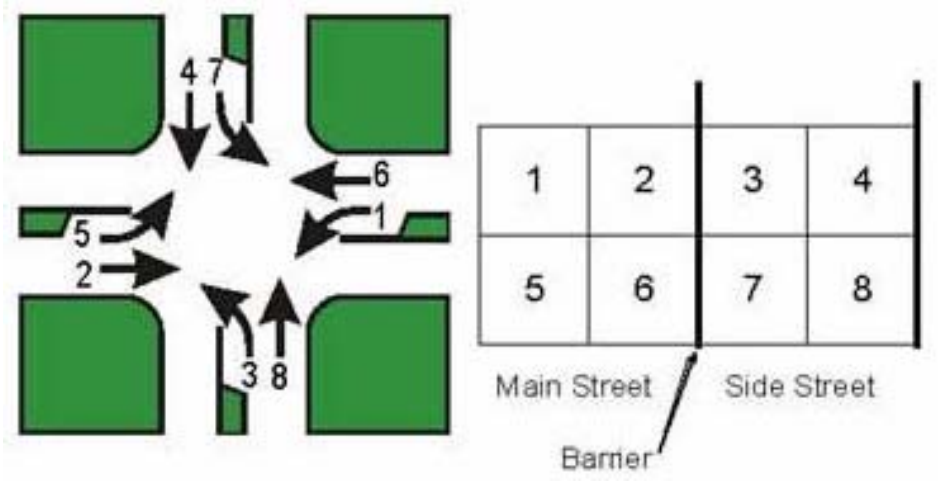

Figure 1.4: Illustration of a typical intersection with NEMA phase labels (Source: FHWA. *Signal Timing on a Shoestring*. Final Report, FHWA-HOP-07-006, Mar. 2005)

It is important to note that only some of the movements can safely go at the same time, which is why these movements are regulated with traffic signals. Using signal indications that are changed in intervals, traffic signals can prevent conflicting movements from having the right of way at the same time. A more systematic way to put all movements together is to use phase and ring diagrams. A phase diagram is a diagram that groups movements into phases, and each phase is shown in a single block. Figure 1.5 gives an example of one possible combination of movements forming a 4-phase diagram. Ring diagrams with barriers ensure that movements do not conflict, thus ensuring drivers' safety (see Figure 1.6). The two rings operate independently except that their control must cross the "barrier" at the same time. In other words, movements on the left side of the barrier must all be terminated before movements on the right side of the barrier can begin. Movements from the same ring cannot be served simultaneously. In the applications discussed in Chapter 3 and Chapter 4, the traffic signals in the field all follow this dual-ring operation.

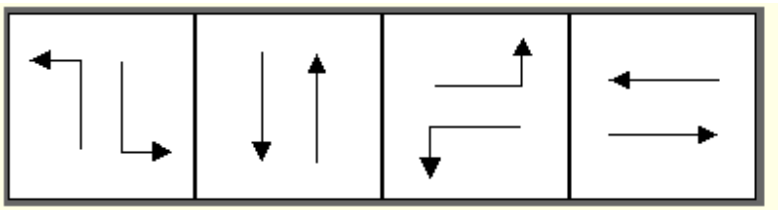

Figure 1.5: Possible case of 4-phase diagram

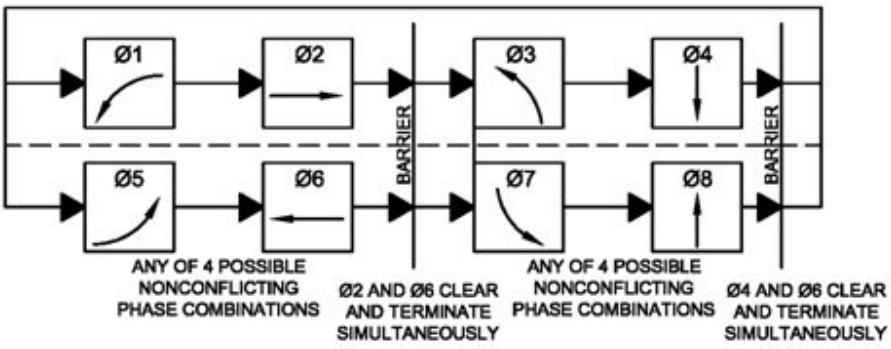

Figure 1.6: Dual-ring diagram (Source: FHWA. *Traffic Control Systems Handbook*. Final Report, FHWA-HOP-06-006, Oct. 2005)

1.3.2 Traffic Signal Control

As the traffic demands increase, it is realized that although traffic signals can prevent the conflicting movement of vehicles and pedestrians, they may lead (under equally safe traffic conditions) to sometimes more or sometimes less efficient traffic network operations. Properly controlled traffic signals can effectively mitigate traffic congestion, reduce energy consumption, and improve air quality [19, 20]. Over the last four decades, traffic signal control strategies have evolved from pre-timed signal control to traffic-responsive signal control, e.g., semi-/full-actuated signal control and adaptive signal control, from isolated intersection control to coordinated corridor control. Most of the following definitions are listed in [17],

- **Pre-timed signal control**: A type of signal control in which the cycle length, phase plan, and phase times are preset to repeat continuously.
- **Semi-actuated signal control**: A type of signal control where point detection (e.g., from an inductive detector loop) is provided for the minor movements only, and the signal timing returns to the major movement and is placed in recall.
- **Fully-actuated signal control**: A type of signal control in which the occurrence and length of every phase are controlled based on the measurements from loop detectors along each approach of the intersection.
- **Adaptive signal control**: A type of signal control concept where vehicular traffic in a network is detected at a point upstream and/or downstream and an algorithm is used to predict when and where traffic will be and to make signal adjustments at downstream intersections based on those predictions.
- **Coordinated signal control**: A type of signal control that synchronizes multiple intersections to enhance the operation of one or more directional movements in a system.

Examples of advanced traffic signal control systems include SCOOT [21], SCAT [22], OPAC [23], PRODYN [24] and RHODES [25]. With the development of novel technologies, the actuated signal control and adaptive signal control are becoming more and more widely used throughout the world. However, pre-timed signal control, the most basic strategy, will still be used for many years in the U.S. due to the costs of installation and maintenance for the advanced traffic signal control systems [26]. In addition, most of the traffic-responsive signal control systems will serve as pre-timed ones when the whole traffic network get congested. Therefore, efforts never cease in developing optimization algorithms for signal timings, even for pre-timed control intersections. Although the applications of the proposed AVL-based adaptive signal control focuses on pre-timed signal control in this thesis, it is straight-forward to apply to actuated signal control systems.

At the same time, a number of traffic signal control algorithms have been developed in the past years, and some of them have already been programmed as commercial software packages. SIGSET [27] is used to minimize total intersection delay (based on Webster's formula) for given traffic demands. MAXBAND [28], PASSER [29] and MULTIBAND [30] focused on optimizing the width of the green band for progression. TRANSIT [31], which is based upon the "platoon dispersion" model and "hill-climb" algorithm, may guarantee a local optimum of system performance but only for under-saturated conditions. Improvements have been achieved in TRANSIT-7F [32] to handle over-saturated cases. SYNCHRO [33] is another macroscopic capacity analysis and optimization software package. Like TRANSIT and TRANSIT-7F, it is most likely not able to reach the global optimal solution. More recently, some researchers proposed a variety of signal control strategies employing numerical solution algorithms, including genetic algorithm [34, 35] and mixed-integer linear programming. Both [36] and [37] formulated the problem based on the Cell Transmission Model (CTM) [38, 39]. However, calibrating and validating the fundamental diagram is a very involved process due to the complexity of urban traffic at signalized intersections.

It is also noted that the adaptive signal control mentioned above is different from what is proposed in this thesis. The former only draws on point detection, e.g., from loop detectors, while the latter works with the automatic vehicle location (AVL) system, which can be either a point detector or a continuous detector.

1.4 Automatic Vehicle Location (AVL) System

The automatic vehicle location (AVL) system is a computer-based system used for tracking the location, speed, and other measures of vehicles—primarily transit buses but also fleets of trucks and automobiles [17, 40, 41]. For the purpose of tracking and locating vehicles, there are mainly two types of AVL systems, signpost-based AVL systems (see Figure 1.7) and GPS-based AVL systems (see Figure 1.8 and Figure 1.9) [40, 42, 43, 44].

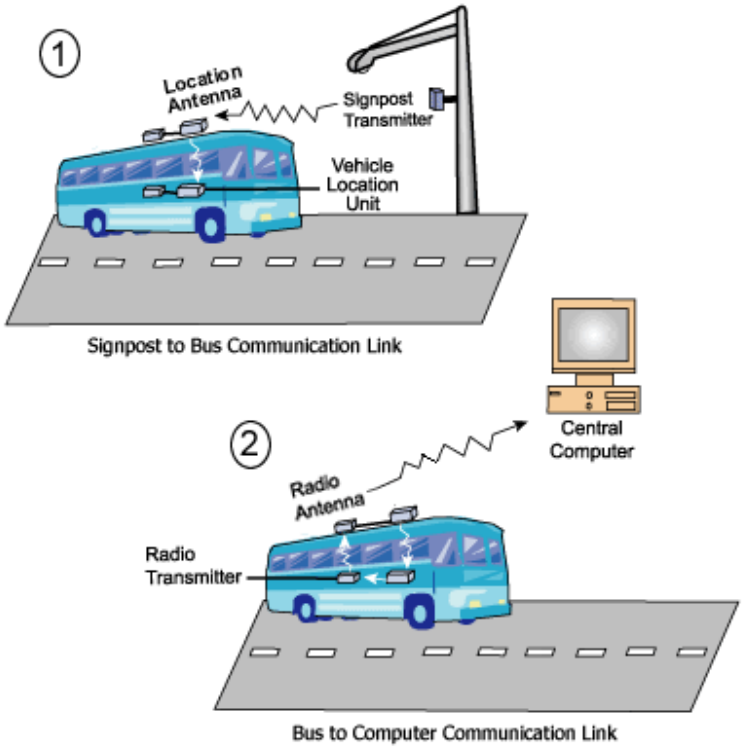

Figure 1.7: Signpost-based automatic vehicle location system

For the signpost-AVL system, the transit vehicle polls transponders or radio-frequency identification (RFID) chips along its route. As each transponder is passed, the moving vehicle would query and receive a handshake, from the signpost transmitter. A transmitter on the vehicle reports the passing of the signpost to a system controller [45]. Such system can also be used inside tunnels or other conveyances where GPS signals are blocked by terrain. For the GPS-based AVL system, a receiver to collect signals from the satellite segment is installed in each vehicle along with a radio to communicate the collected location data with a dispatch point. Figure 1.9 gives an example of another type of GPS-based AVL system. In the applications presented in this thesis, the cellular GPS device as shown in Figure 1.10 is used to track the second-by-second location of the instrumented vehicle (e.g., San Diego trolley). This tracker was developed by researchers at PATH, UC Berkeley.

With the development of GPS positioning and wireless communication systems, the AVL system has been receiving increasingly more attention in fleet and transit management due to its numerous benefits. For example, it can help transit agencies increase fleet utilization and reduce fuel, labor and capital costs. Moreover, it can improve schedule adherence and timed transfers, provide more accessible passenger information, increase availability of data for transit management and planning, and enhance the efficiency/productivity in transit services. References [46] and [47] present examples on improving fleet management with the PATH-developed cellular GPS tracker shown in Figure 1.10. It should be noted that there are also other potential applications for AVL systems beside the fleet management [48, 49, 50].

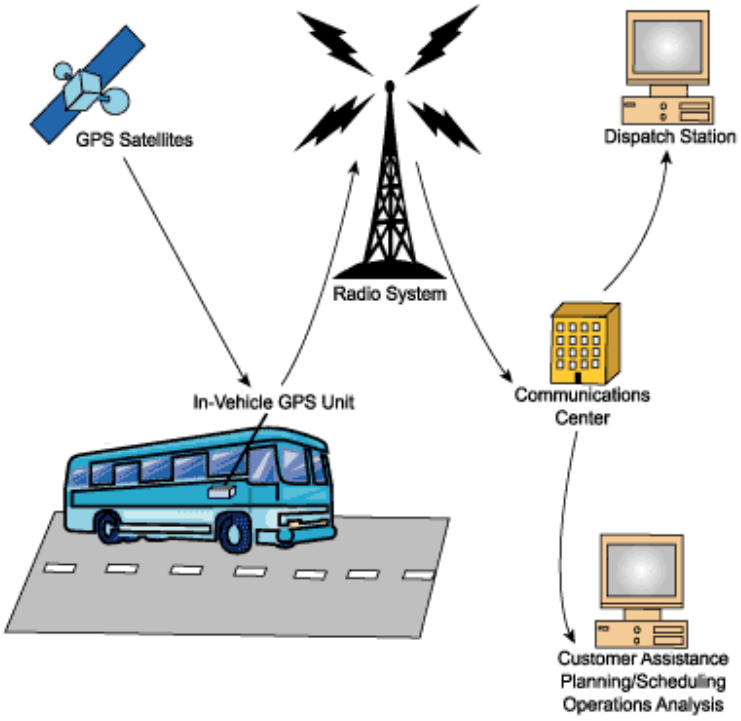

Figure 1.8: GPS-based automatic vehicle location system

1.5 Problem Statement

As mentioned in Section 1.3, traffic signal operation has existed for a long time and the associated control algorithms have been studied for decades. However, the development of signal control strategies based on AVL technology has been very limited.

Even fewer applications of such control system have been implemented for public transit, in particular, rail transit operation.

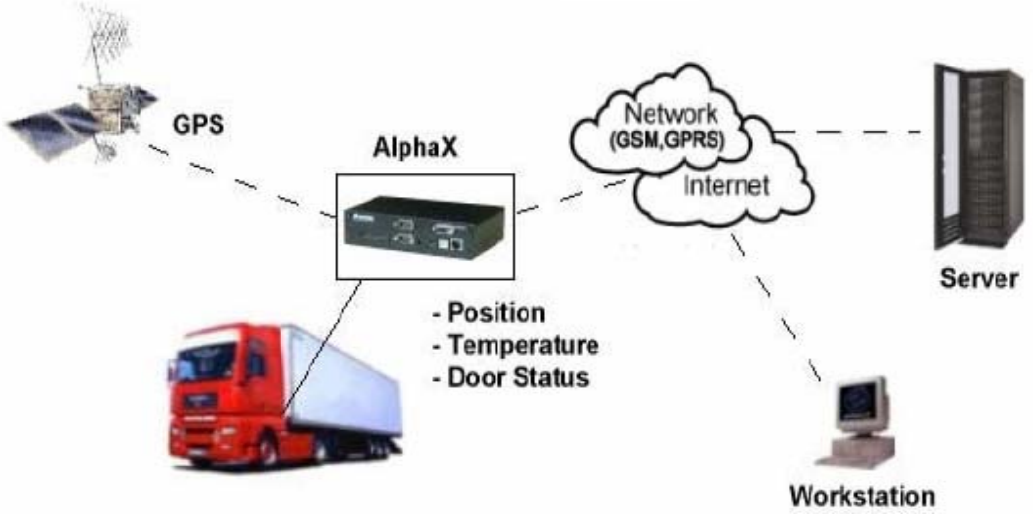

Figure 1.9: Web-based automatic vehicle location system integrated with GPS

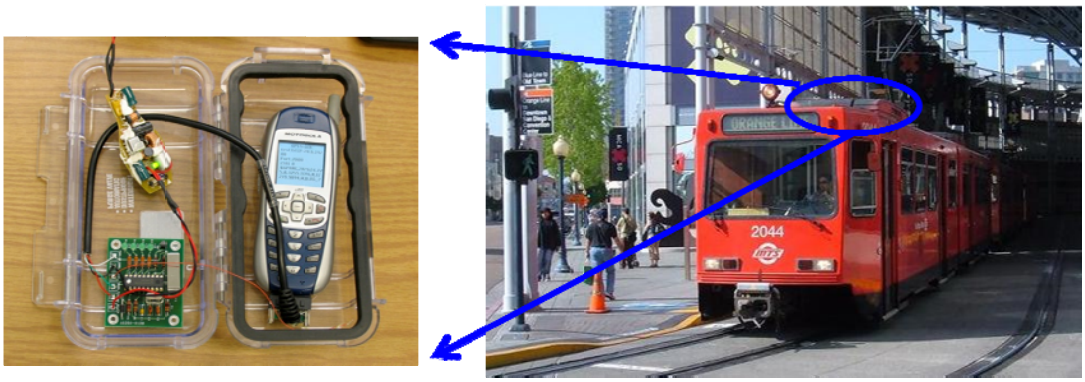

Figure 1.10: PATH-developed cellular GPS tracker equipped on trolley

In conventional rail transit operation under preemption, the traffic flows are interrupted around the grade crossings when the rail transit vehicle is approaching the grade crossing (see Figure 1.2). During the preemption, the traffic signals operate with a coded pre-timed logic regardless of any information on traffic conditions or movements and the location of the transit vehicle. As the frequency of such services become more intensive, the negative impact of interruptions becomes increasingly serious. In cases where the transit vehicle and traffic signals around the grade crossing are operated by different stakeholders, the traffic signal control engineers may not even know when the transit vehicle arrives at the grade crossing. Therefore, it is hard for them to tune the signals to make the traffic system efficient around the grade crossing.

A similar situation can be encountered with the conventional rail transit service under the priority signal operation (see Figure 1.3). Although the interruption of other traffic is less disruptive than with preemption, the movement of the transit vehicle is also controlled by the traffic signal at the grade crossing. Hence, it is impossible to guarantee that there is no stop or delay to the transit vehicle at traffic signals if information on the movement of the light rail transit (LRT) is not available. Even worse, if the traffic signal is not well tuned, severe waste of green time along the transit direction may occur, and the other traffic may be adversely affected by the priority methodology at the same time (see Figure 4.5 in Chapter 4).

Thanks to the development of the AVL system and wireless communication, real-time information on the location and movement of transit vehicles has become available. Based on such detailed and updated information, a more advanced signal control strategy can be developed for those intersections at or around the grade crossings such that the traffic systems operate more efficiently within these regions. For example, if the initiation times and termination times of preemption can be predicted, the traffic signal can be adjusted by taking into account the other traffic conditions to mitigate the congestion or back up of queues caused by the preemption maneuvers. At the same time, some potential safety hazards, such as vehicle/pedestrian traps, can be removed to a certain degree. Similarly, if the arrival times of transit vehicles can be well predicted, then the traffic signals under priority can be tuned to eliminate or reduce the intersection delays due to the operation of LRT. With such an advanced signal control strategy, the schedule adherence can be improved, the pollutant emissions can be decreased, and the negative impact on other motor vehicles may be minimized.

1.6 Research Objective, Framework and Contributions

The objective of this study is to develop an AVL-based adaptive signal control system, in particular for the state-of-practice traffic signal control at/around the highway/railroad grade crossing (HRGC). However, it should be noted that the proposed control system can also be applied to signalized intersections for buses or emergency vehicles. The traffic signal operation will be optimized by balancing both rail transit and other traffic so that the overall traffic system works more efficiently.

Figure 1.11 presents a top-down flow chart for the overall research frame. As is shown in the figure, this study starts from the system design of adaptive signal control (ASC), which provides an overview of the proposed system. The major contribution of this thesis is to develop the core of such an adaptive signal control system, i.e., the algorithm to optimize signal timings. This algorithm takes into consideration both rail transit and other

motor vehicles. The outputs of such a signal optimization algorithm include optimal signal timings for each phase and the user-defined performance measures of the traffic system, such as overall traffic delay and the width of the green band [51]. The applications presented in Chapter 3 and Chapter 4 provide detailed descriptions of how to develop the adaptive signal control algorithm for an isolated signal and a signalized corridor, respectively. After the proposed algorithm is developed, both numerical analysis and simulation tests are conducted to verify its validity. More specifically, Matlab is used for the numerical study, while the simulation results come from PARAMICS. Sensitivity analysis on model parameter(s) is also within the scope of interest if necessary. After gaining enough confidence in the performance measures of the proposed system under the lab and assumed environment, a few field operational tests are conducted to demonstrate how the system works in the real world.

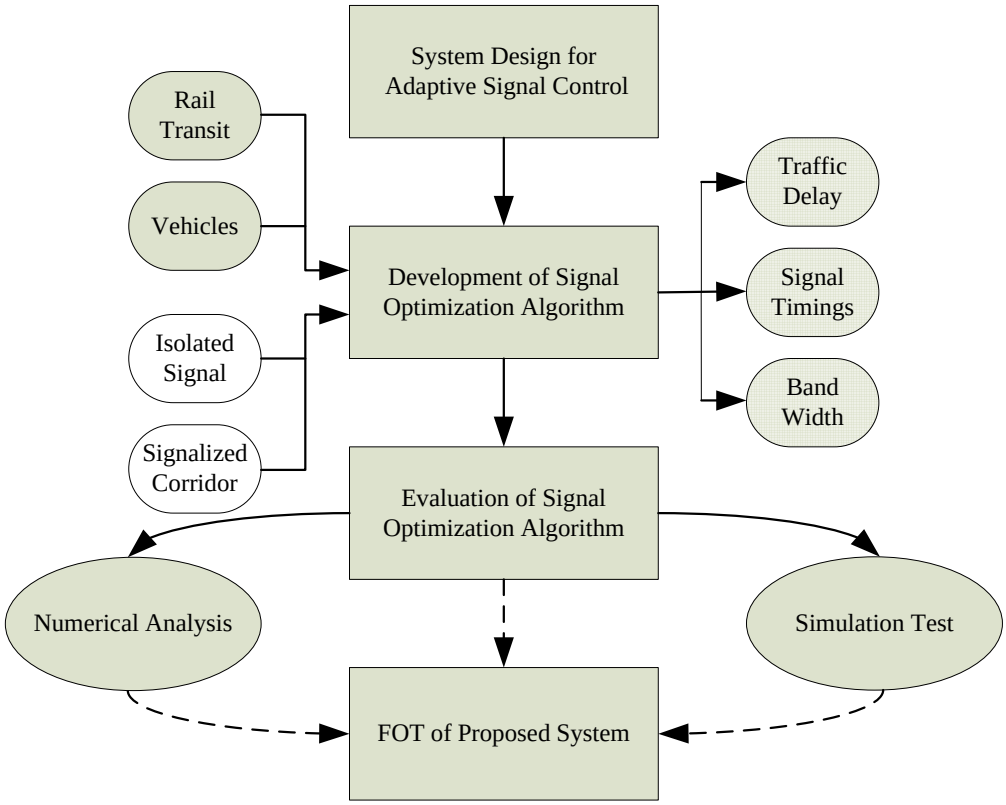

Figure 1.11: Top-down flow chart of research framework

The major contributions of this study include:

- ***Development of the AVL-based adaptive signal control system;***
- ***Modeling of the traffic signal timing optimizer, which is the most important component of the proposed system***.
- ***Application of the proposed system, in particular the adaptive signal control strategy, to two real world cases and attractive results available***

for further research.

1.7 Organization of the Dissertation

The organization of this dissertation is as follows: Chapter 1 has presented the background information on the AVL system, traffic signal operation/control, and preemption/priority logic related to the application examples in the following chapters. Chapter 2 demonstrates the methodology and architecture of the proposed AVL-based adaptive signal control system. A detailed description of the application of the proposed control system to the SPRINTER rail transit service is provided in Chapter 3 to show how to optimize traffic signal operation at an isolated intersection. The problem is identified by results from both simulation and field data and is formulated into a mixed integer quadratic programming (MIQP) problem. By solving the mathematical model, the proposed signal control strategy can adapt to the movement of the SPRINTER rail transit and the traffic volume around the grade crossings and provide benefits for the overall traffic system, which is validated through both numerical analysis and simulation tests. Chapter 4 elaborates the application of the proposed system to a signalized corridor by taking the San Diego trolley system as an example. Sensitivity analysis and simulation studies are conducted to evaluate the system performance. In addition, results from the lab testing and field operational testing are discussed for further research. Chapter 5 concludes this thesis and discusses potential future directions as a continuation of the current research work. Figure 1.12 shows a flow chart on the organization of the whole dissertation.

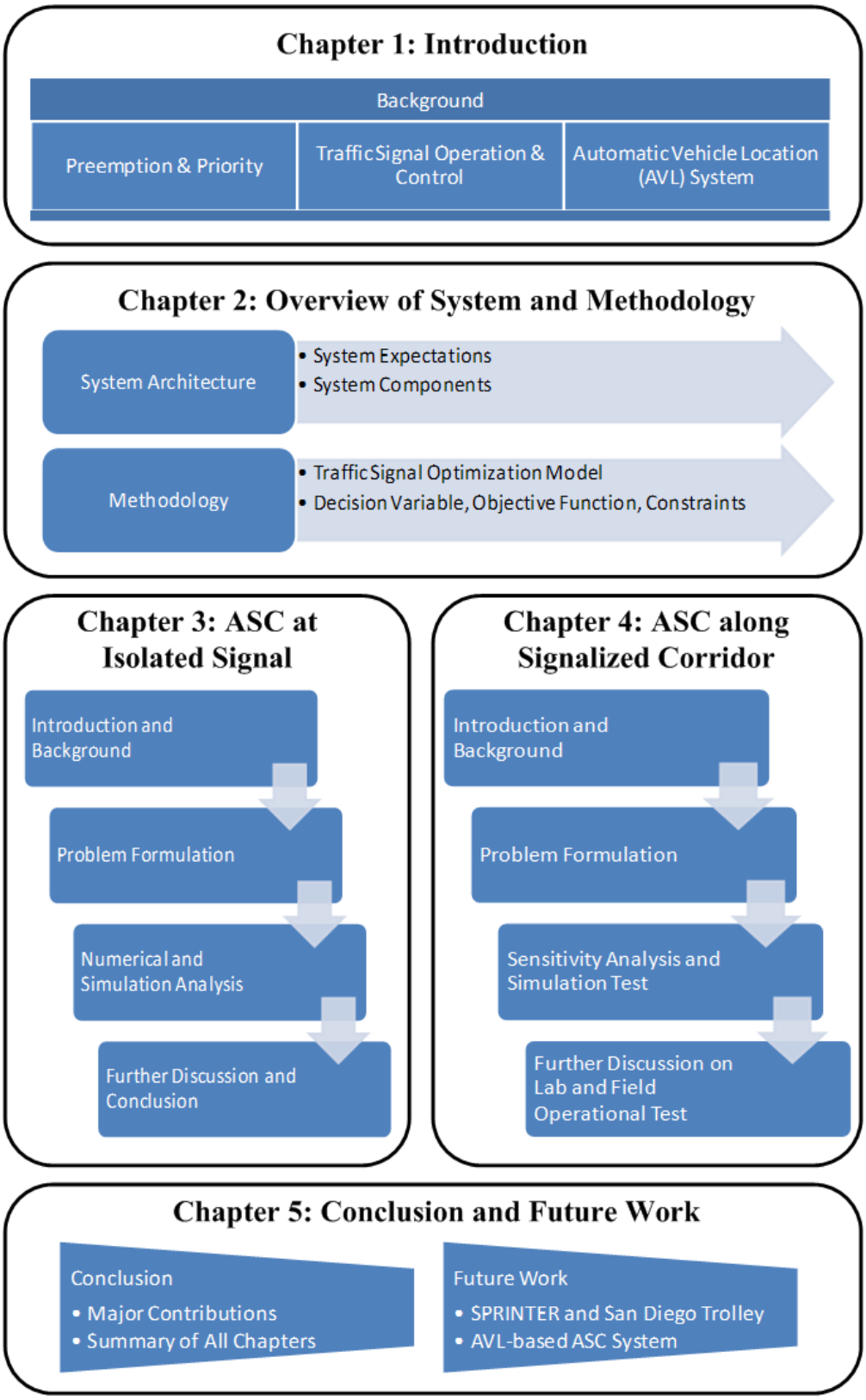

Figure 1.12: Organization flow of the dissertation

Chapter 2

2. Overview of System and Methodology

2.1 Overview of the Proposed Adaptive Signal Control (ASC) System

As mentioned in Chapter 1, the major problem of the conventional traffic signal control strategy at intersections at/around grades crossings lies in the lack of information on the movements of rail transit vehicles. If the AVL system is instrumented on a rail transit vehicle, then the GPS signal can arrive from a satellite to the transit vehicle. The vehicle location is communicated to the PC dispatch software through the internet and the motion information will be available for predicting movements of the rail transit vehicle. Therefore, traffic signal timings can be adjusted to adapt to the prediction of the transit vehicle's movements. For example, Figure 2.1 and Figure 2.2 illustrate the modified AVL

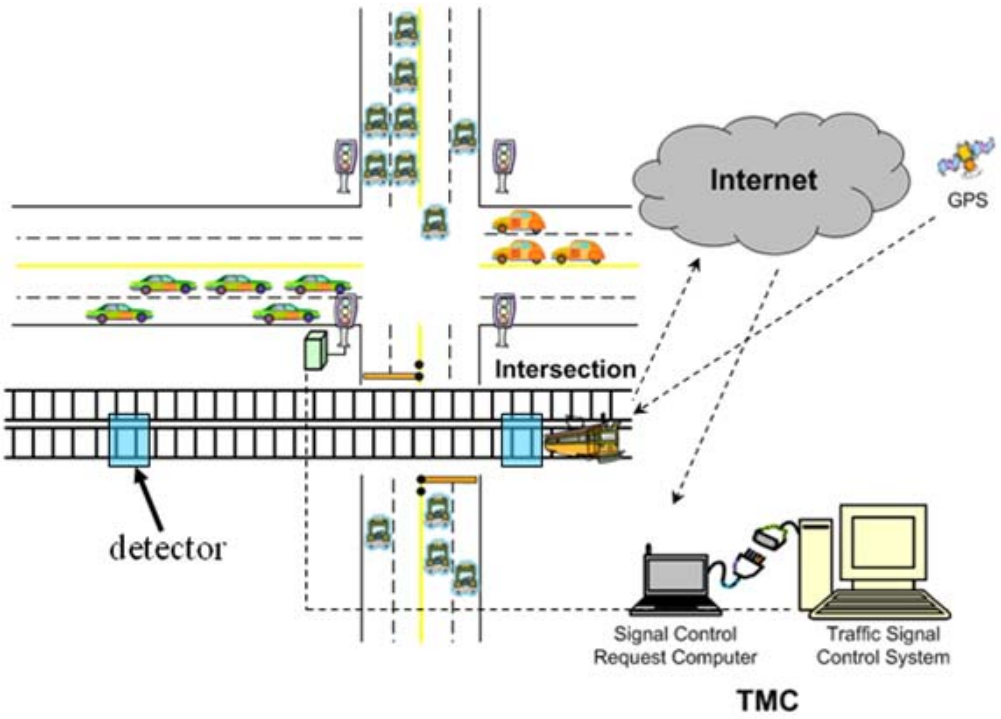

Figure 2.1: Preemption with AVL system

-based traffic signal control systems which employ preemption and priority, respectively.

2.1.1 System Expectations

Based on the updated location/movement information of transit vehicles, the proposed adaptive signal control system is expected to:

- Remove the queue of motor vehicles caused by preemption.
- Reduce the overall traffic delay around the grade crossing caused by preemption.
- Reduce the intersection delays and the number of en-route stops of rail transit vehicles under priority
- Reduce the overall trip travel time.
- Improve the reliability of trip travel time and the schedule adherence of rail transit vehicles under priority.
- Decrease the operational costs of rail transit vehicles, such as fuel consumptions and pollutant emissions, caused by the unnecessary stops at signals under priority.
- Minimize the negative impact (e.g., increased delays) on other traffic under priority.

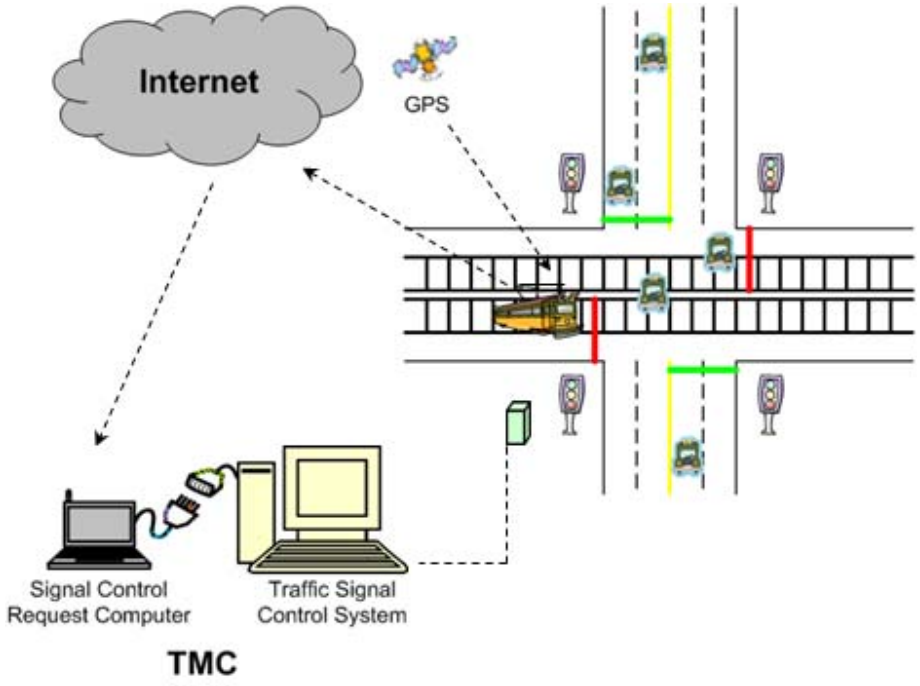

Figure 2.2: Priority with AVL system

All of the expectations mentioned above will be illustrated in Section 2.2. Beside these major expectations, fundamental requirements for the proposed system to obtain better performance are:

- **Cost effectiveness.** To deploy the system in the field, the cost is always one of the major concerns. However, the overall cost of the proposed adaptive traffic signal control system depends on not only the technology that will be implemented, but also the type of transit system deployed, e.g., preemption or priority. As mentioned before, the AVL system used in the applications in this dissertation is the PATH-developed cellular GPS navigator, which is very cost effective. Nevertheless, the signal reception under certain conditions is not satisfactory. For example, the signal blockage by skyscrapers in the downtown area degrades the quality of required information.
- **Minimal interruption with the original system.** Another desired feature of the proposed system is to interrupt the original system as little as possible. For example, in the application of San Diego trolley illustrated in Chapter 4, the decision variables in the field testing are chosen only as force-off points instead of offsets, which can guarantee shorter transition times for traffic signals and less interference with the coordination along cross streets. Further details will be discussed in Section 4.7.
- **System flexibility** [52]**.** The system to be deployed should be user-friendly, which means that it may be flexibly modified to satisfy users' needs. As will be shown in the applications in the following chapters, the proposed adaptive traffic signal control system is very easy and straightforward to adjust the performance index and model constraints based on users' preferences and different situations.
- **As little interaction with transit operators as possible** [52]**.** There is no additional or minimal load to transit operators by implementing the proposed adaptive traffic signal control system. This feature ensures that the system is more reliable without causing further safety issues due to the interaction with transit operators.

The requirements listed above are far from being complete. For example, the Manual on Uniform Traffic Control Device (MUTCD) [53] and California Vehicle Code provide more detailed operational requirements to which the priority for transit vehicles needs to conform.

2.1.2 System Architecture and Components

The architecture of the adaptive signal control system largely depends on several factors including the type and operation of the traffic control system in place, the extent to which traffic congestion interferes with transit operations, the nature of the interference, and the frequency or other characteristics of transit service. Figure 2.3 presents the system architecture for the proposed adaptive signal control.

To be more specific, the proposed system draws on the AVL system equipped onto transit vehicles as a means of continuously detecting vehicles' locations. Then the movements of transit vehicles, e.g., arrival times at signals or leaving times at grade crossings, are predicted by the movement predictor module. Numerous studies have been conducted on transit movement prediction with regression models [54, 55], Kalman filtering [56], artificial neural networks [57, 58, 59], and other methodologies [60]. However, the focus of this dissertation is the development and applications of the signal optimization algorithm for adaptive signal control, so no further efforts are made to predict the transit movement and the predictor described in [55] will be chosen in this thesis. The traffic condition predictors, such as delay and queue length estimators, used in this study only take the simplest form, i.e., deterministic and uniform arrival, due to the limited traffic data from the field. If more detailed information on traffic condition is available from detectors, then more advanced traffic condition predictors can be developed. Nevertheless, this is out of the scope of the thesis. By taking into account the predicted transit movements, predicted traffic conditions and traffic signal status, the adaptive signal control system can provide the optimal signal timings based on the outputs of the optimizer. The set of optimal signal timings are sent to signal controllers in the field.

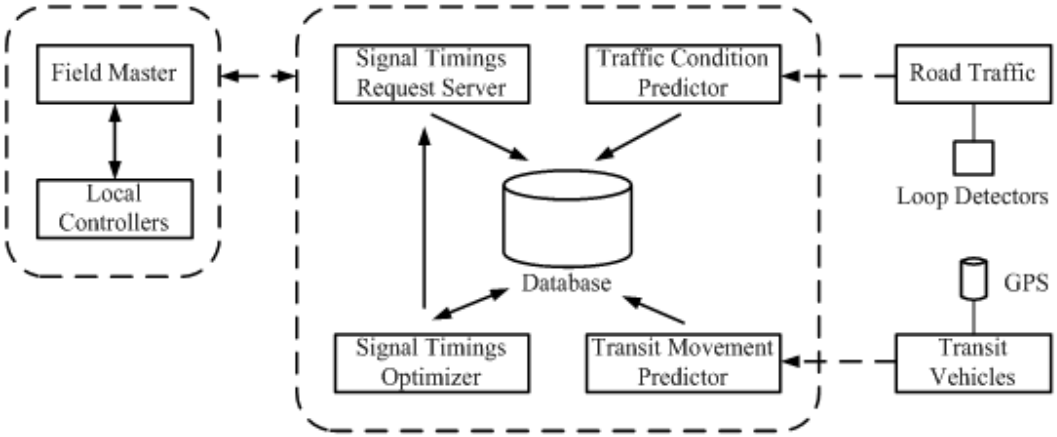

Figure 2.3: System architecture of the proposed adaptive signal control

As is shown in Figure 2.3, the components of the proposed adaptive signal control system are:

- Transit vehicles with location detectors (the AVL systems).
- A traffic surveillance system to monitor the traffic condition.
- Signal controllers to implement the requested traffic signal timings.
- The core of the proposed system to generate the optimal signal timings that adapt to transit vehicles' locations and ambient traffic conditions. More specifically, it includes the transit movement predictor, the traffic condition predictor, the signal timing optimizer, the signal timing request server and the database.

2.2 Overview of the Proposed ASC Methodology

The methodology of the proposed adaptive signal control will be illustrated in the following. A flow chart of the ASC methodology is presented in Figure 2.4. The core of the method is the traffic signal optimization algorithm, which will be elaborated in the next section. The inputs of such algorithm include:

- **Predicted Transit Movement**. With continuous detections of transit vehicles' locations by the AVL system, movements of transit vehicles, such as intersection arrival times and leaving times, are predicted by the algorithm developed in [55], which is based on historical movement data as well as real-time information.
- **Predicted Traffic Condition**. If advanced traffic surveillance systems are available at studied intersections, more accurate and sophisticated methods can be used to predict the states of traffic operation. However, in the applications shown in Chapter 3 and Chapter 4, there are no real-time traffic data available but limited survey data on vehicle turning counts instead. Therefore, the simplest deterministic model is applied to estimate the traffic delays at signals. In Chapter 3, two sub-models are proposed to estimate the queue length along each approach based on the data available.
- **Traffic Signal Timings**. The usage of traffic signal timings is three-fold: a) Traffic signal status should be integrated in the prediction of transit movement (e.g., under priority) because transit vehicle are also controlled by traffic signals; b) Traffic signal timings are necessary for estimating traffic delays, queue lengths or other key performance measures; c) Traffic signal timings cast a portion of constraints on decision variables in formulating the optimization algorithm.
- **Road Characteristics**. Road characteristics determine values of some parameters of the optimization algorithm. For example, *Highway Capacity*

Manual 2000 (*HCM 2000*) [61] recommends the values of saturation flows based on different configurations of intersections. It is noted that parameters in the algorithms presented in Chapter 3 and Chapter 4 are selected based on *HCM 2000*.

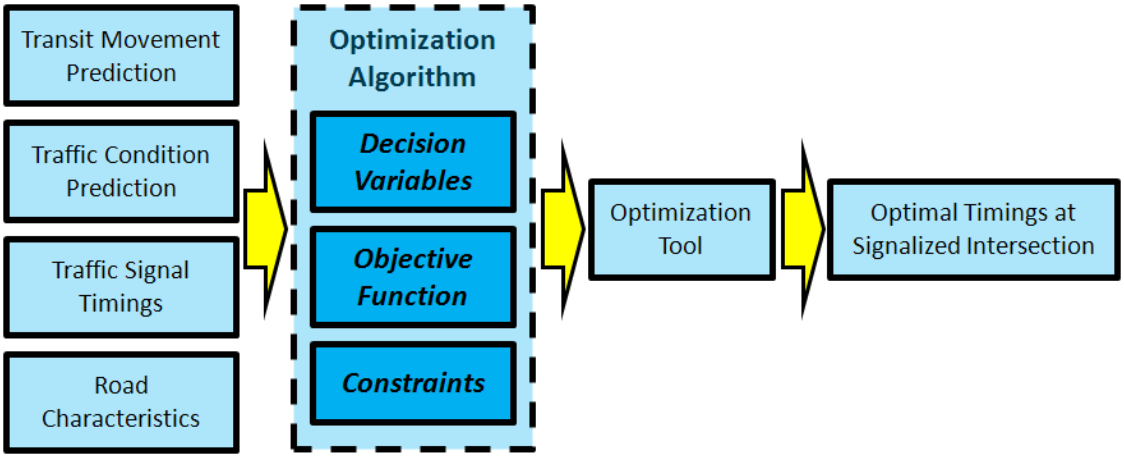

Figure 2.4: Illustration of proposed ASC methodology

2.2.1 Traffic Signal Optimization Algorithm

Optimization algorithms are widely used in traffic signal control. Almost every traffic control system employs at least one optimization algorithm [62, 63]. Different types of optimization algorithms can be set up, depending on the user-defined performance measures, the type of traffic signal operation and transit operation, and other needs. For example, in the SPRINTER rail transit application (Chapter 3), the deterministic delay estimation model is used and the problem is formulated into a mixed integer quadratic programming (MIQP) problem. Then commercial optimization software, such as LINDO API 6.0 [64], and CPLEX [65], can be applied. If Webster's formula [66] or the HCM equation is selected as the delay estimation model, then the problem is formulated into a nonlinear general integer programming (NGIP) problem, which in general is very difficult to solve and there is no guarantee so far to obtain the global optimum or even a local optimum [67, 68]. However, under certain conditions, some of the integer constraints on decision variables in the traffic signal optimization model can be relaxed, and these decision variables are rounded to the nearest feasible integers after solving the linear relaxation counterpart. Therefore, the original NGIP problem can be simplified into a nonlinear programming (NP) problem or nonlinear binary integer programming (NBIP) one, which is computationally tractable, and the corresponding local optimum can be obtained by existing computational tools, such as Matlab. Some

details on the linear programming (LP) relaxation of the proposed ASC are presented in the application to the San Diego trolley system (Chapter 4).

2.2.2 Decision Variables

The choice of decision variables mainly depends on the needs to formulate the problem. In most cases, the decision variables of traffic signal optimization problems include cycle length, green splits, the start point and end point of each phase, and the phase sequence, or more generally, the states of signals at each time step. If the cycle length and the phase sequence are pre-timed, then the times when each phase initiates and terminates become the focus of interest. This is just the case for the applications illustrated in this thesis.

However, based on the author's knowledge from field testing on the San Diego trolley system, a more pragmatic choice of decision variables is the force-off point of each phase or the offset of each local controller rather than the green split if we take into account the real-world operation of a traffic signal controller. More details in selecting decision variables for field implementation will be covered in Chapter 4. Moreover, for the adaptive signal control along a signalized corridor, additional decision variables related to the formation of green bands [51] are entailed to provide sufficient green band widths for transit operation and traffic progression.

2.2.3 Objective Function

In this dissertation, overall traffic/passenger delays at signals, including both transit vehicles and other motor vehicles, are the performance indices of the proposed ASC system. Based on specific needs, other commonly used measurements of effectiveness (MOEs) at signalized intersections can be incorporated into the proposed system and serve as the objective functions. These MOEs include:

- Overall trip travel times
- Numbers or percentages of stops
- Average vehicle speed
- Numbers or rates of accidents
- Overall fuel consumption
- Overall emission of pollutants

Nevertheless, traffic delays at signalized intersections are of particular interest

because the *HCM 2000* adopted the intersection control delay (ICD) as the only MOE to determine the level of service (LOS) of an intersection. In *HCM 2000*, the intersection control delay (ICD) is defined as follows: “Control delay includes initial deceleration delay, queue move-up time, stopped delay and final acceleration delay” [61]. In the simulation results shown for the San Diego trolley system, the LOS is determined by the control delay at the studied intersection.

2.2.4 Constraints

The constraints for traffic signal optimization are problem dependent. Most of the existing algorithms include constraints related to safety (minimum greens and maximum greens [69]), the efficiency of the overall traffic system, e.g., upper bound and lower bound of cycle length [70], and pre-timed mechanisms of traffic signal controllers, such as phase sequences in dual ring signal operations [71]. Beside the commonly used constraints mentioned above, there are still other constraints specific to the problems in this dissertation. For example, there is a constraint to guarantee that the queue accumulated during the preemption should be cleared as soon as possible (Chapter 3). In the application of San Diego trolley system (Chapter 4), constraints are developed to satisfy the geometric relationship of green bands along a signalized corridor and to simplify the original problem.

Chapter 3

3. Application I: ASC at an Isolated Signalized Intersection – SPRINTER Rail Transit

3.1 Introduction

In this chapter, the adaptive signal control algorithm is applied to the transit preemption systems which are mainly operating in the suburban areas. Section 3.2 provides the background of SPRINTER rail transit service and identifies the existing problems related to the operation of SPRINTER. To improve the performance of the overall traffic system at the signalized intersection around the highway/rail grade-crossing right after the preemption, e.g. delay reduction and queue clearance, a mixed integer quadratic programming (MIQP) model is proposed in Section 3.3. To validate the model, both numerical analysis and simulation tests are conducted and the results are presented in Section 3.4. Section 3.5 concludes this chapter and discusses some potential extensions for future research.

3.2 Background

3.2.1 SPRINTER Rail Transit Service

The SPRINTER Rail Transit is located in northern San Diego County. The rail line parallels the heavily-congested SR 78 corridor and was previously used for freight transportation. It was converted into a diesel multiple unit (DMU) passenger rail system which serves 15 stations including a 1.7 mile loop to serve California State University San Marcos (CSUSM). It extends nearly 22 miles and connects four North County cities - Oceanside, Vista, San Marcos, and Escondido, as well as unincorporated areas of San Diego County (Figure 3.1). The train service started on March 9th, 2008.

The existing railroad has been used by Burlington Northern-Santa Fe for freight transportation. The freight trains are typically 1,100ft long and run only three round trips every week during evening and early morning hours. Thus there is very little traffic impacts from the freight operation. The current passenger train service is a shared-track operation with freight trains. Passenger and freight operations will be completely segregated in time – the freight transportation will continue, but will be limited to the hours between 11pm and 4am, and the operating speed will increase to 30 mph. The passenger trains are 85 ft (1 car) or 170 ft (2 cars) long, with the headway of 30 minutes (64 trains per day between 04:00 a.m. and 09:30 p.m.) and a maximum operating speed of 55 mph.

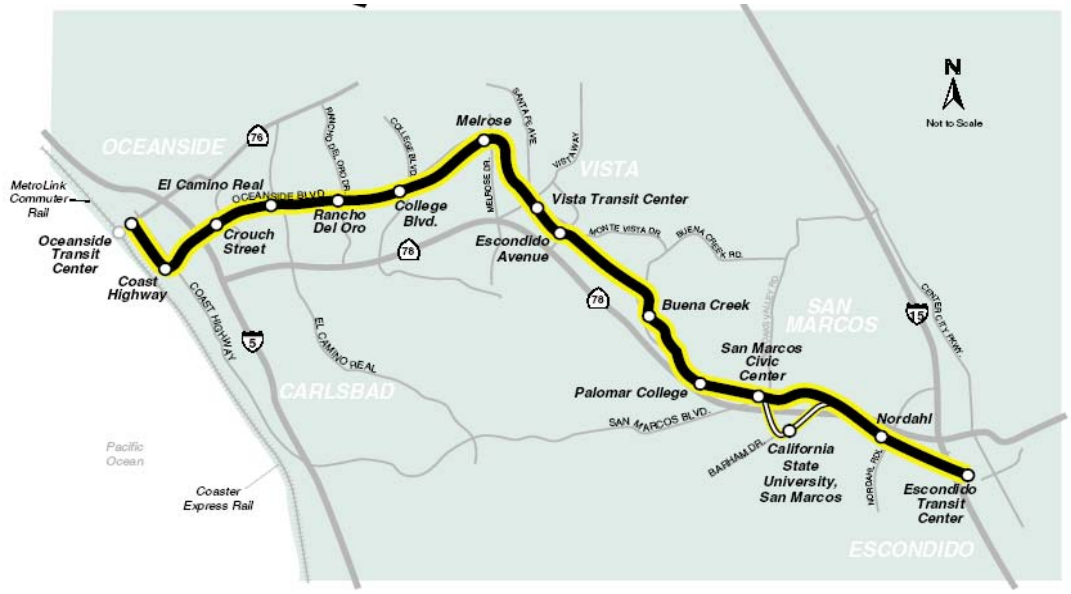

Figure 3.1: SPRINTER project site

The train control uses traditional blocking systems and a centralized train control (CTC) system. The control center is located at the maintenance facility in Escondido. The track circuits provide train presence detection for interlocking control. Near grade crossings, they also provide predicted time-to-arrival within a very limited range at the grade crossing.

The corridor served by this project parallels SR78, which is currently congested throughout the entire route during rush hours. The project will serve large intermodal transit centers in both Oceanside and Escondido, and a dispersed mix of commercial, industrial, and single-/multiple-family residential developments between corridors. It has also been estimated that the number of residents living in communities served by the rail line will increase by 74 percent, with employment increasing at nearly the same rate.

Thus, current traffic volumes are projected to increase by more than 50 percent in the year 2015, ranging from 150,000 to 200,000 vehicles per day.

3.2.2 Railroad Preemption Procedure

Typical railroad preemption procedures at signalized intersections include:

- **Prior to the train crossing**: The railroad crossing controller will receive a train approaching signal from the detection equipment, and initiate the warning devices and the necessary traffic signal preemption events (including the clearance of tracks).
- **During the train crossing**: The warning device will be activated for at least a minimum amount of time prior to the arrival of the train at the crossing. When the automatic crossing gate is lowered and all movements across the track have been stopped, the traffic signal may implement a limited phasing sequence.
- **After the train crossing**: The railroad crossing controller will trigger the automatic gate to rise and the flashing signal and audible warning to stop. Then, the traffic is allowed to proceed normally.

Table 3.1 [72] shows the minimum time interval of each step during the preemption at a grade crossing. The selection of time intervals for SPRINTER service is more conservative due to safety concerns, as illustrated in Figure 3.2.

Table 3.1: Time for traffic interruption at grade crossings

Warning bells prior to gate activation (gates are not down but traffic should stop once bells begin to sound)	5 seconds
Gate activation prior to train arrival	20 seconds
Time for Train to pass crossing (200 ft long train traveling at 20 mph min)	7 seconds
Equipment reaction time to all calls	3 seconds
Time for gates to clear crossing after train passes	5 seconds
Total	40 seconds

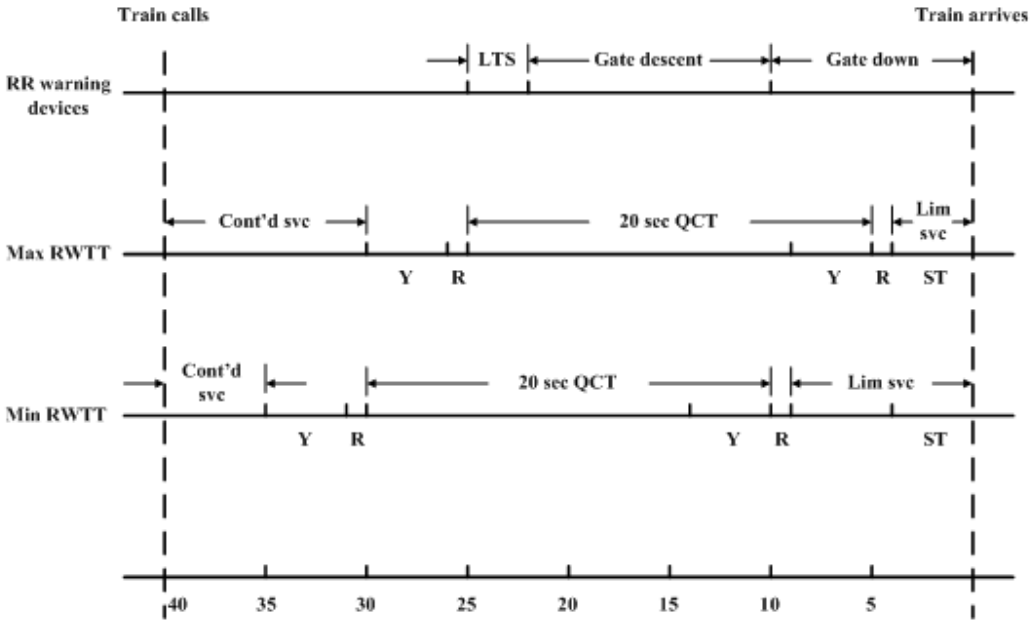

* RR – Railroad
** RWTT – Right-of-the-way transfer time
*** QCT – Queue clearance time

Figure 3.2: An example of preemption logic used in SPRINTER

3.2.3 Problem Identification

3.2.3.1 Project Meetings with Local Jurisdictions

The SPRINTER line started revenue service on March 9, 2008. The freight trains that previously ran on the track only operate during late evening hours and do not have obvious impacts on traffic. The concerns raised by the traffic engineers are mostly perceived negative impacts.

In the project area, traffic congestion is already prevalent. With the traffic signal preemption provided to more frequent train services, traffic engineers from the cities along the SPRINTER line expect that the traffic congestion problem will further deteriorate because the signal timing is not optimized to handle preemption interruptions.

3.2.3.2 Simulation in PARAMICS

To get further insight into the potential problem, a simulation network was coded in PARAMICS to model the traffic system under the current signal operation. All field data including SPRINTER operation, traffic volumes, road characteristics and traffic signals at grade crossings, were used to calibrate the microscopic simulation model. Figure 3.3 shows the whole SPRINTER railroad about 22 miles long through City of Oceanside, Vista, San Marcos and Escondido in the San Diego North County region. More details in simulation setups will be presented in Section 3.4.

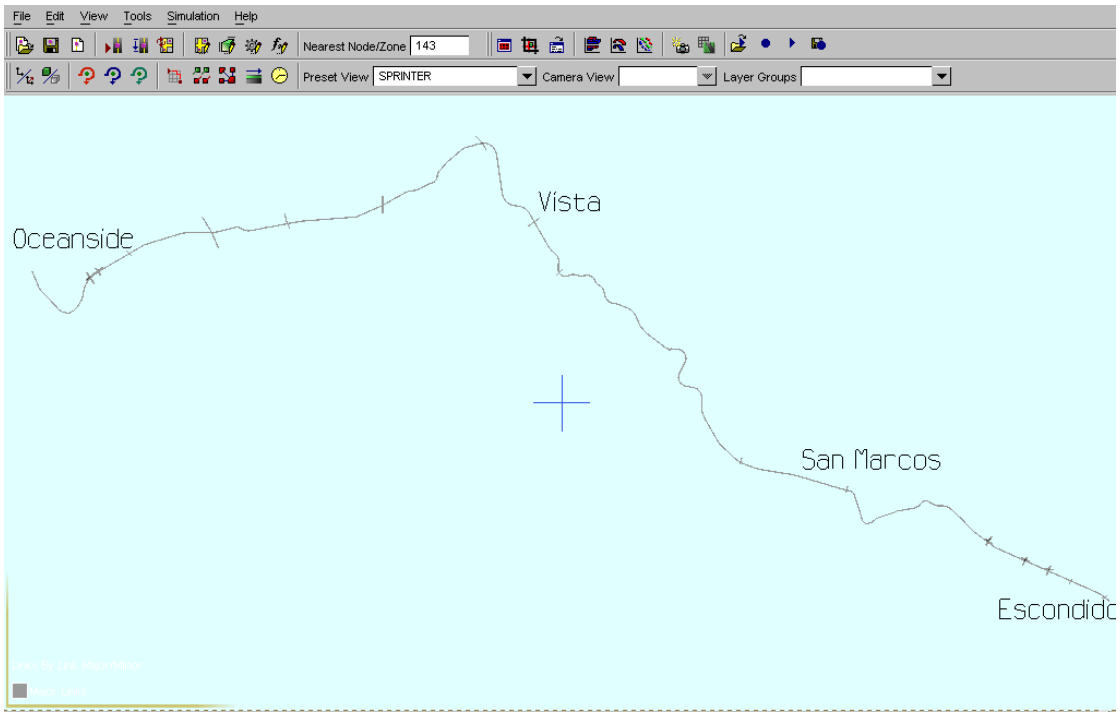

Figure 3.3: Overview of the network coded in PARAMICS

The following study sites are selected and corresponding system performances of traffic operation are compared with and without preemption impacts: I-5 Southbound Ramp @ Oceanside Blvd., the I-5 Northbound Ramp @ Oceanside Blvd., Enterprise @ Oceanside Blvd., Andreasen Dr. @ Oceanside Blvd., Vista Village Dr. @ Olive, Vista Village Dr. @ Santa Fe Ave., Main @ Santa Fe Ave, Pala Dr. @ Escondido Ave. and Phillips St. @ Escondido Ave. The results are illustrated in the following figures.

I-5 SB/NB Ramp @ Oceanside Blvd.

Figure 3.4 shows the comparison results where **65.1 percent** and **69.1 percent**

increases in average vehicle delay (sec) during the cycle right after the preemption is attributed to the operation of SPRINTER at *I-5 Southbound (SB) @ Oceanside Blvd*. and *I-5 Northbound (NB) @ Oceanside Blvd*., respectively.

Enterprise/Andreasen Dr. @ Mission Rd.

From Figure 3.5, it can be observed that there are **23.2 percent** and **49.1 percent** increases in traffic delay per vehicle (sec) within the cycle right after the preemption, due to the impacts from the operation of SPRINTER at *Enterprise @ Mission Rd.* and *Andreasen Dr*. *@ Mission Rd*., respectively.

Vista Village Dr. and Santa Fe Ave.

Figure 3.6 shows the traffic delays along intersections: *Vista Village Dr*. *@ Olive*, *Vista Village Dr*. *@ Santa Fe Ave*. and *Main @ Santa Fe Ave*., with and without preemption under the original signal timings. It can be observed that there are **98.5 percent**, **28.3 percent** and **127.3 percent** increases in average vehicle delay (sec), respectively, owing to the operation of SPRINTER.

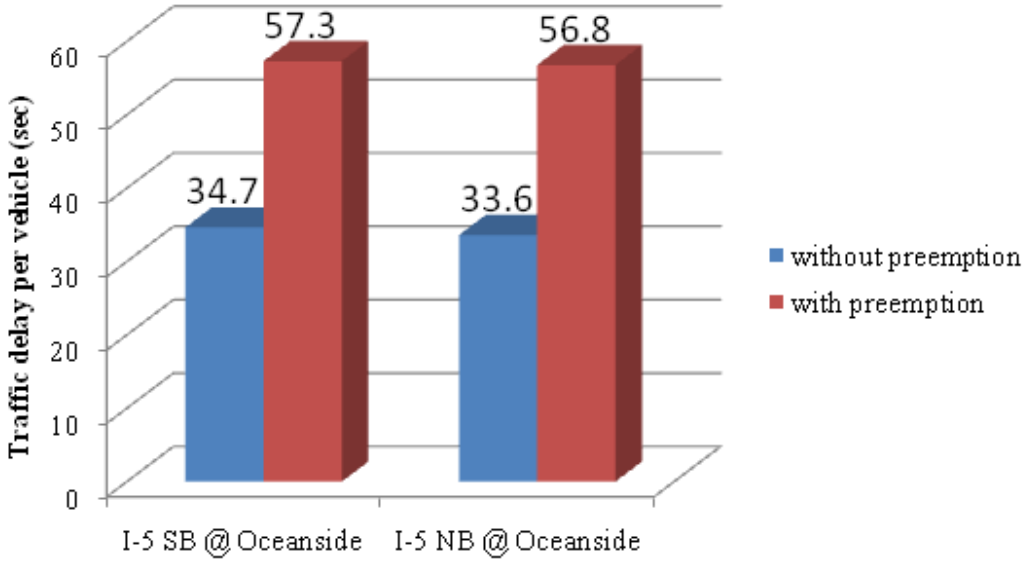

Figure 3.4: Comparison results for I-5 SB/NB Ramp @ Oceanside Blvd. from simulation with and without preemption

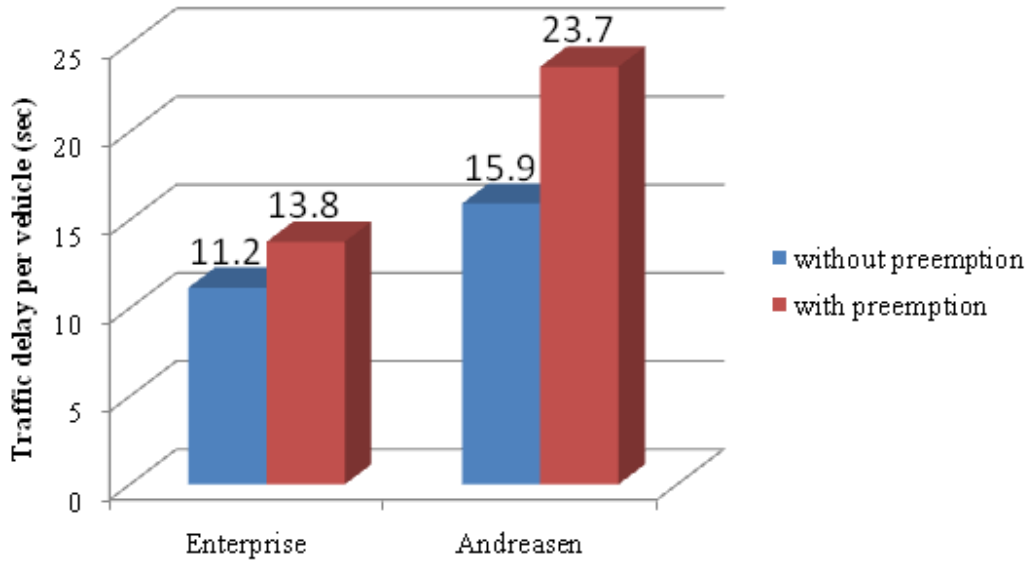

Figure 3.5: Comparison results for Enterprise/Andreasen Dr. @ Mission Rd. from simulation with and without preemption

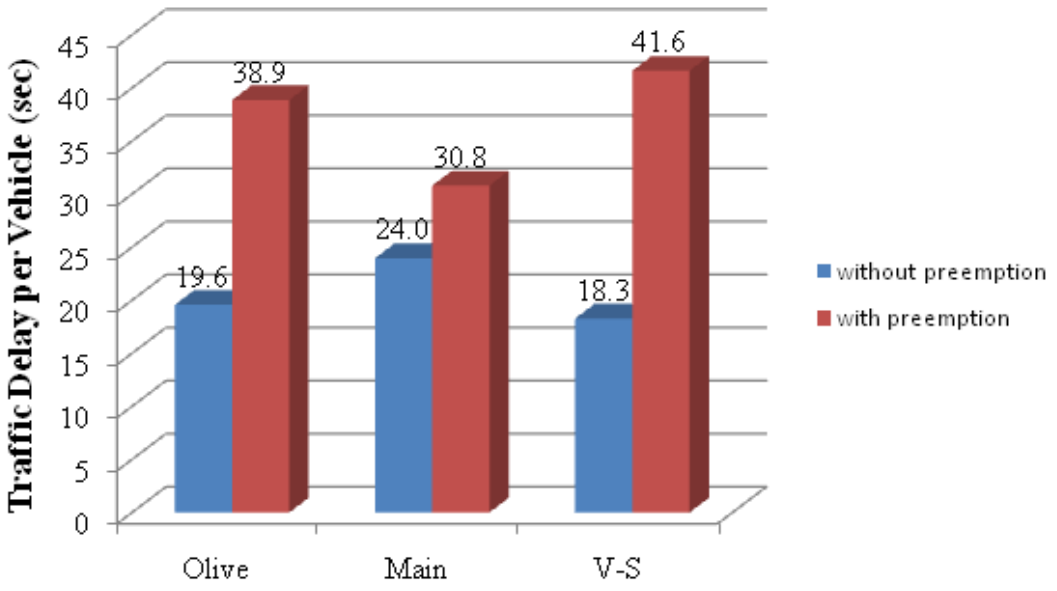

Figure 3.6: Comparison results for Vista Village Dr. and Santa Fe Ave. from simulation with and without preemption

Pala Dr./Phillips St. @ Escondido Ave.

In Figure 3.7, the interruption of SPRINTER operation is responsible for the growth of traffic delays by as high as **66.6 percent** and **29.0 percent** at *Pala Dr. @ Escondido Ave*. and *Phillips St. @ Escondido Ave*., respectively.

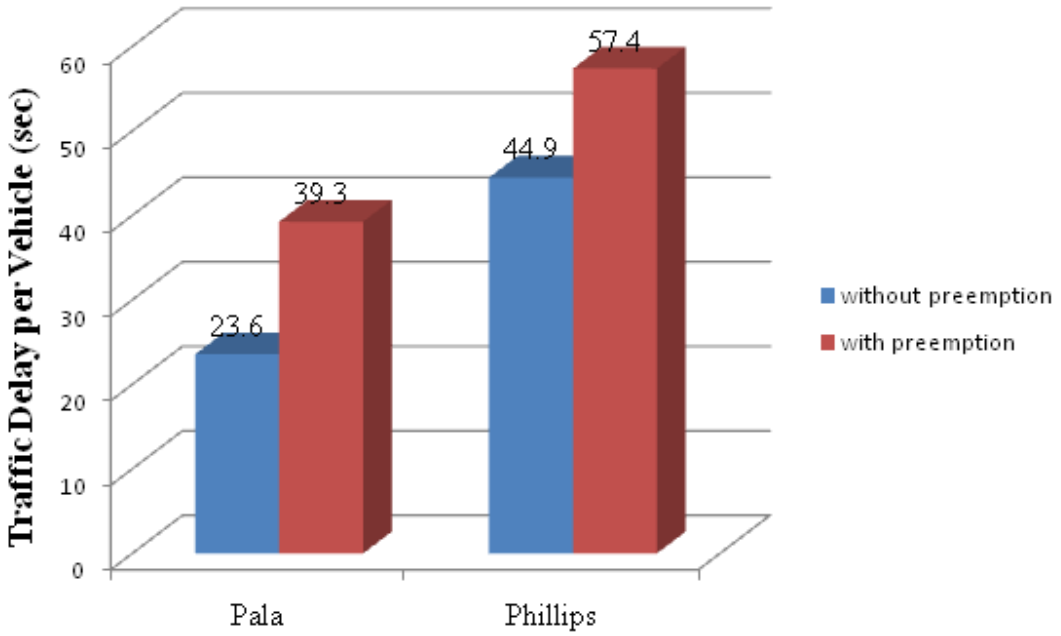

Figure 3.7: Comparison results for Pala Dr./Phillips St. @ Escondido Ave. from simulation with and without preemption

3.2.3.3 AVL-based Data Analysis

Six PATH-developed cellular devices (Figure 1.10) were installed on SRPINTER trains as GPS loggers [83]. These cellular GPS trackers keep sending trains' GPS locations and speed information back to the server at PATH with one-second resolution. Using these GPS data, the trains' movements of interest can be precisely tracked. For instance, the following figure (Figure 3.8) plots a train's trajectory for one typical day.

The signal preemption starts when a train triggers an arrival detector. However, if the train station is a near-side station, then a pre-set 30-second dwell time is assumed, i.e., the preemption starts 30 seconds after the train stops at a ***near-side station***. This assumption could lead to unnecessary traffic delays if the actual dwell time is longer than 30 seconds and to safety concerns if the actual dwell time is much shorter than 30

seconds. With the GPS data, a more accurate dwell time and arrival/departure time at each station along each direction can be obtained. Figure 3.9 and Figure 3.10 show examples of station dwell time statistics. As can be observed from the figure, the dwell times range from 25 seconds to 50 seconds and vary with different stations. Even for the same station, the dwell time statistics are also different along different direction.

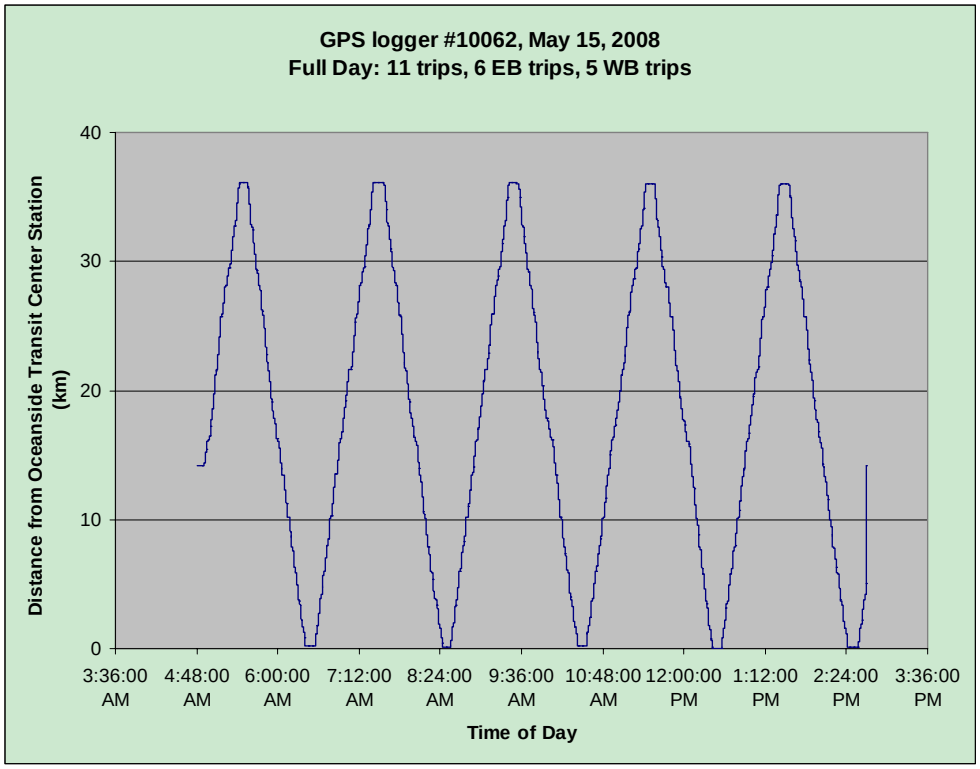

Figure 3.8: Train trajectory

3.2.4 Relative Study

The sub-optimality of traffic signal operations near grade crossings may cause non-trivial delays to traffic, particularly after the preemption. Nevertheless, the standard signal optimization strategy [37, 73, 74] and the adaptive priority strategy proposed in [71] do not apply due to the special logic of the preemption. In [75], an improved transition preemption strategy (ITPS) was designed to provide more green time to the phases that will be blocked during the preemption, as compared to the normal traffic signal mode and the transition preemption strategy (TPS) algorithm [76], but the optimality of overall traffic performance cannot be guaranteed.

At the same time, to quantify the system performance, e.g. traffic delay, at a signalized intersection, it is critical to have a good estimation of the queue length along each approach and the associated queue clearance time. At those intersections affected by the preemption, the backup vehicle queue becomes even worse. Therefore, the delay estimation largely depends on the residual queue length due to the preemption. Development on queue length estimation methodologies has been an active research area for years [77 – 81]. Some methodologies employ the results from simulation tools while others are based on the assumption of a known arrival pattern or the availability of a sophisticated surveillance system. In this chapter, with the limited information on turning counts along each phase from historical surveys, a deterministic model is applied with modifications by two sub-models to obtain a more accurate estimate of the queue length along each phase after the preemption.

In the following section, the methodology presented in Chapter 2 will be introduced to minimize overall intersection delays after the preemption.

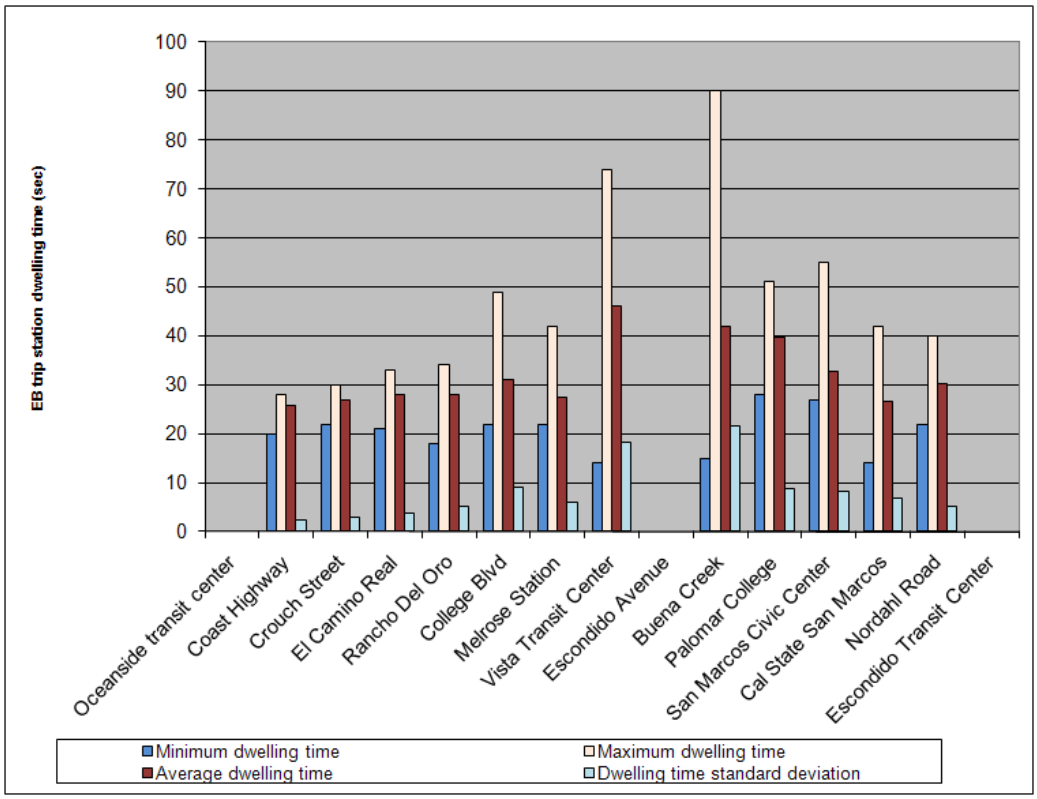

Figure 3.9: Station dwell time of east bound trips

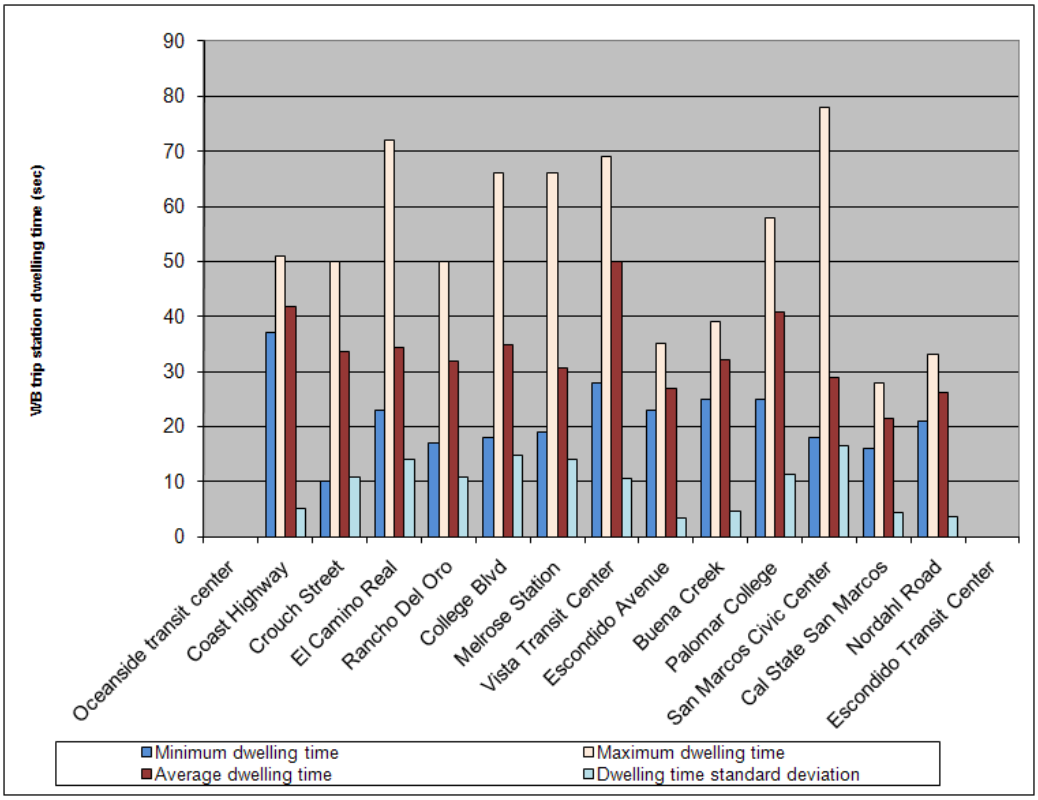

Figure 3.10: Station dwell time of west bound trips

3.3 Problem Formulation

As identified in the previous section, the negative impacts on motor vehicles around the grade crossings due to SPRINTER operation cannot be negligible under the original traffic signal timings. To solve this problem, the proposed adaptive signal control algorithm for the SPRINTER is to adjust the signal timings around the grade crossings right after the preemption such that the overall intersection traffic delays can be minimized within a certain time window (e.g. one or multiple cycles). In addition, the residual queue caused by the preemption along each approach can be dissipated as quickly as possible. A mixed integer quadratic programming (MIQP) model is proposed to optimize traffic signal operation at the studied intersections affected by preemption, such that the movements of trains and motor vehicles at these sites can be well coordinated and the overall traffic system performance can be improved. The flow chart of methodology is shown in Figure 3.11.

In summary, to relieve the impacts on normal traffic incurred by the interruption of SPRINTER trains, the queue length along each approach right after the preemption is first estimated. The overall intersection traffic delay can then be quantified based on

queue length estimation. Finally, a delay minimization model is formulated and solved by mathematical programming to obtain a set of optimal traffic signal timings operated within a specified time window right after the preemption at each intersection around the grade crossing. This set of traffic signal timings are aimed to relieve the traffic congestion caused by SPRINTER operations. After the congestion is mitigated, the traffic signal timings can be transitioned back to the original ones or others depending on users' needs.

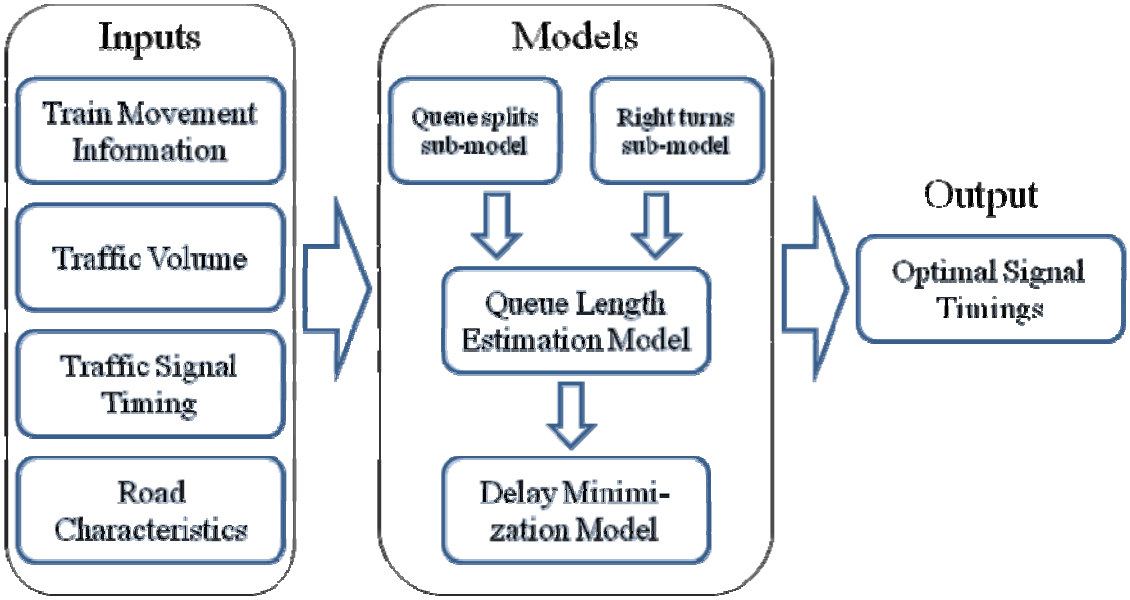

Figure 3.11: The proposed optimization strategy

In addition, data collection is indispensible, since these data will not only serve as inputs to both the queue length estimation model and the overall intersection traffic delay minimization model, but also be used in the network construction of the simulation model. At the same time, both the numerical model and the simulation model are calibrated by the collected data. Roughly speaking, the required data for analysis in this chapter can be divided into the following four types:

- **SPRINTER rail/train data**. To formulate the traffic signal optimization problem and construct the SPRINTER rail/train microscopic simulation model, it is required to obtain the train physical/dynamic parameters, operating schedule, the number and location of stations, the GPS coordinates of the entire SPRINTER track-way, and movement data of SPRINTER trains;
- **Traffic volume**. Traffic volumes and turning counts are used in estimating the queue length right after the preemption. The estimated queue length is used to obtain traffic delays under either original signal timings or our proposed signal timing;
- **Traffic signal timing**. Traffic signal timings are critical to construct both the

numerical model and the simulation model. On the other hand, the queue length along each approach immediately after preemption largely depends on the original traffic signal timings at the associated intersection near the grade crossing. Therefore, signal timings under both normal condition and preemption are required;

- **Geometric information at signalized intersections**. Geometric parameters of signalized intersections around grade crossings, such as the number of lanes along each approach, and one/two way(s), are indispensable in building up the numerical model and the simulation network.

3.3.1 Queue Length Estimation

To quantify the traffic performance at the grade crossing right after the preemption, the number of waiting vehicles along each phase needs to be estimated. Two sub-models are developed to conduct such estimation by analyzing the data on traffic signal operation, traffic turning counts and road characteristics. In addition, the estimated queue length is a function of time points when the transit vehicle checks in and checks out of the grade crossing.

3.3.1.1 Assumptions

To develop the proposed queue length estimation model, the following assumptions are required

- Isolated intersection is taken into account instead of a coordinated corridor;
- Motor vehicles uniformly arrive at signals;
- The dissipation rate along each phase is a constant;
- The right-turn maneuver is permitted when signal is red;
- For drivers, the “smart” lane choice rule – selecting the lane with shorter queue if not mandatory – always holds. The rule sometimes may not apply to the real case since drivers tend to avoid lane changings due to the safety concerns.

Based on the assumptions mentioned above, the queue length can be estimated along each phase, even at the lane level, by integrating the following two sub-models.

3.3.1.2 Sub-model I: Simulation-based Queue Split Estimation on

the Shared Lane

Drivers' behavior will affect the queue development along each lane in the multi-lanes case, thus resulting in the variation of the number of waiting vehicles along each phase. Based on the assumption that the incoming drivers can make "smart" decisions on following the queue with the shortest length when approaching and waiting for a signal, a queue split model, i.e. the relationship between queue split and other factors, such as traffic demand, initial queue and road characteristics, may be developed. However, it is hard to get a close form for such a model by considering all the aforementioned factors. Instead, an approximate model is proposed by using simulation in Matlab.

Simulation results for a road arm configuration with one left-turn lane and one shared (for both left-turn and through movements) lane are presented in Figure 3.12 through Figure 3.15. According to these figures, some observations can be summarized below:

- If the incoming demand of left-turn traffic is much higher than that of through traffic, then the resulting numbers of waiting vehicles on both lanes are almost the same.
- In the reverse case, the numbers of waiting vehicles along the left-turn lane and shared lane approximate the corresponding incoming demands, respectively.
- If the difference in incoming demand is trivial between the through traffic and the left-turn traffic, then the difference in the number of waiting vehicles between these two lanes is also trivial. In addition, the variation of queue length along each lane is noticeably greater than any of those in the two cases mentioned before.
- The effect caused by the discrepancy of initial queues is remarkable when the demand of through traffic is much higher than that of the left-turn traffic, due to the fact that the left-turn vehicles can use both lanes but the through vehicles can only use the shared lane in this simulation scenario.

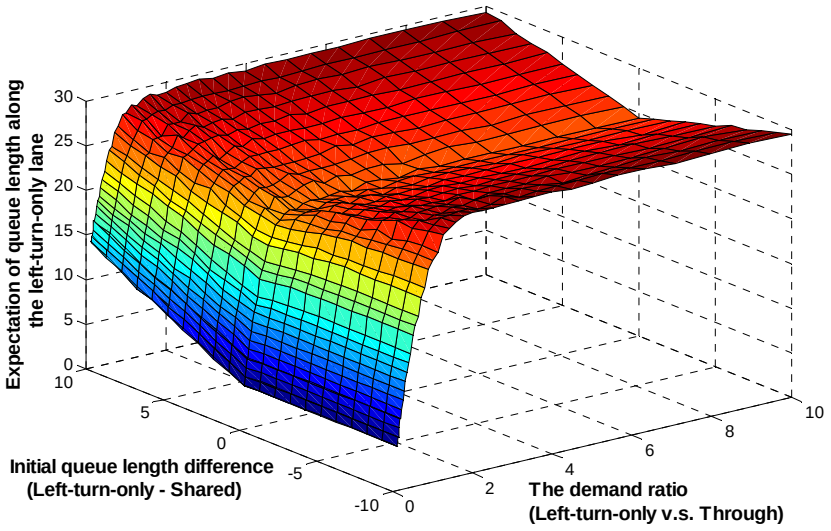

Figure 3.12: Mean of the number of waiting vehicles along the left-turn lane

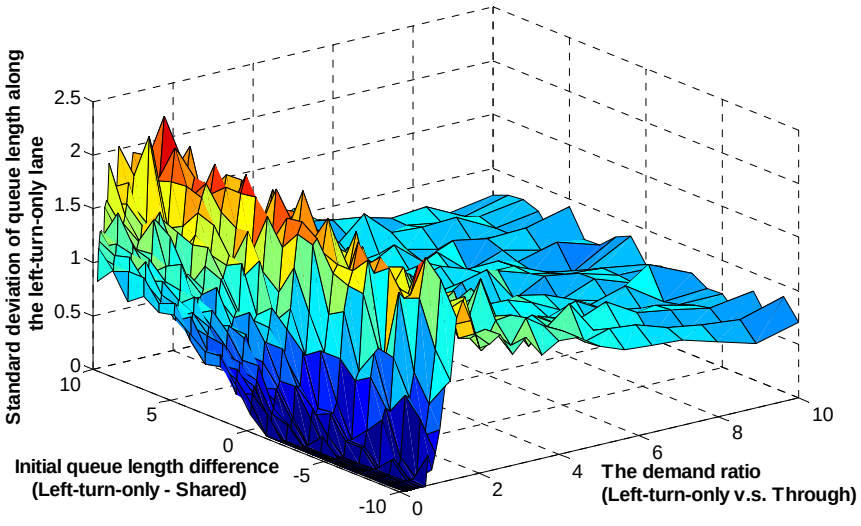

Figure 3.13: STD of the number of waiting vehicles along the left-turn lane

For different study sites, the proposed simulation-based model is modified based on associated traffic demands and road geometric features. With the outputs of such simulation-based models, the queue splits can be estimated along the left-only lane(s), right-only lane(s), through lane(s) and the shared lane(s) for any road geometric features.

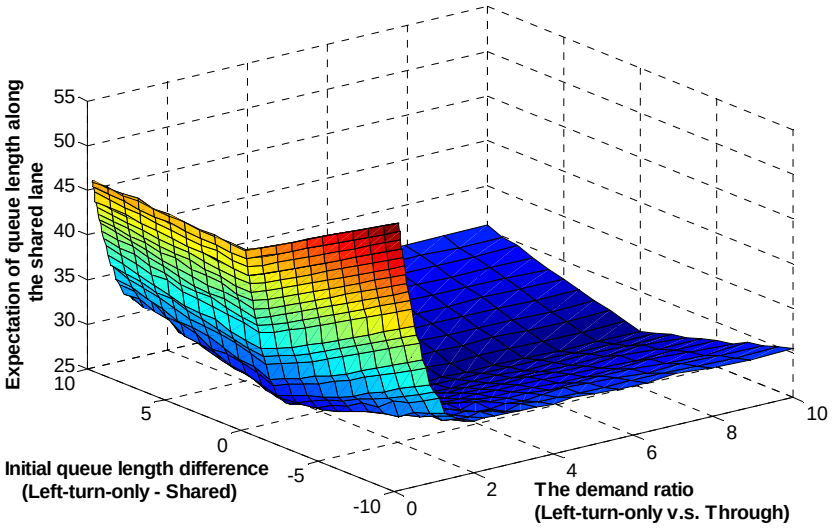

Figure 3.14: Mean of the number of waiting vehicles along the shared lane

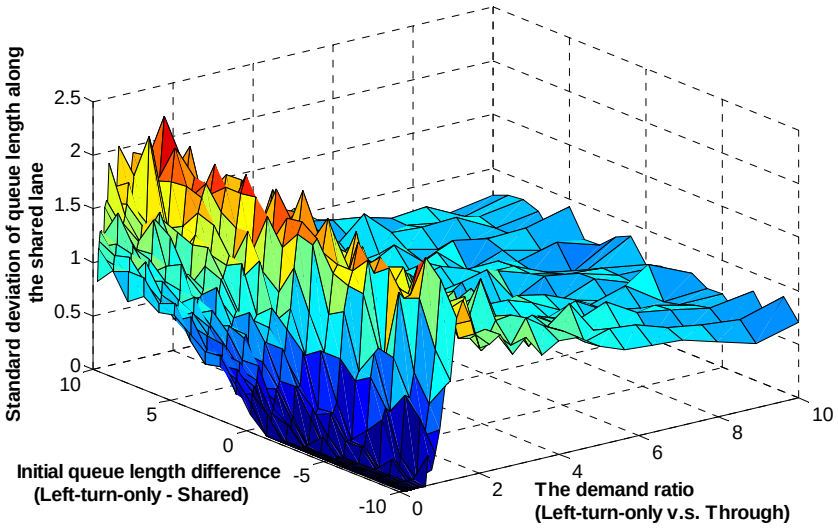

Figure 3.15: STD of the number of waiting vehicles along the shared lane.

3.3.1.3 Sub-model II: Right-turn Counts on the Shared Lane

On the other hand, if the right-turn maneuver is permitted when the signal phase is red, which is very common throughout the U. S., then another sub-model is required to modify the estimated number of waiting vehicles along the shared lane for both through (and/or left-turn) and right-turn traffic.

To illustrate the proposed sub-model, let us consider the case where there are n_1 through vehicles and n_2 vehicles that will make right turns forming a waiting queue along a shared lane. The random variable, *X*, is defined as the queue index for the first vehicle that will go through the intersection. A probability model is developed in the following to calculate the number of waiting vehicles along this shared lane, by taking into account the impact of right-turn traffic.

Proposition 1: The probability that the first through vehicle happens to be the *i*th vehicle along this shared queue with $n_1 + n_2$ vehicles is

$$P(X = i) = \frac{C(n_2, i-1) \cdot (i-1)! \cdot C(n_1, 1) \cdot (n_1 + n_2 - i)!}{(n_1 + n_2)!} \qquad \forall\, 1 \le i \le n_2 + 1$$

Proposition 2: Under the assumption that all right-turn vehicles at the very beginning of the queue will make turns in red, the estimated queue length, *L*, of waiting vehicles along this shared lane is

$$E(L) = \sum_{i=1}^{n_2+1} (n_1 + n_2 + 1 - i) \cdot P(X = i)$$

The number of waiting vehicles along each phase estimated from the above two sub-models will serve as an input into the traffic delay minimization model elaborated in the following section.

3.3.2 Delay Minimization

As specified before, the goal is to design green splits for different phases after the preemption, such that the overall intersection delays can be minimized over the controlled time period. A deterministic queue model is used for delay calculation. Before the model is developed, the following assumptions should hold

- Isolated intersection is taken into account;
- The arrival rate, a_i for each phase is uniform and constant;
- The dissipation rate, d_i, is constant and relates to the road characteristics;
- In most cases, the controlled time-span is one cycle after the train clears the grade-crossing, but the model can be extended to the controlled time-span of multiple cycles (see Section 3.5.1);
- The traffic condition is under-saturated;

- Vehicles accelerate and decelerate instantaneously, which implies that all drivers behave identically. In other word, they follow the average driving pattern;
- In timing optimization, the sequence of phases (lead/lag relationship) keeps untapped, which can be a potential topic for further research;
- The dual-ring signal controller is used for traffic control at the intersection.

The controlled time-span is a user-defined quantity, and the model extension will be illustrated later in this chapter. Although the deterministic queue model implemented here does not represent normal queuing behavior and may not accurately represent the exact number of queued vehicles at a given instant, it does not bias the delay estimation process over an entire queue formation and dissipation process [82], and is therefore a valid simplification when only considering delay calculations. In the proposed optimization model, the actual green splits, instead of the effective green splits, are considered at a signalized intersection. However, trivial modifications on constraints of the model can be conducted, such that the effective signal intervals rather than the actual green splits can be used and the additional delays due to drivers' reaction times and vehicles' acceleration/deceleration times can be taken into account. In addition, because of the lack of detailed information on traffic, the uniform arrival rate, instead of Poisson or non-Poisson arrival distribution, is adopted to calculate the traffic delay, even though the latter model may capture the randomness of traffic flows. In the future research, the sequence of phases will be also incorporated into decision variables for the purpose of traffic signal optimization.

3.3.2.1 Delay quantification

Before the traffic signal optimization algorithm is elaborated, the symbols are listed, which will be used in the following sections.

M = The cycle index set, i.e. $M = \{1, 2, \dots, m\}$;

D_1 = The phase set of the first ring in the dual ring signal controller in our case study, $D_1 = \{3, 4, 1, 2\}$;

D_2 = The phase set of the first ring in the dual ring signal controller in our case study, $D_2 = \{7, 8, 5, 6\}$;

C = The cycle length (sec);

TTA = The time of the local clock when the train triggers the preemption, or the preemption initiation time (sec);

PD = Preemption duration (sec);

$n_i(\cdot,\cdot)$ = The number of waiting vehicles along the *i*-th phase after the preemption, it is a function of TTA and PD (veh);

a_i = The arrival rate of traffic along the *i*-th phase (veh/sec);
d_i = The departure rate of traffic along the *i*-th phase (veh/sec);
$g_{i,1}$ = The green start along the *i*-th phase on the local clock (sec);
$g_{i,2}$ = The green clear point along the *i*-th movement on the local clock (sec). If the queue is cleared, then $g_{i,2} = \left[n_i(TTA, PD) + d_i \cdot g_{i,1}\right]/(d_i - a_i)$, else, $g_{i,2} = g_{i,3}$;
$g_{i,3}$ = The green end along the *i*-th phase on the local clock (sec);
G_i^{max} = The maximum green along the *i*-th phase on the local clock (sec);
G_i^{min} = The minimum green along the *i*-th phase on the local clock (sec);
y_i = The yellow duration along the *i*-th phase on the local clock (sec);
r_i = The red clearance along the *i*-th phase on the local clock (sec);
p_j^k = The *k*-th phase in the *j*-th ring;

Since the goal is to minimize the overall traffic delay at the signalized intersection near the grade crossing after the preemption, it is important to quantify the overall traffic delays. As shown in either Figure 3.16 or Figure 3.17, a_i (the slope of line AC in Figure 3.18) represents the arrival rate of vehicles (veh/sec) while d_i (the slope of line FH in Figure 3.19) denotes the vehicle departure rate. Therefore, the shadow area represents the overall delays (in veh*sec) that vehicles may undergo along a certain phase within a cycle for two cases: 1) the queue is cleared at the end of green, and 2) the queue remains when the green terminates. Based on the fundamental geometric knowledge, the shadow area (e.g. the one in Figure 3.16) can be calculated as explained in Figure 3.18 and Figure 3.19. Therefore,

$$\text{Area}_{\text{shadow}} = (\text{Area}_{\text{ABC}} + \text{Area}_{\text{ABDE}}) - \left(\text{Area}_{\text{FGH}} + \text{Area}_{\text{FJKG}} + \text{Area}_{\text{JLDK}}\right)$$

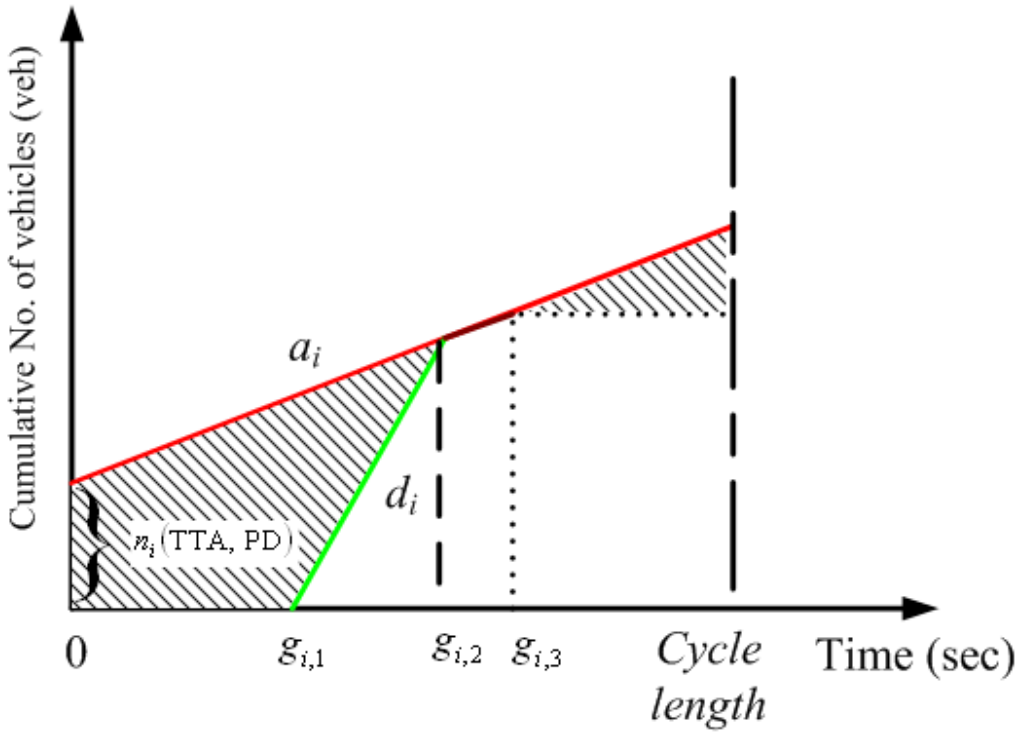

Figure 3.16: Illustration of delay calculation where queue is cleared

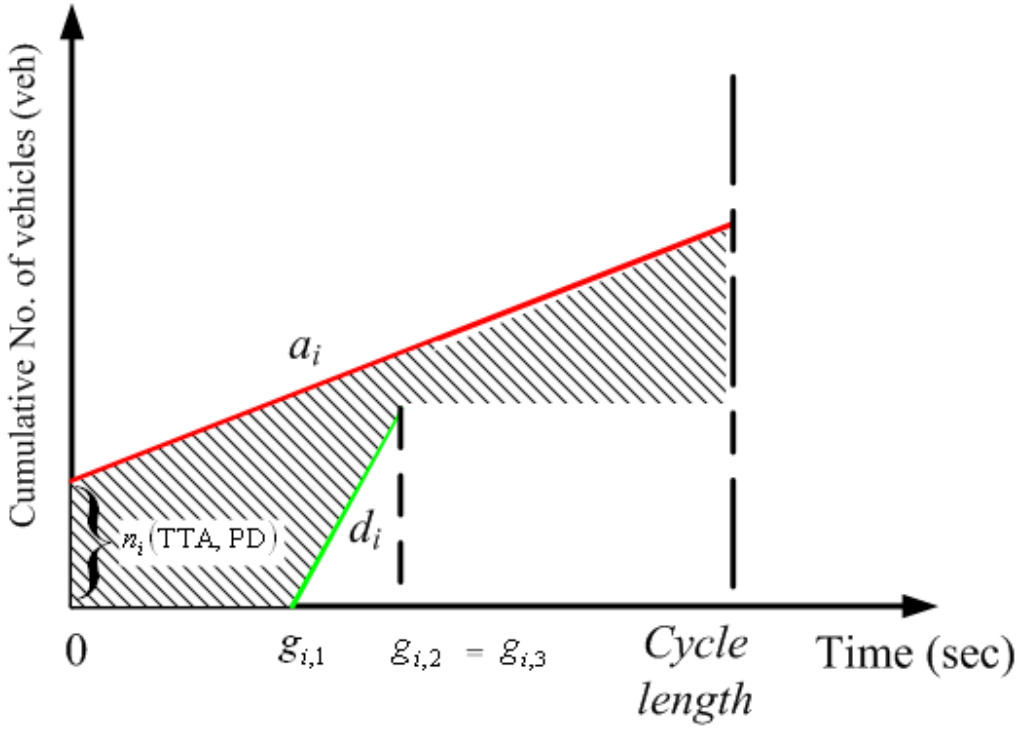

Figure 3.17: Illustration of delay calculation where queue is not cleared

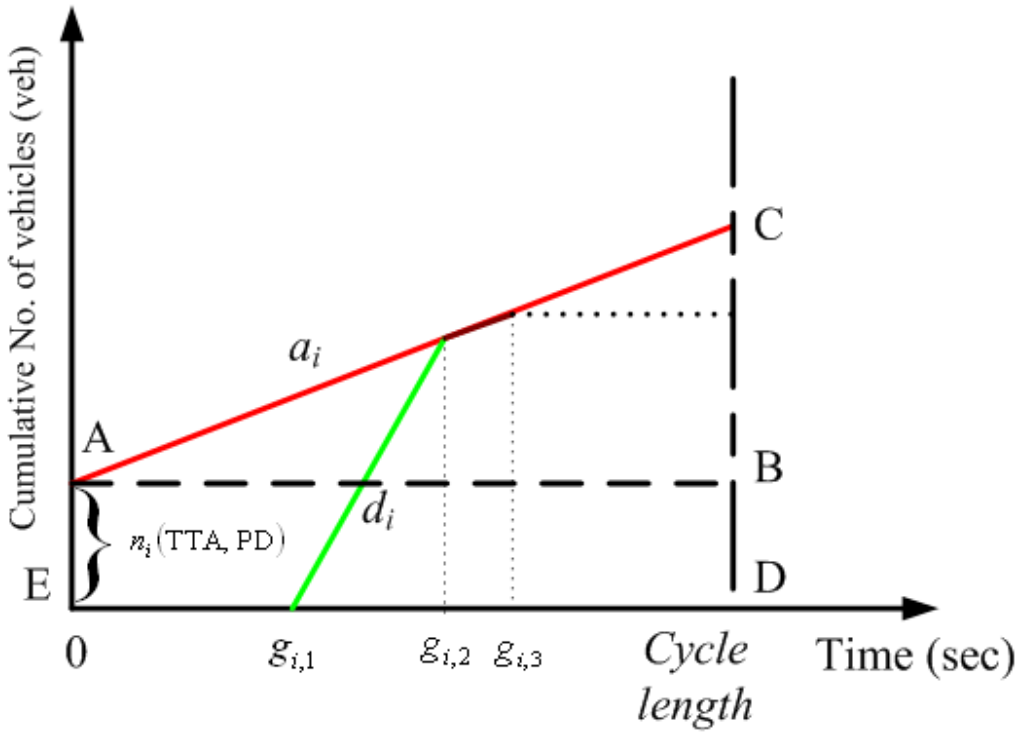

Figure 3.18: Illustration I of the shadow area calculation for Figure 3.16

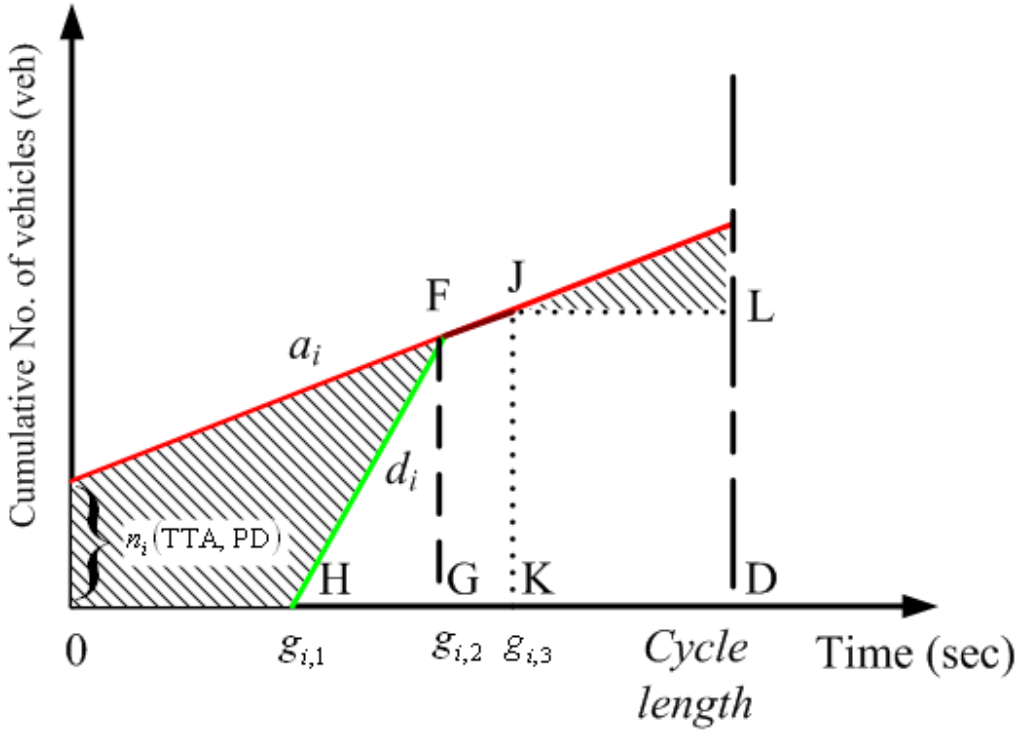

Figure 3.19: Illustration II of the shadow area calculation for Figure 3.16

3.3.2.2 Constraints

Most of the constraints come from the mechanism of the dual-ring signal controller, such as the sequence of phases, the barrier constraint and the bound on adjustable parameters. The sequence of phases is dependent on the specific site. For example, in the model shown below, there are eight phases and the lag phases are 2, 4, 6, and 8. The ring-phase diagram is as shown in Figure 1.6. However, modifications on constraints can be easily made for other phase sequences. For safety, the designed length of each green phase should not exceed the maximum green, but must be longer than the minimum one.

3.3.2.3 Mixed-integer Quadratic Programming (MIQP)

Problem Formulation

Combining the performance index and the constraints, the problem is formulated into a mixed integer quadratic programming (MIQP) problem to minimize the overall traffic delays at the intersection near the grade crossing after the preemption by selecting $g_{i,1}$, $g_{i,2}$ and $g_{i,3}$ ($i \in D_j \; and \; j = 1, 2$). As mentioned before, the performance index represents the sum of traffic delay along each phase within one cycle after the preemption. The first two terms demonstrate the areas of 1 and 2 in Figure 3.18, respectively. The rest terms calculate the areas of 3 through 5 shown in Figure 3.19.

$$\min \sum_{j=1,2} \sum_{i \in D_j} \Big\{ n_i(TTA, PD) \cdot C + \frac{1}{2} \cdot a_i \cdot C^2 - \frac{1}{2} \cdot d_i \cdot \left(g_{i,2} - g_{i,1}\right)^2 - \frac{1}{2} \cdot \left[2 \cdot d_i \cdot \left(g_{i,2} - g_{i,1}\right) + a_i \cdot \left(g_{i,3} - g_{i,2}\right)\right] \cdot \left(g_{i,3} - g_{i,2}\right) - \left[d_i \cdot \left(g_{i,2} - g_{i,1}\right) + a_i \cdot \left(g_{i,3} - g_{i,2}\right)\right] \cdot \left(C - g_{i,3}\right) \Big\}$$

subject to

$$n_i(TTA, PD) - d_i \cdot \left(g_{i,2} - g_{i,1}\right) \leq 0 \qquad i \in D_j \; and \; j = 1, 2 \qquad (3\text{-}1)$$

$$d_i \cdot \left(g_{i,2} - g_{i,1}\right) - \left[n_i(TTA, PD) + a_i \cdot g_{i,2}\right] \leq 0 \qquad i \in D_j \; and \; j = 1, 2 \qquad (3\text{-}2)$$

$$g_{i,3} - g_{i,1} - G_i^{max} \leq 0 \qquad i \in D_j \; and \; j = 1, 2 \qquad (3\text{-}3)$$

$$g_{i,1} - g_{i,3} + G_i^{min} \leq 0 \qquad i \in D_j \; and \; j = 1, 2 \qquad (3\text{-}4)$$

$$g_{p_j^{k+1},1} - g_{p_j^k,3} - y_{p_j^k} - r_{p_j^k} = 0 \qquad j = 1,2, and\ k = 1,2,3 \qquad (3\text{-}5)$$

$$g_{p_j^1,1} - y_{p_j^4} - r_{p_j^4} = 0 \qquad j = 1,2 \qquad (3\text{-}6)$$

$$g_{p_1^1,1} - g_{p_2^1,1} = 0 \qquad and \qquad g_{p_1^3,1} - g_{p_2^3,1} = 0 \qquad (3\text{-}7)$$

$$g_{p_j^4,3} - C = 0 \qquad j = 1,2 \qquad (3\text{-}8)$$

$$0 \le g_{i,1} \le g_{i,2} \le g_{i,3} \le C \qquad i \in D_j\ and\ j = 1,2 \qquad (3\text{-}9)$$

Constraint (3-1) guarantees that vehicles will not wait for more than one cycle, and constraint (3-2) represents the restriction on the value that $g_{i,2}$ can take. Constraints (3-3) and (3-4) relate the safety concerns on minimum and maximum green for each phase. Constraints (3-5) – (3-6) are the connectivity (sequence) condition for phases in each ring, where p_j^k means the *k*-th phase in the *j*-th ring. Constraint (3-7) represents the barrier condition for the dual ring signal controller, which means that phase(s) must terminate their timing and cross the "barrier" together. Constraint (3-8) ensures the cycle length will not change. The last constraint shows the upper bound and lower bound for each decision variable, where $g_{i,1}'s$ and $g_{i,3}'s$ should be general integers.

3.4 Evaluation of Effectiveness and Benefits

Both numerical analysis and microscopic simulation are conducted to evaluate the effectiveness and benefits of the proposed adaptive signal control algorithm.

3.4.1 Numerical Analysis

Based on the proposed strategy, numerical analysis has been conducted for the following intersections: *I-5 Southbound Ramp @ Oceanside Blvd*. (Caltrans), *I-5 Northbound Ramp @ Oceanside Blvd.* (Caltrans), *College Ave @ Oceanside Blvd.* (City of Oceanside), *Enterprise @ Mission Rd.* (City of Escondido), *Andreasen Ave @ Mission Rd.* (City of Escondido), *Vista Village Dr. @ Olive* (City of Vista), *Vista Village Dr. @ Santa Fe Ave.* (City of Vista), *Main @ Santa Fe Ave.* (City of Vista), *Pala Dr. @ Escondido Ave.* (City of Vista) and *Phillips St. @ Escondido Ave.* (City of Vista). In this dissertation, not all the numerical results will be presented. However, readers of interest

can refer to the technical report [83].

Due to the preemption logic, the estimated queue length along each phase may vary with different time-to-arrival (TTA) of the SPRINTER rail transit on the local clock and different preemption duration under the assumption of uniformly deterministic traffic arrival and dissipation rates. Therefore, the optimal timings at each intersection may also vary with either the preemption initiation time on the local clock or the preemption duration.

In the numerical analysis, the performance index, i.e. the overall intersection delays within one cycle right after the preemption, is compared between the scenario under original signal timings and the one under proposed signal timings. Then the numerical analysis results are investigated site by site and illustrated by using 3-D diagrams.

3.4.1.1 Examples on Site-by-site Results

I-5 Southbound Ramp @ Oceanside Blvd.

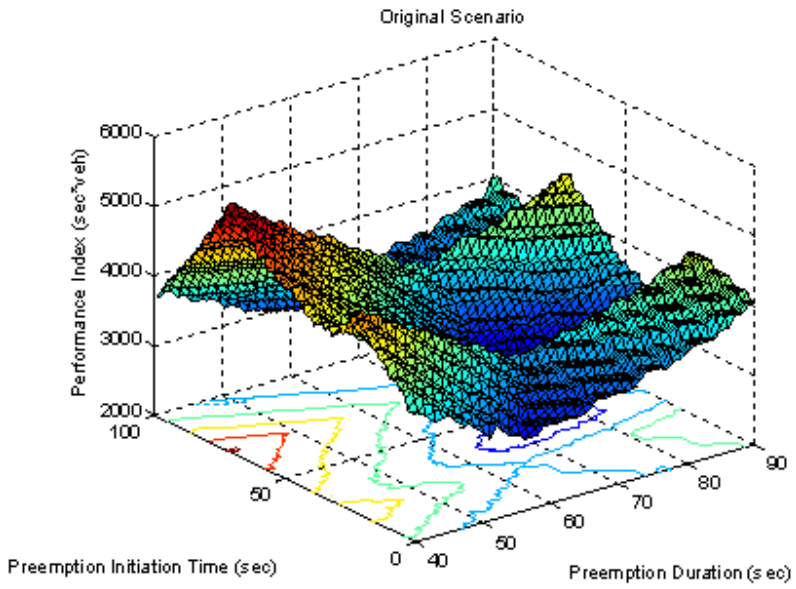

Figure 3.20: Performance index under original scenario at I-5 SB ramp @ Oceanside Blvd.

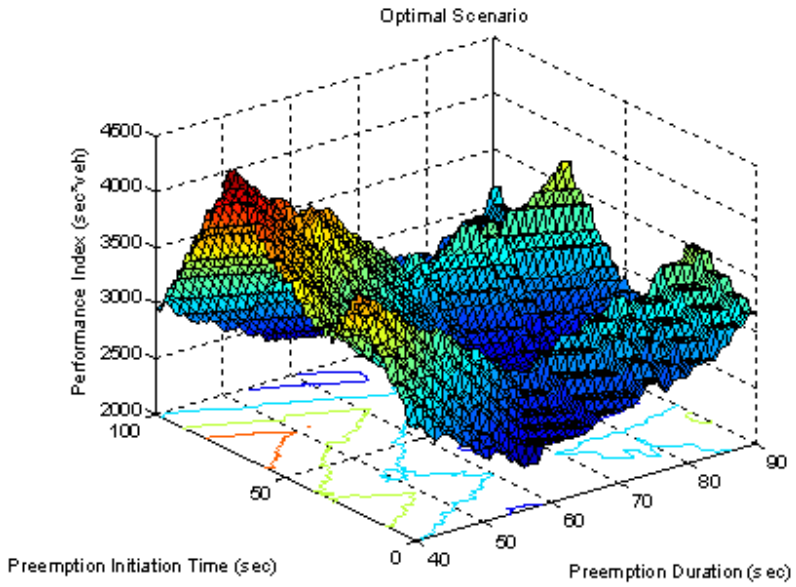

Figure 3.21: Performance index under proposed scenario at I-5 SB ramp @ Oceanside Blvd.

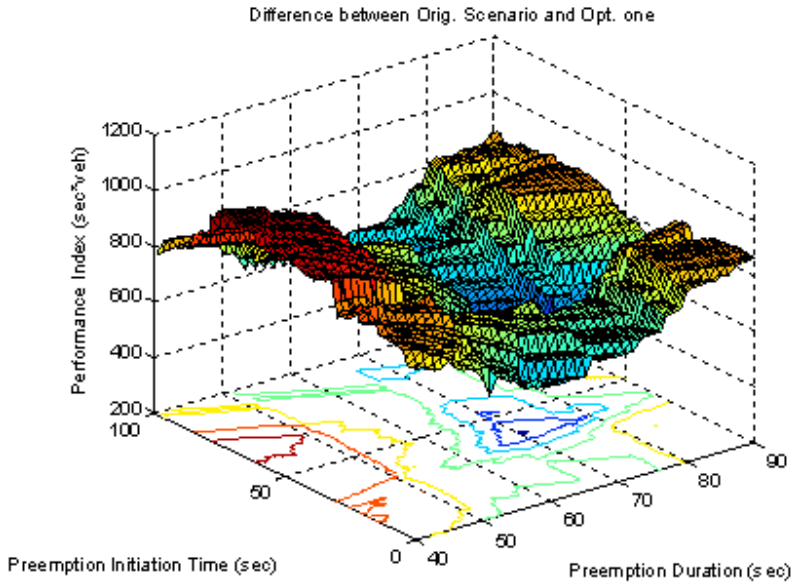

Figure 3.22: Absolute differences in performance index between original and proposed scenarios at I-5 SB ramp @ Oceanside Blvd.

As shown in Figure 3.20 through Figure 3.23, by implementing the optimal green splits, not only can the queue along each phase be cleared within one cycle after the preemption, but also the overall intersection delays can be reduced by as much as **24**

percent at the *I-5 Southbound Ramp @ Oceanside Blvd.* Furthermore, it can be observed that there is a **20.2 percent** reduction in traffic delay per vehicle **on average** during the cycle after preemption.

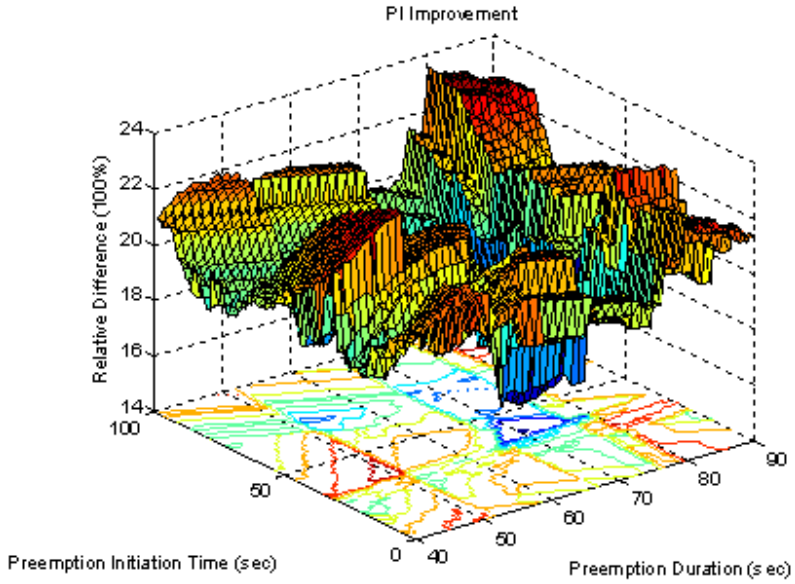

Figure 3.23: Relative differences in performance index between original and proposed scenarios at I-5 SB ramp @ Oceanside Blvd.

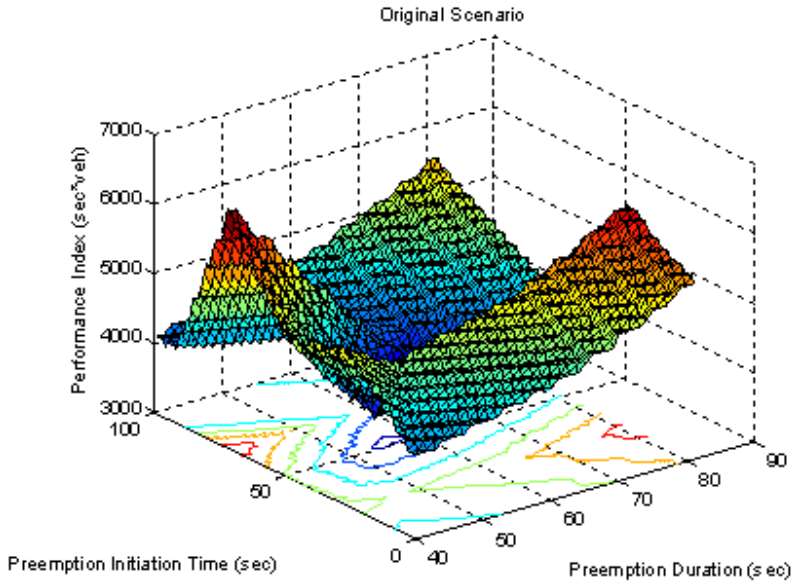

Figure 3.24: Performance index under original scenario at I-5 NB ramp @ Oceanside Blvd.

I-5 Northbound Ramp @ Oceanside Blvd

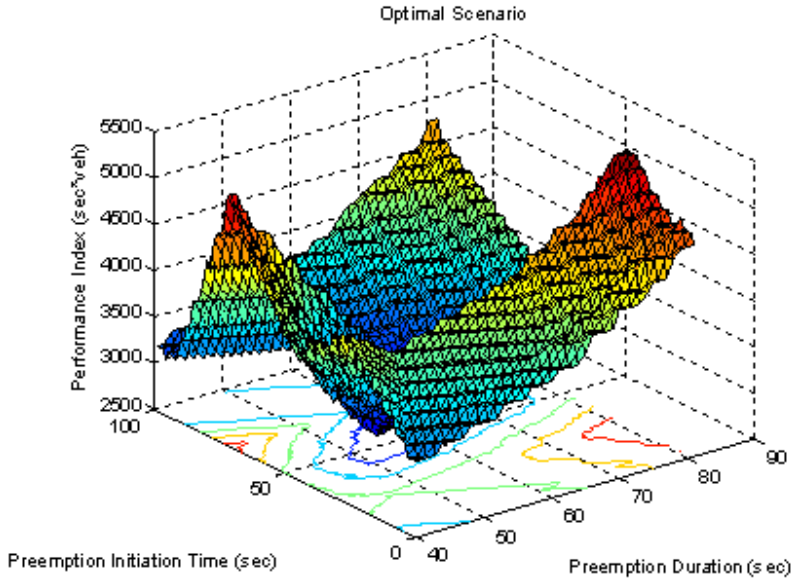

Figure 3.25: Performance index under proposed scenario at I-5 NB ramp @ Oceanside Blvd.

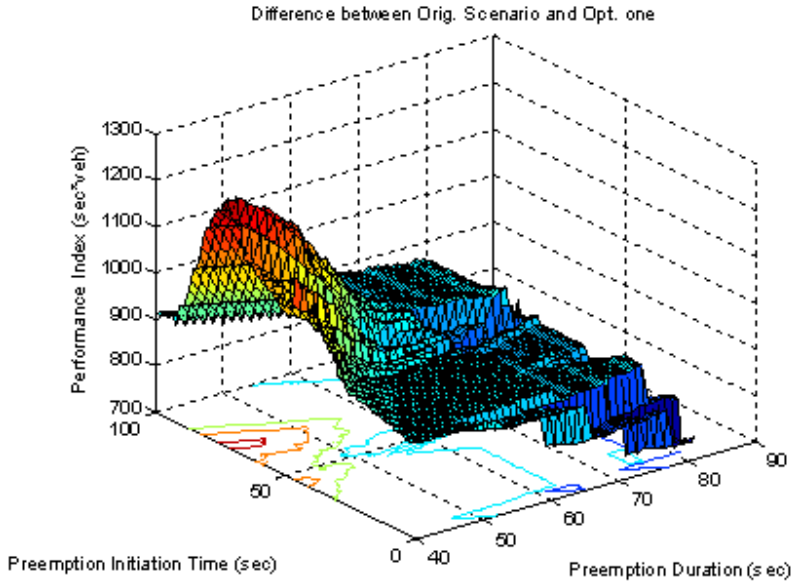

Figure 3.26: Absolute differences in performance index between original and proposed scenarios at I-5 NB ramp @ Oceanside Blvd.

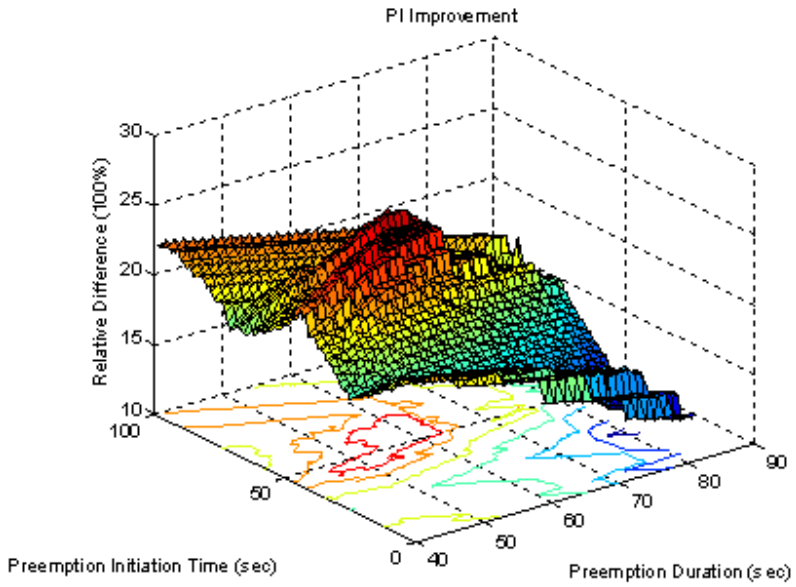

Figure 3.27: Relative differences in performance index between original and proposed scenarios at I-5 NB ramp @ Oceanside Blvd.

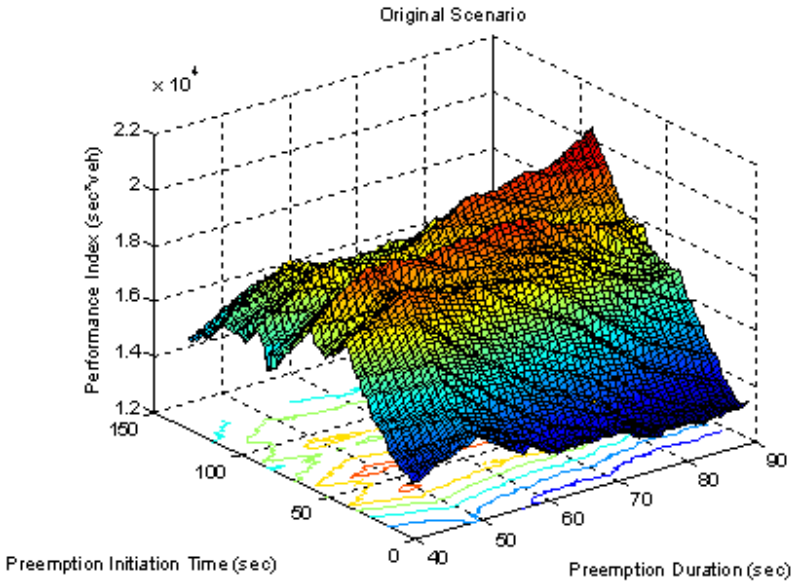

Figure 3.28: Performance index under original scenario at College Ave. @ Oceanside Blvd.

Similarly, from the numerical analysis, as much as a **25 percent** improvement in the performance index can be witnessed at *I-5 Northbound Ramp @ Oceanside Blvd.* if the proposed traffic signal timings are conducted instead of the original ones. Moreover, the results shown in Figure 3.24 through Figure 3.27 indicate that there is, **on average**,

approximately a **19.3 percent** improvement in the performance index.

College Ave. @ Oceanside Blvd.

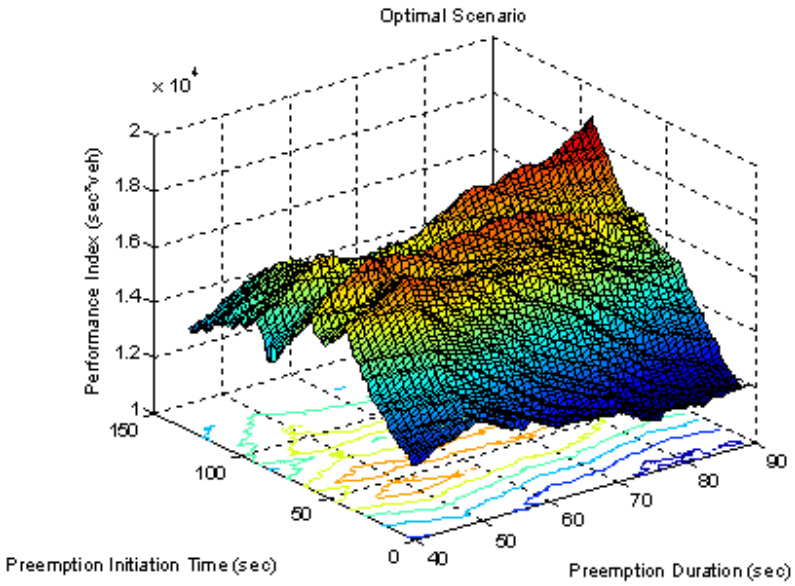

Figure 3.29: Performance index under proposed scenario at College Ave. @ Oceanside Blvd.

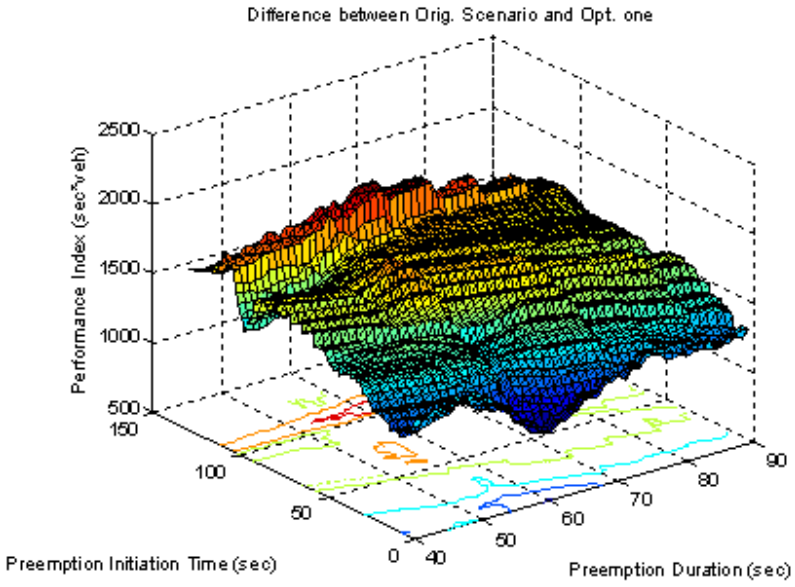

Figure 3.30: Absolute differences in performance index between original and proposed scenarios at College Ave. @ Oceanside Blvd.

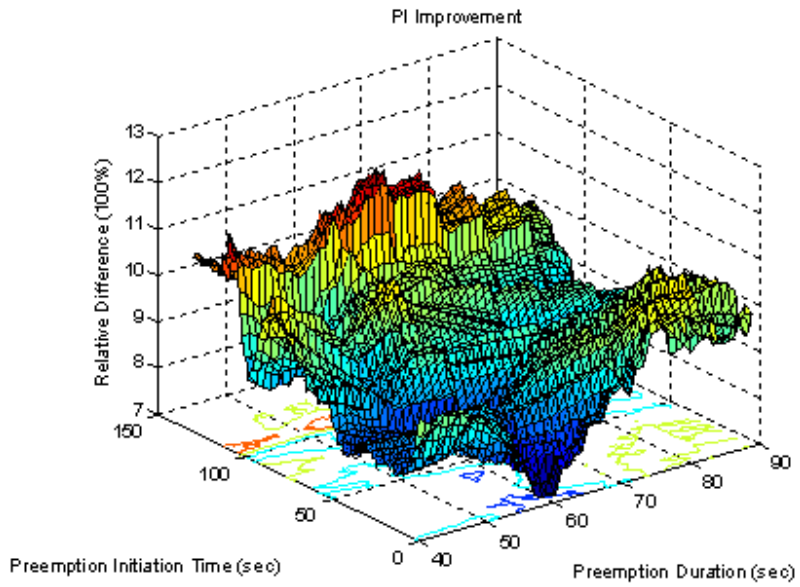

Figure 3.31: Relative differences in performance index between original and proposed scenarios at College Ave. @ Oceanside Blvd.

Based on the results shown in Figure 3.28 through Figure 3.31, there is around an **average** of **9.5 percent** drop, compared with the original scenario, in overall traffic delays at *College Ave. @ Oceanside Blvd.* if the proposed traffic signal timings are implemented. Numerical results of other sites will not be elaborated here.

3.4.1.2 Summary of Numerical Analysis

To get further insight into the numerical results from the proposed algorithm, not only are the overall intersection delays (within one cycle right after the preemption) compared under the original signal timings and under the proposed ones, but also the performance index (for one normal cycle) is calculated under the original signal timings without preemption. The results are illustrated in Figure 3.32 through Figure 3.37 for the study intersections mentioned above.

Based on the numerical analysis results, we note the following points:

- The overall intersection delays may vary with different combinations of preemption initiation time and preemption duration;
- As shown in figures, within one cycle after the preemption, the overall intersection delays under optimal timings are consistently less than those

under current timings;

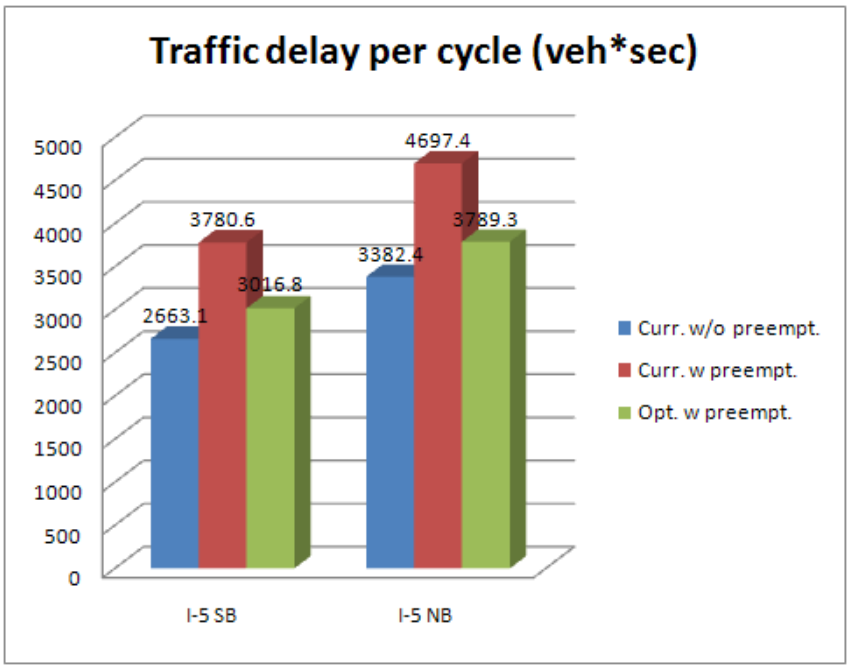

Figure 3.32: Comparison on numerical results at I-5 SB/I-5 NB @ Oceanside Blvd.

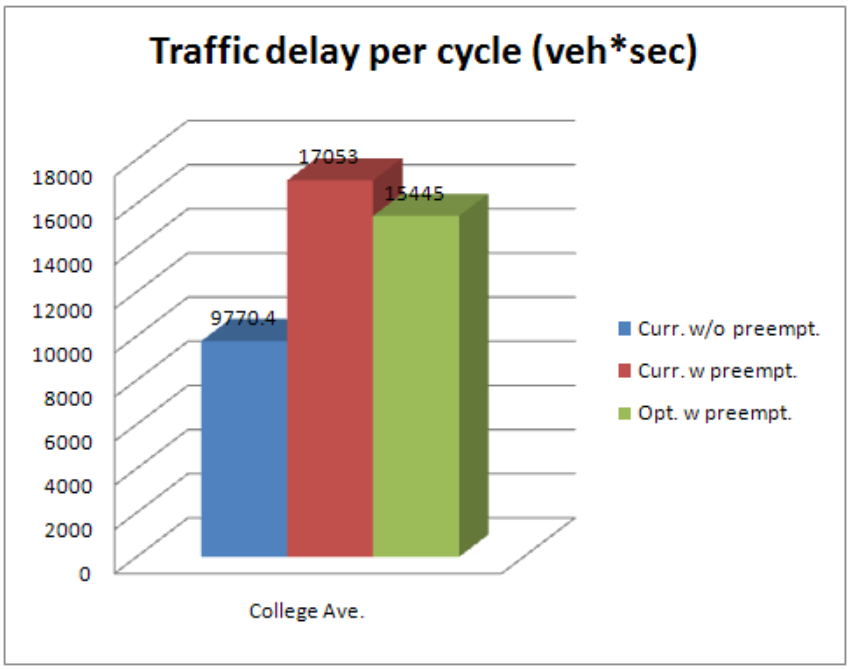

Figure 3.33: Comparison on numerical results at College Ave @ Oceanside Blvd.

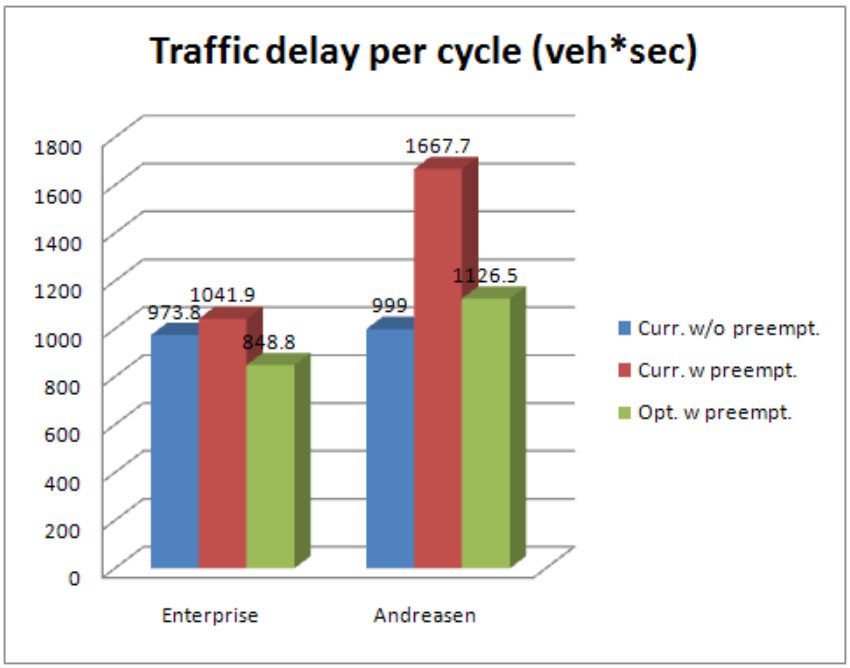

Figure 3.34: Comparison on numerical results at Enterprise/Andreasen @ Mission Rd.

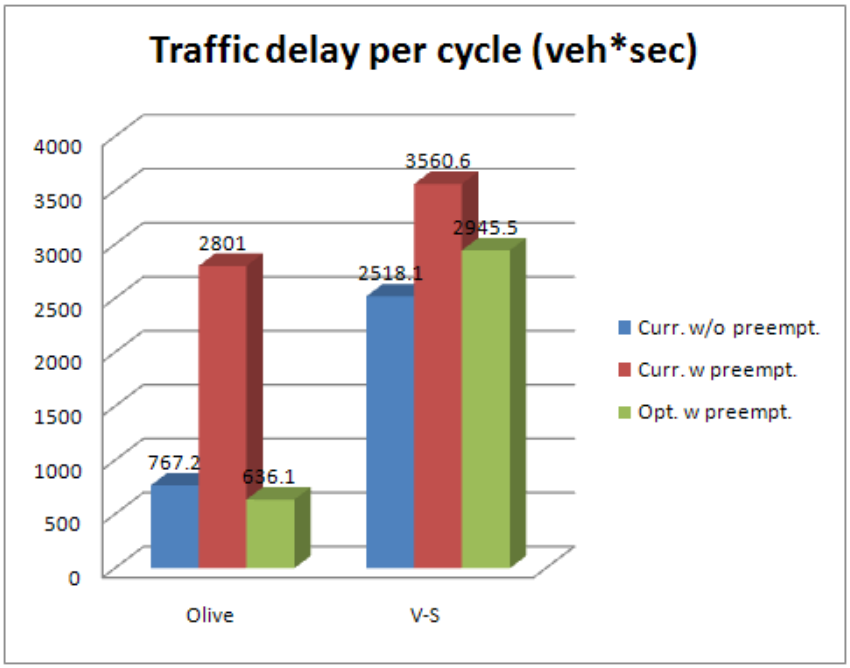

Figure 3.35: Comparison on numerical results at Olive/Santa Fe Ave. @ Vista Village Dr.

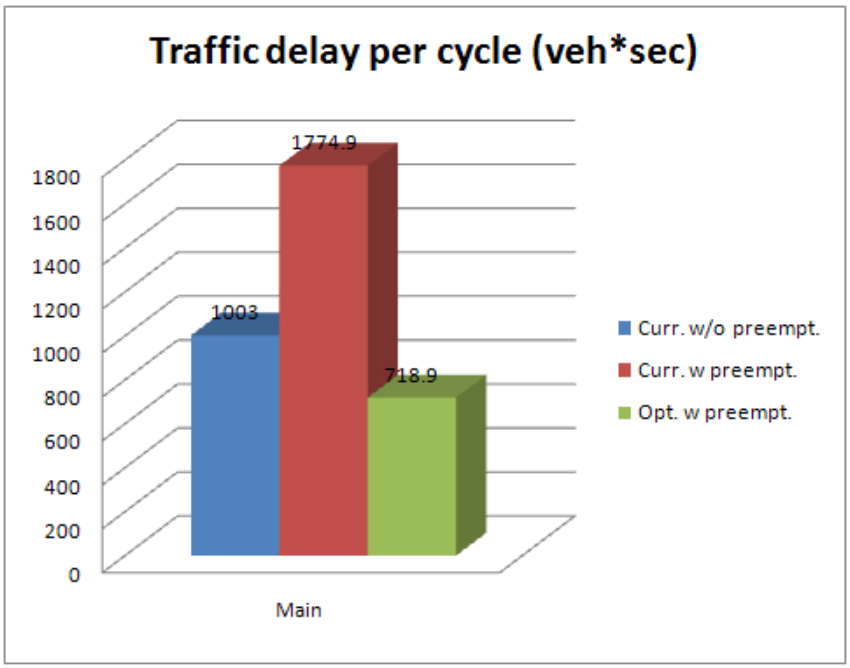

Figure 3.36: Comparison on numerical results at Olive/Santa Fe Ave. @ Vista Village Dr.

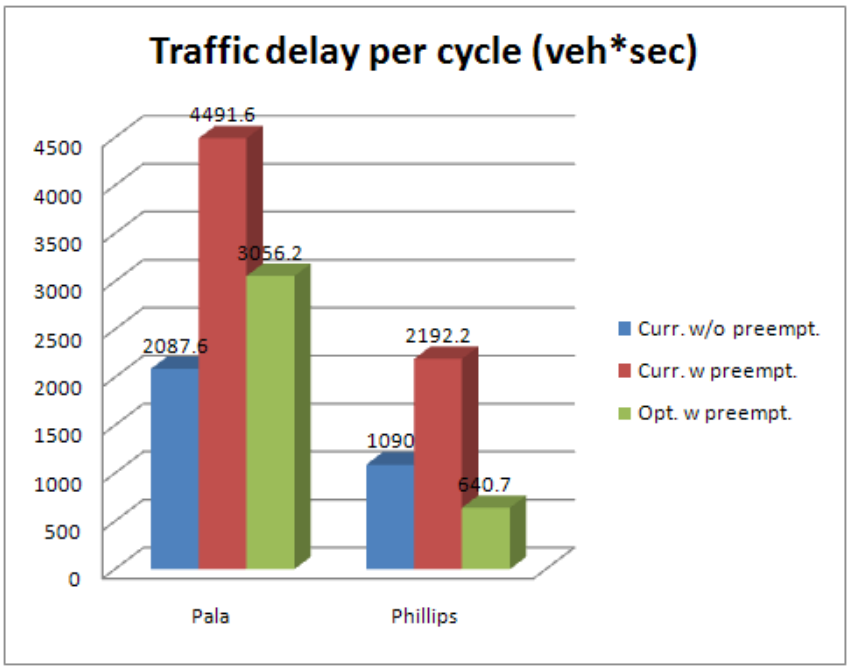

Figure 3.37: Comparison on numerical results at Pala/Phillips @ Escondido Ave.

- Note that in those 3-D diagrams, the preemption initiation time varies from 0 to the cycle end (w.r.t. the local clock) while the preemption duration

ranges from 40 sec to 90 sec. According to the preemption logic currently used in SPRINTER, such range of preemption duration is wide enough to cover almost all kinds of situations, even for those intersections with near-side stations;

- At *I-5 Southbound Ramp @ Oceanside Blvd.* and *I-5 Northbound Ramp @ Oceanside Blvd.*, although the overall intersection delays (under either original signal timings and/or proposed ones) may vary noticeably, the normalized performance index, i.e. traffic delay per vehicle within the impacted cycle, are very close, no matter in original scenario or optimal scenario (see Figure 3.32, Figure 3.43 and Figure 3.44);
- From Figure 3.32 to Figure 3.34, it can be observed that for the four study intersections: *I-5 SB/I-5 NB @ Oceanside Blvd*., *Andreasen @ Mission Rd.*, and *College Ave. @ Oceanside Blvd.*, there are non-trivial negative impacts on traffic under the original signal timings due to the interruption of SPRINTER train. However, such degradation can be greatly mitigated if the proposed signal timings are implemented, especially for the first three sites;
- An interesting finding from some figures (e.g. at *Enterprise @ Oceanside Blvd*.) is that better system performance can be obtained with preemption by optimization than that without preemption if the original signal timings are not well tuned.

3.4.2 Simulation Study

To further validate the proposed strategy as well as the numerical analysis, a simulation network was built up in PARAMICS Modeler V5.22. Two scenarios are simulated: one is under original signal timings while the other is under proposed signal timings. Figure 3.3 shows the whole SPRINTER railroad about 22 miles long, parallel to the Highway 78 corridor. This railroad traverses City of Oceanside, City of Vista, City of San Marcos and City of Escondido in San Diego's North County region. The snapshots of *I-5 Southbound Ramp @ Oceanside Blvd.*, *I-5 Northbound Ramp @ Oceanside Blvd.*, *Enterprise @ Mission Rd.*, *Andreasen @ Mission Rd.*, *Olive/Santa Fe Ave. @ Vista Village Dr./Main St.* and *Pala/Phillips @ Escondido Ave.* in the simulation model are illustrated in Figure 3.38 through Figure 3.42.

3.4.2.1 Setups of Simulation Model

Simulation Network

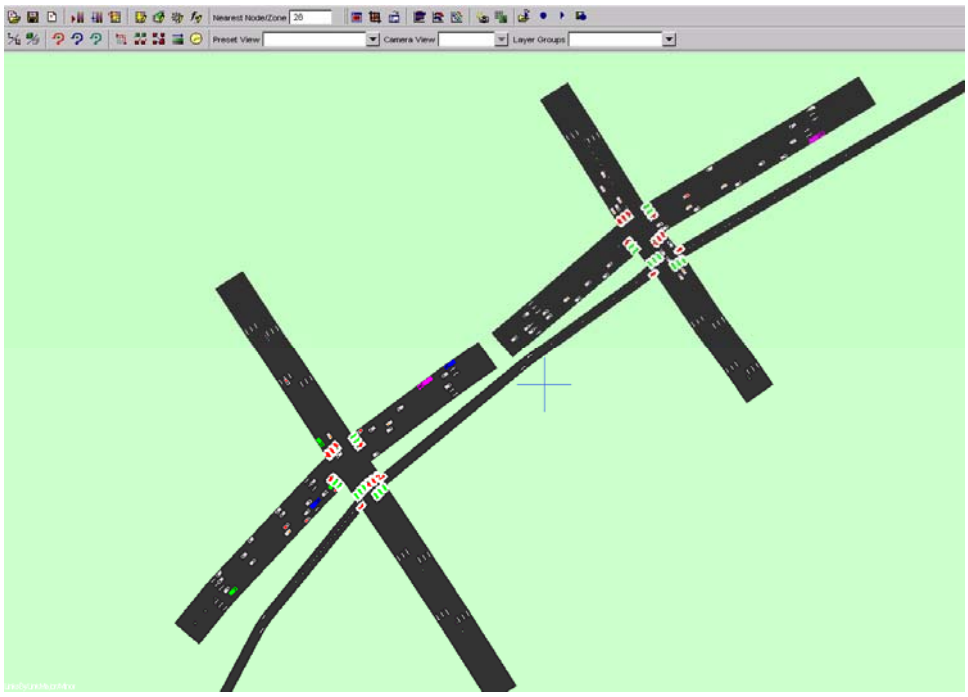

Figure 3.38: Snapshot of I-5 Ramp @ Oceanside Blvd. in PARAMICS

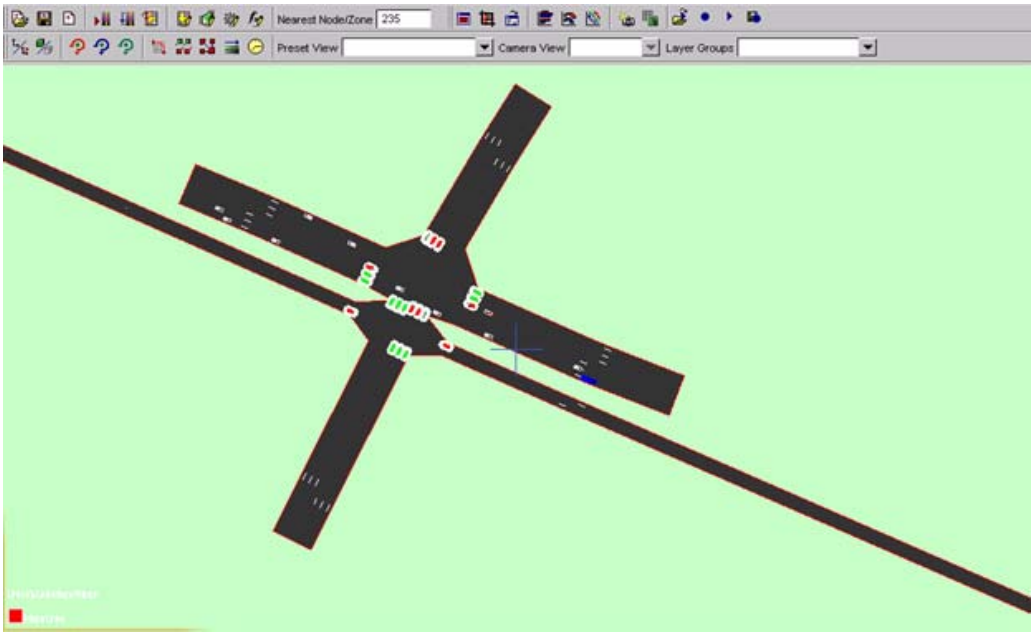

Figure 3.39: Snapshot of Enterprise @ Mission Rd. in PARAMICS

By manually capturing the coordinates of nodes from Google Earth, these nodes were linked to build up the SPRINTER railroad and roadways of study sites. According to documents from local jurisdiction, roadway characteristics and locations of stations

can then be determined.

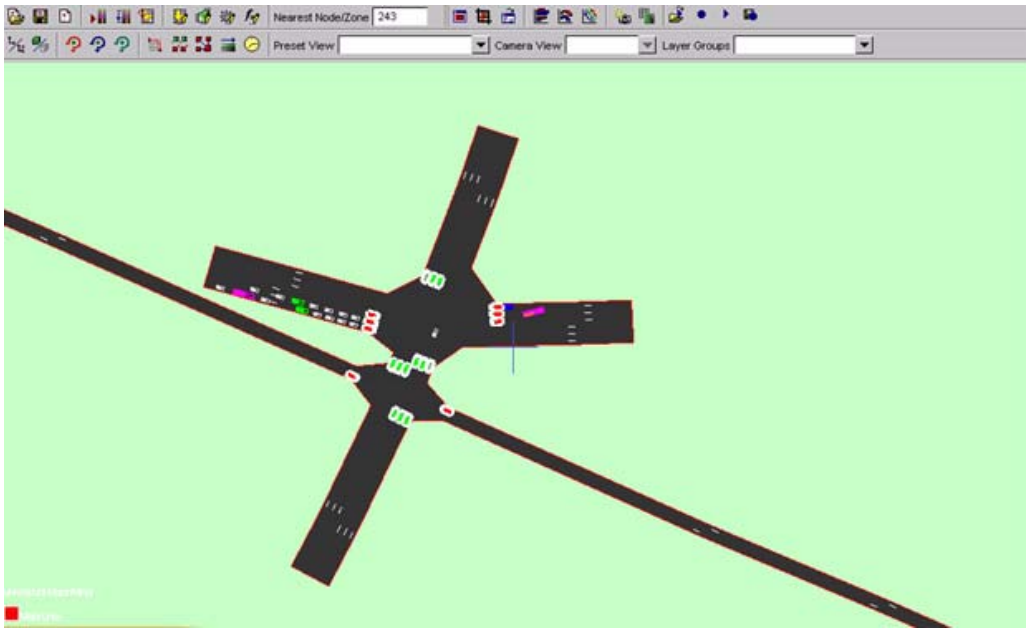

Figure 3.40: Snapshot of Andreasen @ Mission Rd. in PARAMICS

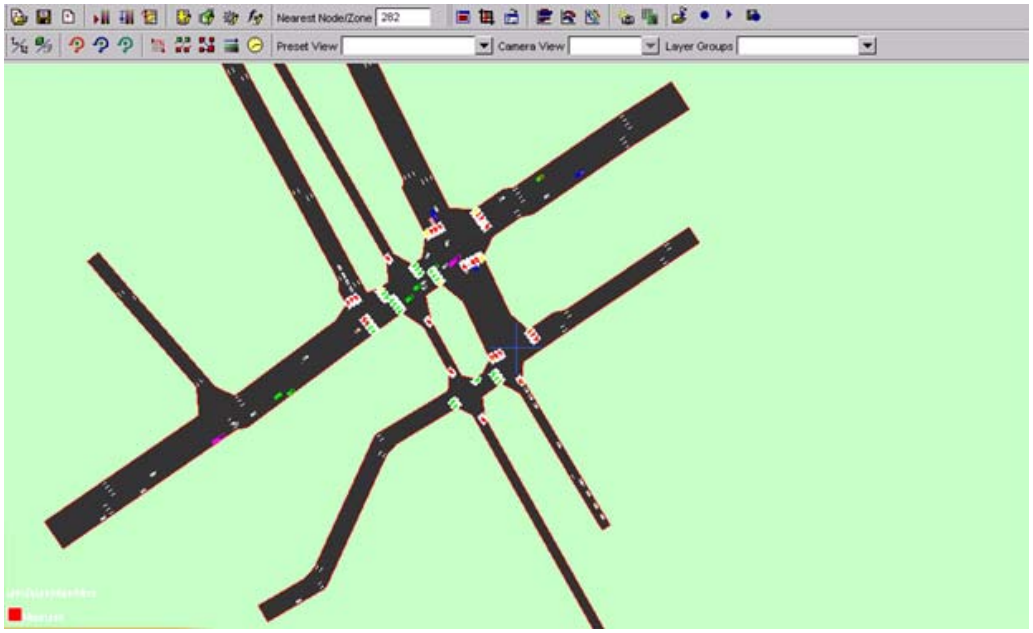

Figure 3.41: Snapshot of Olive/Santa Fe Ave. @ Vista Village Dr./Main in PARAMICS

Based on the traffic volume/ratio data and signal timing tables provided by each city, study sites in the simulation network are signalized and the associated origin-destination (O-D) matrices are coded. Parameters for the operation of SPRINTER

rail transits are input into the simulation model according to the information available from SPRINTER webpage, including physical/dynamical parameters of rail transit vehicles and the SPRINTER online schedule.

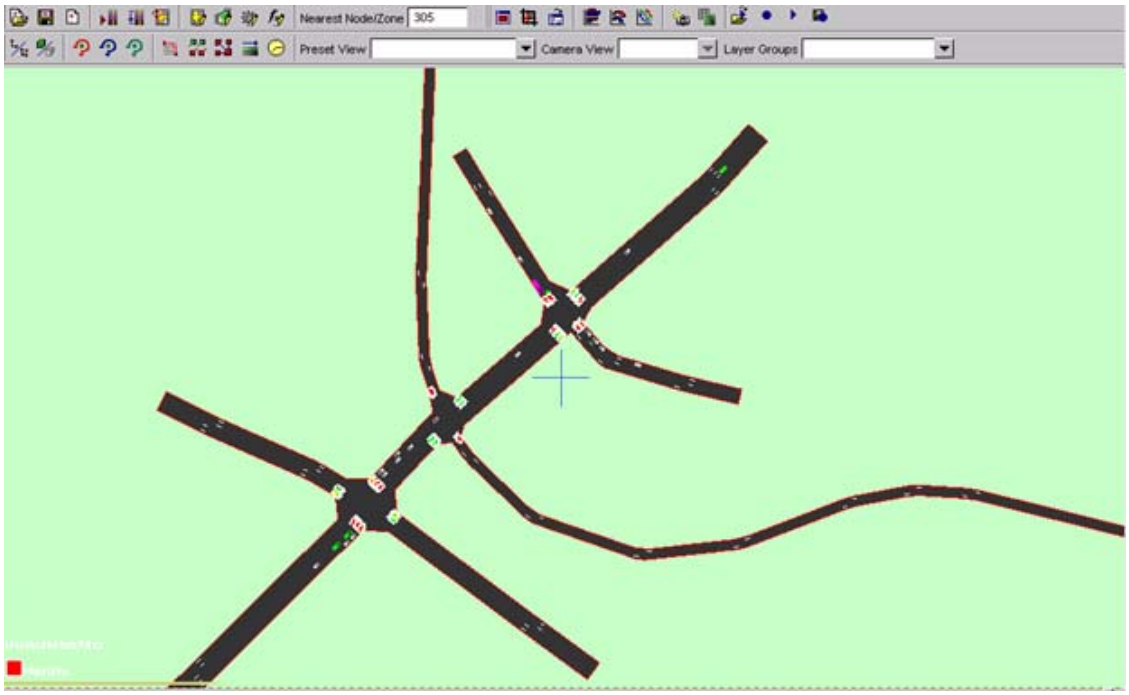

Figure 3.42: Snapshot of Pala/Phillips @ Escondido Ave. in PARAMICS

Simulation Time Settings

In the simulation, the morning peak hours of a typical weekday, i.e. from 06:00 a.m. to 09:00 a.m., are selected as the testing time intervals. Within this simulation time period, the first eastbound SPRINTER train starts from Oceanside Transit Center at 06:03 a.m. while the first westbound SPRINTER train starts from Escondido Transit Center at the same time. The average trip time is about 53 minutes and the headway is around 30 minutes along each bound. Therefore, there are totally 12 trips (6 trips along each bound) during 3 hours of simulation time. In addition, the step length of simulation time is set as 0.1 second.

Codes in the Simulation Model

Besides the setups of simulation network, it is necessary to program, such as APIs, to implement the proposed strategy in PARAMICS. Basically speaking, there are three types of codes:

- **Preemption Logic Related**. PARAMICS Modeler itself does not provide the dedicated public transit (PT) preemption logic function. However, by

coding ‘plans’ and ‘phases’ files to call the vehicle actuated signal (VAS) function which is self-contained in PARAMICS suite, SPRINTER train preemption can be implemented with a certain degree of flexibility, such as preemption duration. For example, at *I-5 Southbound Ramp @ Oceanside Blvd.* and *I-5 Northbound Ramp @ Oceanside Blvd.*, user-defined preemption duration, 50 sec, was coded due to the fact that the train speed almost keeps constant in simulation and there is no ***near-side station*** around these two grade crossings.

- **Adaptive Signal Timing Related**. At our study sites, traffic signal controllers are running fixed timings during the simulation in the original scenario. However, in the proposed scenario, traffic signal timings adapt to not only when the train initiates the preemption, but also how long the preemption lasts, which requires the actuated signals API functions to be coded. Relying on the detection of a train’s movements, the optimization algorithm is triggered right after the train clears the grade crossing.
- **Data Collection Related**. To obtain MOEs and compare overall intersection delays between the original scenario and the proposed scenario at those study sites, “virtual” detector loops and data collection API functions are also coded to obtain the delay for each vehicle passing the controlled (signalized) intersection. Simply speaking, for vehicle *i*,

$$Delay_i = T_{act} - \frac{D}{V_{ff}}$$

where T_{act} is the actual travel time for vehicle *i* between the upstream “virtual” loop and the downstream one; D is the distance between the upstream “virtual” loop and the downstream one; and V_{ff} is the user-defined free flow speed or link speed limit. Obviously, the delay calculated in this way is the overall controlled delay, including the vehicle’s acceleration/deceleration time, start-up loss time and stop time at a signal. On the other hand, SPRINTER trains’ location data and all “virtual” loop detector data are also collected for the purpose of model calibration.

3.4.2.2 Simulation Results

By analyzing all 12 trips (6 trips each bound), or say 12 preemption impacted cycles at each study sites, simulation results are obtained under two different scenarios – original signal timings and proposed signal timings. The comparison results between these two scenarios are presented below.

I-5 Southbound Ramp @ Oceanside Blvd.

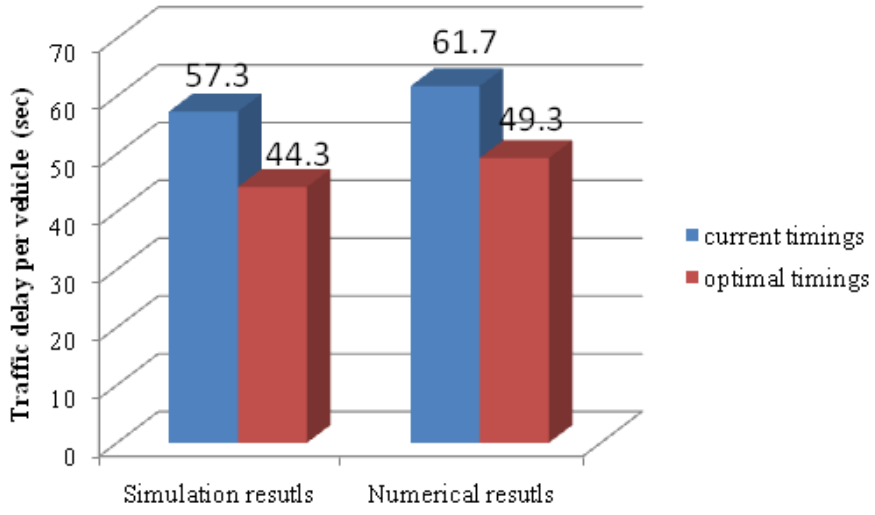

Figure 3.43: Comparison results on simulation and numerical analysis at I-5 Southbound Ramp @ Oceanside Blvd where preemption duration is 50 seconds.

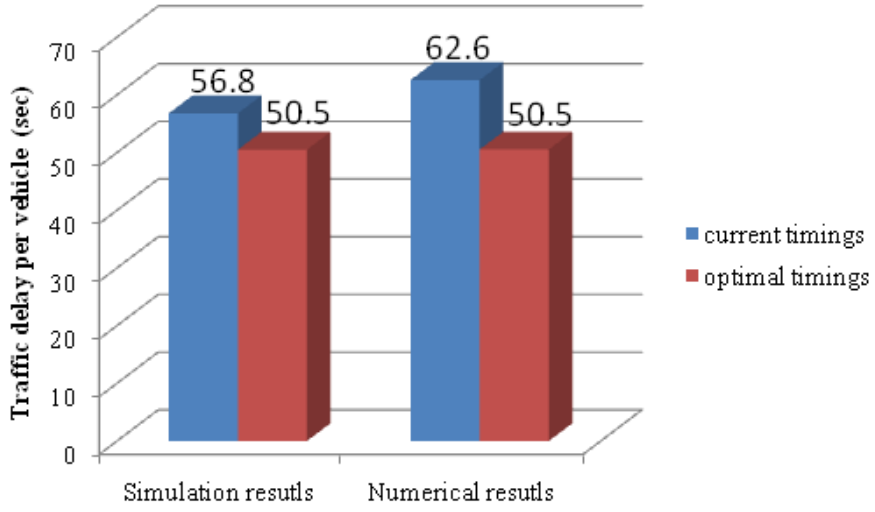

Figure 3.44: Comparison results on simulation and numerical analysis at I-5 Northbound Ramp @ Oceanside Blvd where the preemption duration is 50 seconds.

Based on the simulation results, the average delay per vehicle is **57.3 sec** and **44.3 sec** under original signal timings and proposed ones, respectively. Numerical

analysis is further validated against the simulation test, and the difference between the numerical results and simulation ones under different scenarios are **7.7 percent** and **11.3 percent**, respectively. As shown in Figure 3.43, the improvement in the simulation test is **22.7 percent** by using optimal timings, while the average vehicle delay decreases as much as **20.1 percent** in the numerical analysis.

I-5 Northbound Ramp @ Oceanside Blvd.

Simulation results shows that the average delay per vehicle is **56.8 sec** and **50.5 sec** under original signal timings and proposed ones, respectively. The difference between the numerical results and simulation ones under different scenarios are **10.2 percent** and **0.0 percent**, respectively. As can be seen in Figure 3.44, the improvement is as low as **11.1 percent** by using optimal timings in simulation, but the average vehicle delay decreases as much as **19.3 percent** in numerical analysis. Explanation of simulation results for other sites will not be elaborated in this thesis, but the results are shown in graphical form. Readers of interest can refer to [83] for detailed explanation.

Enterprise @ Mission Rd.

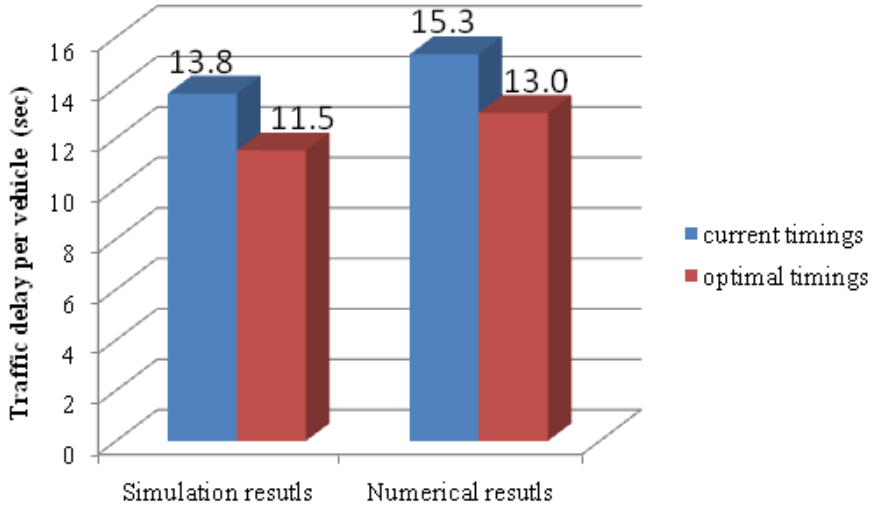

Figure 3.45: Comparison results on simulation and numerical analysis at Enterprise @ Mission Rd. where preemption duration is 50 seconds.

Andreasen Dr. @ Mission Rd.

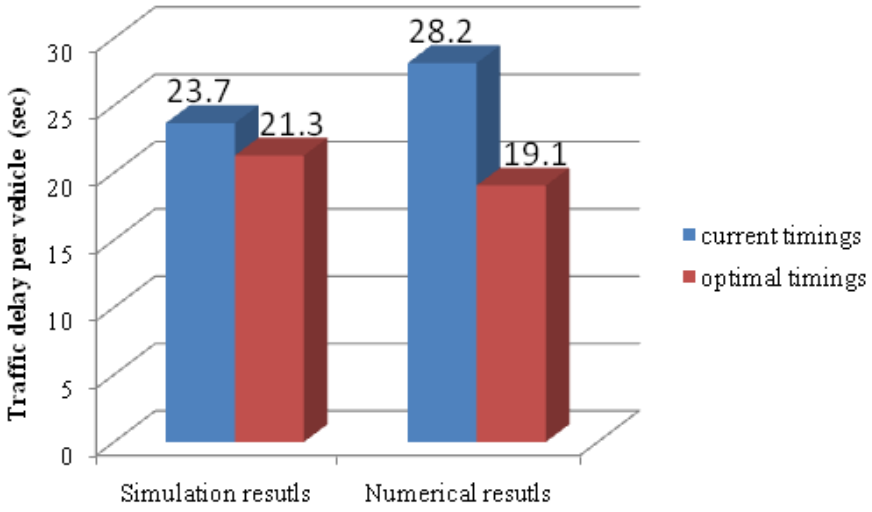

Figure 3.46: Comparison results on simulation and numerical analysis at Andreasen Dr. @ Mission Rd. where the preemption duration is 50 seconds.

Olive @ Vista Village Dr.

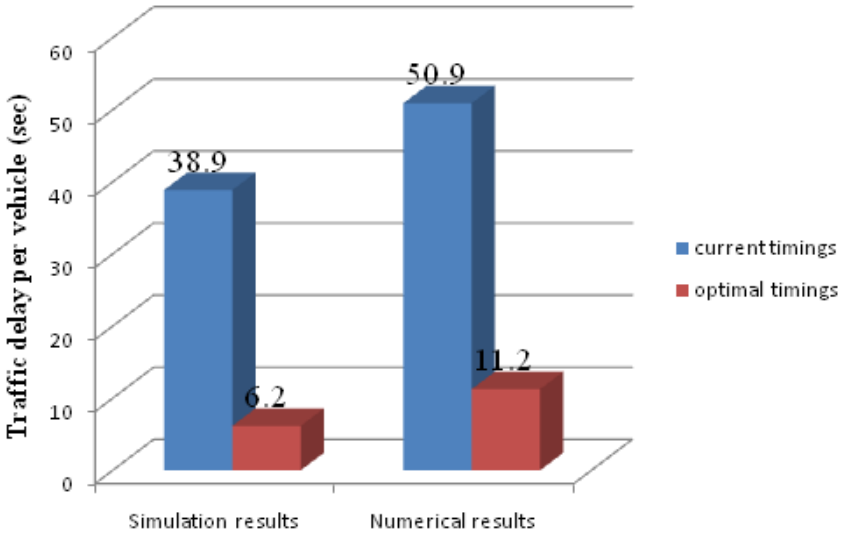

Figure 3.47: Comparison results on simulation and numerical analysis at Olive @ Vista Village Dr. where the preemption duration is 50 seconds.

Santa Fe Ave. @ Main

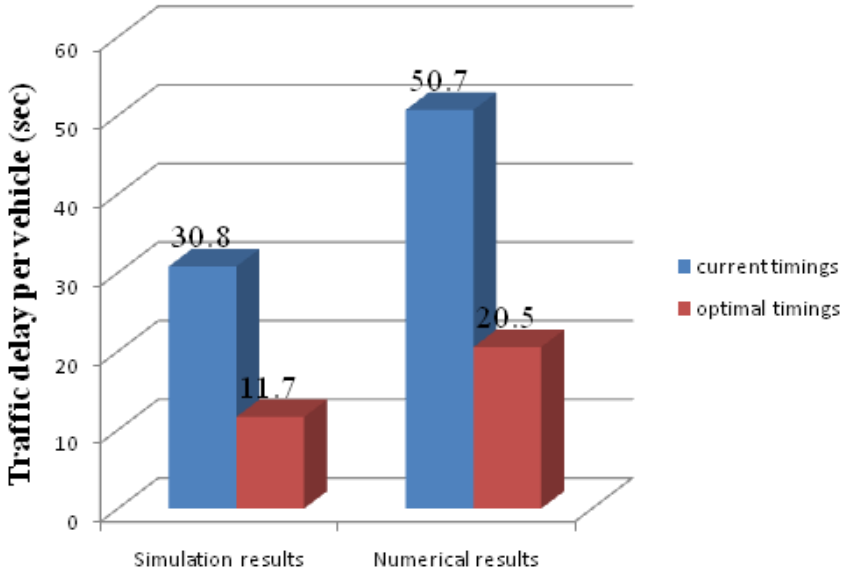

Figure 3.48: Comparison results on simulation and numerical analysis at Santa Fe Ave. @ Main where the preemption duration is 50 seconds.

Santa Fe Ave. @ Vista Village Dr.

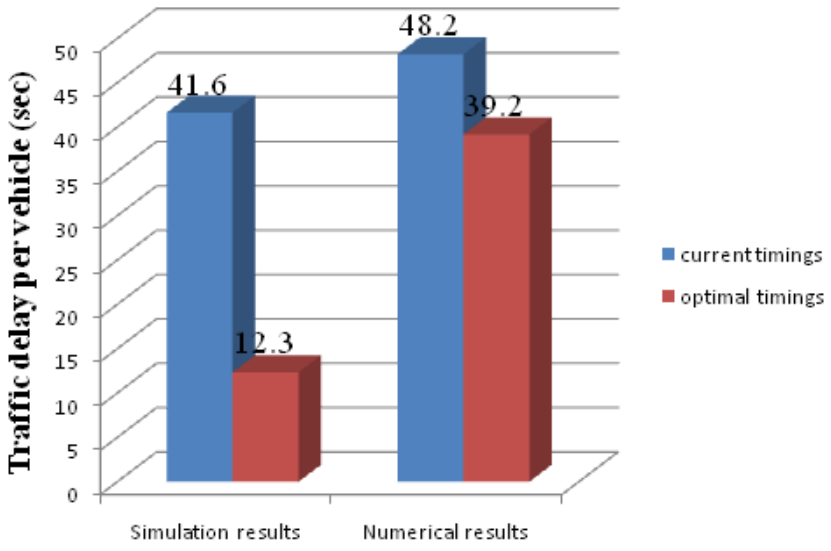

Figure 3.49: Comparison results on simulation and numerical analysis at Santa Fe Ave. @ Vista Village Dr. where the preemption duration is 50 seconds.

Pala @ Escondido Ave.

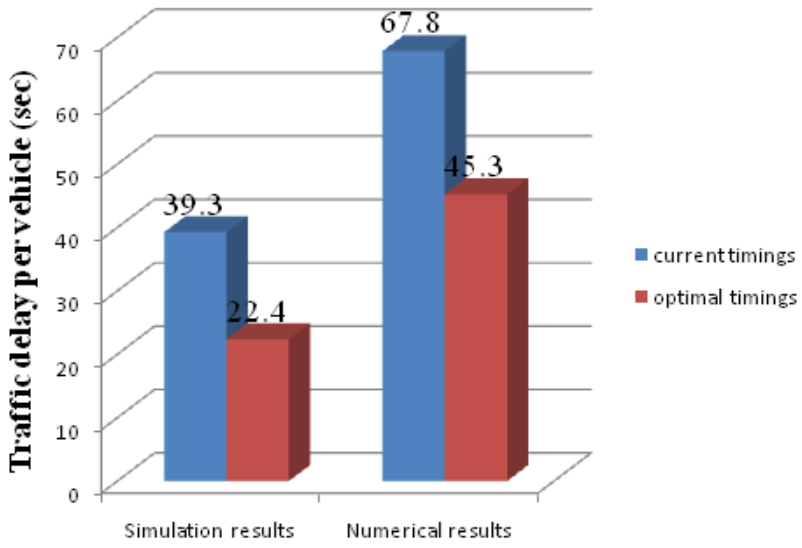

Figure 3.50: Comparison results on simulation and numerical analysis at Pala @ Escondido Ave. where the preemption duration is 50 seconds.

Phillips @ Escondido Ave.

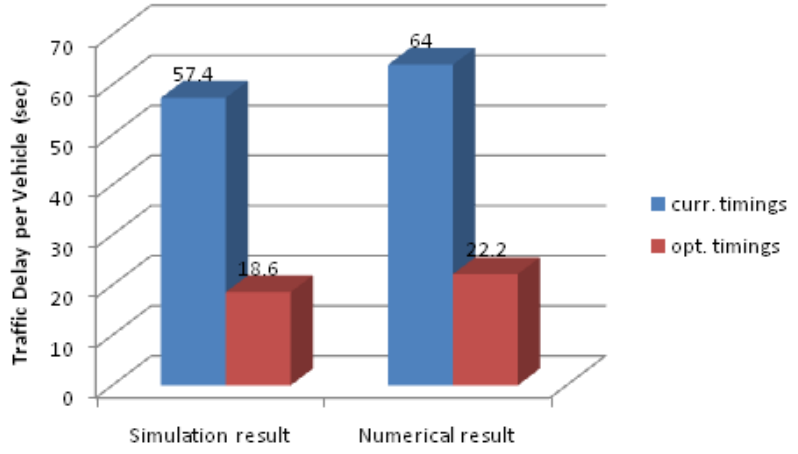

Figure 3.51: Comparison results on simulation and numerical analysis at Phillips @ Escondido Ave. where the preemption duration is 50 seconds.

3.5 Further Discussion and Conclusion

3.5.1 Multiple-Cycle Optimization

When the traffic volumes along the coordinated phases increase and/or the preemption duration is too long, a feasible solution might not be obtained if the optimization model mentioned in previous sections is applied. The infeasibility is due to the ambition to clear the queue that is backed up during preemption within a single cycle. By modification, a more generalized MIQP problem can be formulated, i.e. a multi-cycle version of traffic signal optimization problem. The queue does not necessarily have to be cleared up within one cycle, but within $m(\geq 2)$ cycles, where m is a user-defined value. In addition, it is evident that the optimization model presented in the previous section is a special case of the multi-cycle version of optimization problem where $m = 1$. The generalized MIQP problem is formulated as follows:

$$\begin{aligned} min \sum_{j=1,2} \sum_{k \in D_j} \Big\{ & n_k(TTA, PD) \cdot m \cdot C + \frac{1}{2} \cdot a_k \cdot (m \cdot C)^2 \\ & - \sum_{i \in M} \Big\{ \frac{1}{2} \cdot d_k \cdot \left(g_{i,k,2} - g_{i,k,1}\right)^2 + \frac{1}{2} \\ & \cdot \left[2 \cdot d_k \cdot \left(g_{i,k,2} - g_{i,k,1}\right) + a_k \cdot \left(g_{i,k,3} - g_{i,k,2}\right)\right] \cdot \left(g_{i,k,3} - g_{i,k,2}\right) \\ & + \left[d_k \cdot \left(g_{i,k,2} - g_{i,k,1}\right) + a_k \cdot \left(g_{i,k,3} - g_{i,k,2}\right)\right] \cdot \left(m \cdot C - g_{i,k,3}\right) \Big\} \Big\} \end{aligned}$$

subject to

$$n_k(TTA, PD) + a_k \cdot (i-1) \cdot C - d_k \cdot \sum_{l=1}^{i} \left(g_{l,k,2} - g_{l,k,1}\right) \leq 0 \qquad \forall i \in M, j = 1,2, and\ k \in D_j \qquad (3\text{-}10)$$

$$d_k \cdot \sum_{l=1}^{i} \left(g_{l,k,2} - g_{l,k,1}\right) - \left[n_k(TTA, PD) + a_k \cdot g_{i,k,2}\right] \leq 0 \qquad \forall i \in M, j = 1,2, and\ k \in D_j \qquad (3\text{-}11)$$

$$g_{i,k,3} - g_{i,k,1} - G_k^{max} \leq 0 \qquad \forall i \in M, j = 1,2, and\ k \in D_j \qquad (3\text{-}12)$$

$$g_{i,k,1} - g_{i,k,3} + G_k^{min} \leq 0 \qquad \forall i \in M, j = 1,2, and\ k \in D_j \qquad (3\text{-}13)$$

$$g_{i,p_j^{k+1},1} - g_{i,p_j^k,3} - y_{p_j^k} - r_{p_j^k} = 0$$

$$\forall i \in M, j = 1,2, and\ k = 1,2,3 \qquad (3\text{-}14)$$

$$g_{i,p_j^1,1} - g_{i-1,p_j^4,3} - y_{p_j^4} - r_{p_j^4} = 0$$

$$\forall i \in M, and\ j = 1,2 \qquad (3\text{-}15)$$

$$g_{0,p_j^4,3} = 0 \qquad \forall j = 1,2 \qquad (3\text{-}16)$$

$$g_{i,p_1^1,1} - g_{i,p_2^1,1} = 0 \ \ and\ g_{i,p_1^3,1} - g_{i,p_2^3,1} = 0 \qquad \forall i \in M \quad (3\text{-}17)$$

$$g_{i,p_j^4,3} - i \cdot C = 0 \qquad \forall i \in M, and\ j = 1,2 \qquad (3\text{-}18)$$

$$(i-1) \cdot C \leq g_{i,k,1} \leq g_{i,k,2} \leq g_{i,k,3} \leq i \cdot C$$

$$\forall i \in M, j = 1,2, and\ k \in D_j \qquad (3\text{-}19)$$

Similar to the single-cycle version, the performance index demonstrates the calculation of the shadow area shown in Figure 3.18 and Figure 3.19.

Constraint (3-15) represents the connectivity condition for the last phase of (*i*-1)-th cycle and the first phase of *i*-th cycle. The explanation of other constraints and definition of decision variables are similar to the single-cycle version, except the following:

$g_{i,j,1}$ = The green start along the *j*-th phase on the local clock in the *i*-th cycle after the preemption (sec);

$g_{i,j,2}$ = The green clear point along the *j*-th phase on the local clock in the *i*-th cycle after the preemption (sec);

$g_{i,j,3}$ = The green end along the *j*-th phase on the local clock in the *i*-th cycle after the preemption (sec).

3.5.2 Coordination with Other Signals

Based on the meetings in NCTD and correspondence with traffic engineers from City of Vista, there are a lot of concerns on the traffic signal coordination after preemption at the following sites in City of Vista: *Olive @ Vista Village Dr.*, *Santa Fe Ave. @ Vista Village Dr.* and *Santa Fe Ave @ Main.* In addition, these three signalized

intersections are very close to one another and the distance between two grade crossings is only 90 meters. If the traffic signals are not coordinated, long queues and inefficiency of traffic network around these sites may be expected. In addition, the queue backed up along an intersection may spill over to the upstream intersection.

An extension of integration of traffic signal coordination may be developed by introducing a green band into the problem formulation. More details of the green band are available in [51]. To take into account the coordination of several signalized intersections around grade crossings and simplify the problem statement, the following assumptions need to be made:

- The stretch of interest consists of ***three*** traffic signals and these signals are coordinated under the normal operation. For more signals, the model can be extended but may be much more complex.
- Only the intermediate signal will be interrupted by train preemption.
- No signal timings need to be adjusted for the other two signals except the intermediate one.
- Movement 2 and 6 of the intermediate intersection are coordinated, where movement 2 represents bound 1, and movement 6 represents bound 2 in the following problem formulation
- The studied intersection is running fixed timings;
- The arrival rate, a_i for each phase is uniform and constant;
- The dissipation rate, d_i, is constant and relates to the road characteristics;
- In most cases, the controlled time-span is one cycle after the train clears the grade-crossing, but the model can also be extended to the controlled time-span of multiple cycles.
- The traffic condition is under-saturated.
- Vehicles accelerate and decelerate instantaneously, which implies that all drivers behave identically, i.e. they follow average driving patterns.
- In timing optimization, the sequence of phases (lead/lag relationship) keeps untapped during the controlled time-span.
- The dual-ring signal controller is used for traffic control at the intersection.

More decision variables related to the green band formation will be used in the following:

$GB_{i,j}^{S}$ = The start point of green band along *j*-th bound at the *i*-th intersection;

$GB_{i,j}^{E}$ = The end point of green band along *j*-th bound at the *i*-th intersection;

$Tr_{k,k+1}$ = The travel time from the *k*-th intersection to the (*k*+1)-th intersection.

Under the assumptions listed above, a modified MIQP model can be written as:

$$min \sum_{j=1,2} \sum_{i \in D_j} \Big\{ n_i(TTA, PD) \cdot C + \frac{1}{2} \cdot a_i \cdot C^2 - \frac{1}{2} \cdot d_i \cdot \left(g_{i,2} - g_{i,1}\right)^2 - \frac{1}{2}$$
$$\cdot \left[2 \cdot d_i \cdot \left(g_{i,2} - g_{i,1}\right) + a_i \cdot \left(g_{i,3} - g_{i,2}\right)\right] \cdot \left(g_{i,3} - g_{i,2}\right)$$
$$- \left[d_i \cdot \left(g_{i,2} - g_{i,1}\right) + a_i \cdot \left(g_{i,3} - g_{i,2}\right)\right] \cdot \left(C - g_{i,3}\right) \Big\} - \omega_1$$
$$\cdot \left(GB_{2,1}^E - GB_{2,1}^S\right) - \omega_2 \cdot \left(GB_{2,2}^E - GB_{2,2}^S\right)$$

subject to

$$n_i(TTA, PD) - d_i \cdot \left(g_{i,2} - g_{i,1}\right) \leq 0 \qquad i \in D_j \; and \; j = 1,2 \quad (3\text{-}20)$$

$$d_i \cdot \left(g_{i,2} - g_{i,1}\right) - \left[n_i(TTA, PD) + a_i \cdot g_{i,2}\right] \leq 0 \quad i \in D_j \; and \; j = 1,2 \quad (3\text{-}21)$$

$$g_{i,3} - g_{i,1} - G_i^{max} \leq 0 \qquad i \in D_j \; and \; j = 1,2 \quad (3\text{-}22)$$

$$g_{i,1} - g_{i,3} + G_i^{min} \leq 0 \qquad i \in D_j \; and \; j = 1,2 \quad (3\text{-}23)$$

$$g_{p_j^{k+1},1} - g_{p_j^k,3} - y_{p_j^k} - r_{p_j^k} = 0 \qquad j = 1,2, and \; k = 1,2,3 \quad (3\text{-}24)$$

$$g_{p_j^1,1} - y_{p_j^4} - r_{p_j^4} = 0 \qquad j = 1,2 \quad (3\text{-}25)$$

$$g_{p_1^1,1} - g_{p_2^1,1} = 0 \qquad and \qquad g_{p_1^3,1} - g_{p_2^3,1} = 0 \quad (3\text{-}26)$$

$$GB_{k+1,1}^S - GB_{k,1}^S = Tr_{k,k+1} \; and \; GB_{k+1,1}^E - GB_{k,1}^E = Tr_{k,k+1} \qquad k = 1,2 \quad (3\text{-}27)$$

$$GB_{k,2}^S - GB_{k+1,2}^S = Tr_{k+1,k} \; and \; GB_{k,2}^E - GB_{k+1,2}^E = Tr_{k+1,k} \qquad k = 1,2 \quad (3\text{-}28)$$

$$g_{k,2,1} + O_k + C \cdot n_{k,1} \leq GB_{k,1}^S, GB_{k,1}^E \leq g_{k,2,3} + O_k + C \cdot n_{k,1} \qquad k = 1,2,3 \quad (3\text{-}29)$$

$$g_{k,6,1} + O_k + C \cdot n_{k,2} \leq GB_{k,2}^S, GB_{k,2}^E \leq g_{k,6,3} + O_k + C \cdot n_{k,2} \qquad k = 1,2,3 \quad (3\text{-}30)$$

$$GB_{k,l}^E - GB_{k,l}^S \geq GB_l^{min} \qquad k = 1,2,3 \; and \; l = 1,2 \quad (3\text{-}31)$$

$$g_{p_j^4,3} - C = 0 \qquad j = 1,2 \quad (3\text{-}32)$$

$$0 \leq g_{i,1} \leq g_{i,2} \leq g_{i,3} \leq C \qquad i \in D_j \; and \; j = 1,2 \quad (3\text{-}33)$$

Compared with the single-cycle version, the performance index also includes terms of weighted widths of green bands for both directions,

$$\omega_1 \cdot \left(GB_{2,1}^{E} - GB_{2,1}^{S}\right) + \omega_2 \cdot \left(GB_{2,2}^{E} - GB_{2,2}^{S}\right).$$

where ω_1 and ω_2 are user-defined weighting factors.

Constraints (3-27) – (3-30) are feasibility conditions for green bands of both bounds along the stretch of interest. Users can define the minimum width of green band of each bound by changing the right hand side (RHS) of constraint (3-31). Constraint (3-32) ensures that the cycle length will not change. Similarly, explanations of other constraints and definitions of most of decision variables are the same as those in the single-cycle version of optimization problem.

3.5.3 Conclusion

This chapter focuses on the application of AVL-based adaptive signal control system on an isolated signalized intersection by elaborating on the case of improving post-preemption traffic signal operation efficiency at the intersection near a grade-crossing. Simulation results at the studied sites under current signal timings endorse jurisdictions' concerns. A mixed integer quadratic programming (MIQP) problem is formulated to minimize the overall intersection delays within one cycle after the preemption. Computation experiments demonstrate the validity of the proposed ASC strategy. Further simulation tests are conducted to compare the system performance under the original signal timings and the optimized ones.

Furthermore, the following points could be the continuing aspects of this study:

- **Robust optimization**. The estimation of queue length and calculation of traffic delay are highly dependent on traffic volumes, which cannot be constant and are hard to obtain accurately in practice. Therefore, the optimization results should be valid for not only specific values of traffic volume but also a larger range of traffic volumes.
- **Pre-preemption signal optimization**. Based on the information of both the train and motor vehicles, traffic signals should be optimized even before the preemption is triggered. This can further mitigate the potential congestion after the preemption.
- **Pedestrian and vehicle safety**. The safety concern is critical to the operation at highway/rail grade crossings. The adaptive signal control algorithm proposed in this chapter mainly focuses on relieving the traffic

congestion caused by the preemption. A combination of safety and efficiency of rail operation under preemption are more desirable.

Chapter 4

4. Application II: ASC along a Signalized Corridor – San Diego Trolley System

4.1 Introduction

In this chapter, the adaptive signal control algorithm is applied to transit priority systems which are mainly operating in the downtown areas. Section 4.2 provides the background of the project on the San Diego Trolley (SDT) System. To improve system performance metrics for the light rail transit (LRT), such as schedule adherence and delay reduction, without penalizing too much on the cross-street traffic, the adaptive signal optimization model is proposed in Section 4.3. To validate the model, numerical analysis is conducted along a section of C Street in the downtown of San Diego. Sensitivity analysis is presented in Section 4.4. In Section 4.5, the proposed algorithm is further evaluated by microscopic traffic simulation tests in PARAMICS. The last section discusses other issues which have raised in both lab testing and field testing.

4.2 Background

4.2.1 San Diego Trolley (SDT) System

Within the realm of priority, there are two different strategies: passive and active. Passive priority presets the signal timing to favor transit vehicles, whereas active priority adjusts signal timings upon the detection of a transit vehicle.

The San Diego Trolley (SDT) system has implemented passive priority in the downtown area for about 15 years (Figure 4.1). The system works as follows:

- The trolley dwells in the station till the beginning of the next green light at the first downstream signal;
- The trolley departs within 5 sec after the beginning of the green light.

- If the departure window is missed, the trolley must wait till the beginning of the next green light;
- As long as the trolley leaves the station during the departure window, it will receive green lights at all of the downstream signals till it reaches the next station;
- The two-phase, fixed-time signal timing favorable to the trolley is always in place (no matter the trolley is present or not) and is fitted into a larger network of signals.

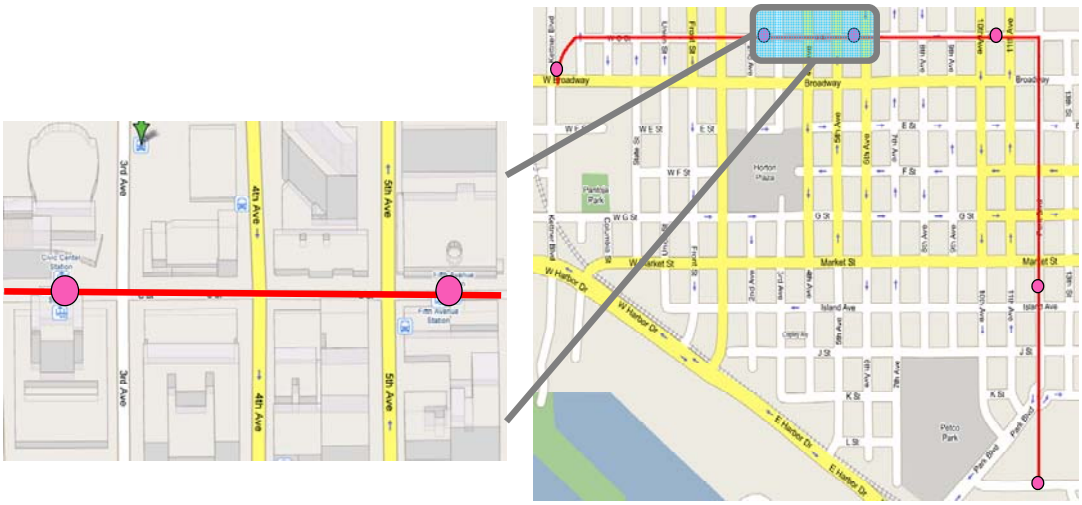

Figure 4.1: C St. and Park Blvd. in San Diego downtown where the passive priority is implemented

The trolley priority system has proven to be successful in increasing the efficiency of trolley operations through downtown San Diego [84]. Also, the system is a simple and easily implemented solution to the complex problem of accommodating motor vehicles, pedestrians and trolleys. However, there are still some concerns regarding this system. First, a significant train delay is experienced if the train operator is not ready to depart the station during the initial green light. Second, there is no clear indication for the departure window and the trolley operator have to guess in borderline situations, thus sometimes the trolley misses the window and hits a red light before reaching the next station. Third, a train waiting for the green light might block the following train from entering the station platform. In even worse situations, two trains could block one or more intersections and thus mess up the entire traffic flow. Finally, the passive priority strategy typically makes the overall intersection operation less efficient, in particular when traffic demand is high, because the signal settings still favor trolleys even if there are no transit vehicles present. Therefore, an active priority system is preferable to improve the efficiency of the whole system, including both trolleys and motor vehicles.

4.2.2 Proposed Adaptive Signal Control System

The proposed adaptive signal control system consists of four major components: train detector, train movement (including travelling and dwelling) predictor, priority request generator, and traffic signal controllers. The train detection means is the GPS based AVL system, but it can be also traditional point detection system, such as the loop detector.

The priority request generator is the "brain" of the proposed system. A trolley route is divided into several independent sections, each starting from a station and ending at the closest downstream station, as shown in Figure 4.1. Intersections between two adjacent stations belong to the same section. Within each section, three priority schemes based on train schedule adherence are designed below:

- When a trolley is running late, for example 3 minutes behind its schedule, scheme I with a timing optimization algorithm adapted to the movement of the trolley, which will be elaborated in the following section, is applied.
- When a trolley is running early or on-time, scheme II with pre-optimized signal timings is implemented.
- When there is no train approaching in the next cycle, the minimum green for pedestrians is provided along the trolley direction.

In essence, scheme II and III are rule based signal control algorithms which can be implemented by two sets of fixed-time signal plans. When the two schemes are triggered, the priority request generator just loads the appropriate signal plan on signal controllers. However, for scheme I, as shown in Figure 4.2, the priority request generator need to obtain the predicted time-to-arrival (TTA) at the downstream section by the movement predictor. If no priority request has been placed for the downstream section, the signal timing optimization algorithm will obtain new timing plans for all intersection of the downstream section. Finally, the priority request generator will send those optimized timing plans to signal controllers in the downstream section.

Unlike most of the existing transit signal priority systems, such as TTI's improved transition preemption strategy (ITPS) system [8] and PATH's adaptive transit signal priority (ATSP) system [55], the proposed system optimizes signal timings for multiple intersections or a signalized corridor rather than focusing on one isolated intersection. Furthermore, the system proposed here is not just dedicated to the transit operation, but to consider the overall performance of the traffic system as a whole. It should be also noted that although the system is initially designed for traffic signals under two-phased fixed-timing control (as shown in Figure 4.3), it can be also applied to those under semi-actuated or fully-actuated control. This thesis is not intended to discuss the

technical details of the system applicability on either 170/2070 controllers or NEMA controllers. But rather, the focus is on modeling a general problem and evaluating the system performances. Since the motivation of this study is to solve the aforementioned problems in the existing SDT system, some of the model assumptions are based on current situations in San Diego, they may be modified to fit other situations.

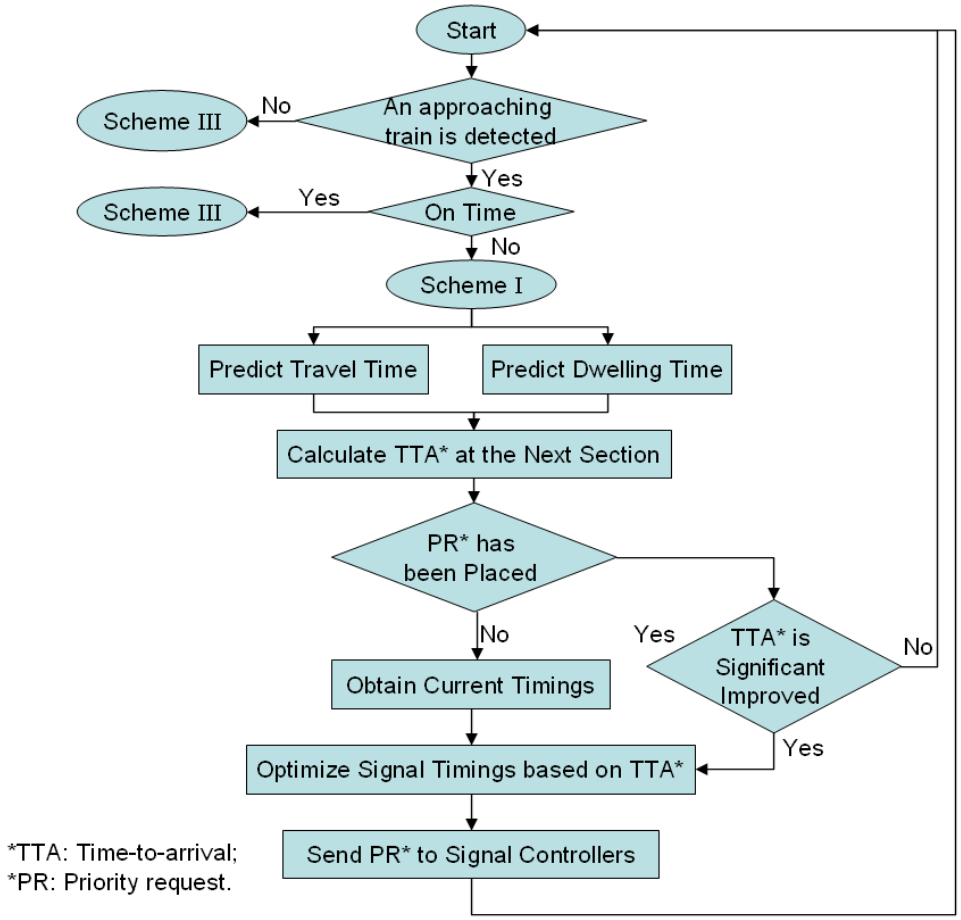

Figure 4.2: Flow chart of adaptive signal control algorithm

As mentioned in the previous chapter, it is crucial for the proposed adaptive traffic signal control system to update the information on LRV's movement and predict its arrival time at intersections. The details in travel time prediction and dwelling time estimation are available in [55, 85], and are not the focuses of this thesis. Here it is assumed that such information is ready to use for setting up the adaptive traffic signal optimization algorithm at urban highway/railroad grade crossings.

The performance index (PI) adopted in this chapter is called the overall passenger delays (OPDs), which is composed of passengers' delays from both light rail

transit and cross-street traffic. Based on different requirements, other performance criteria can be used. However, delay is one of the most critical performance indices that are used in the optimization of traffic signal timings.

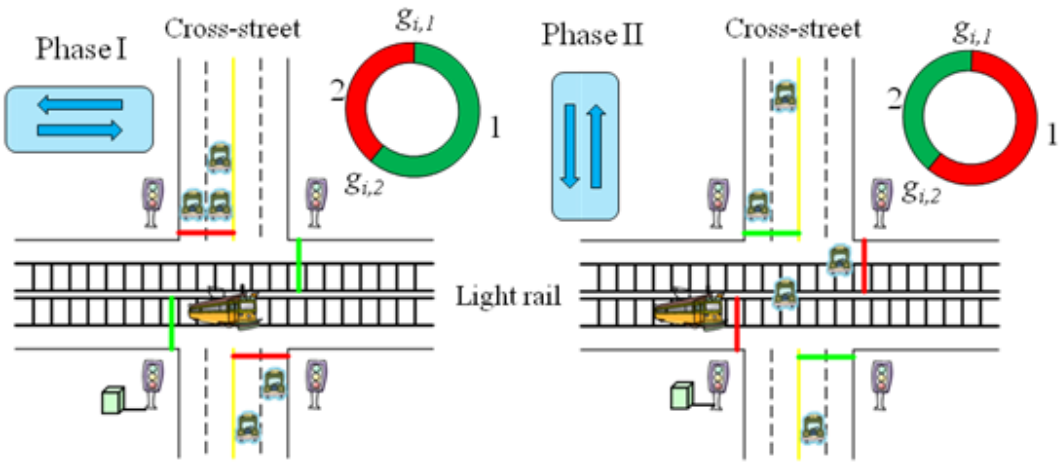

Figure 4.3: Illustration of two-phased signal with fixed-timing control

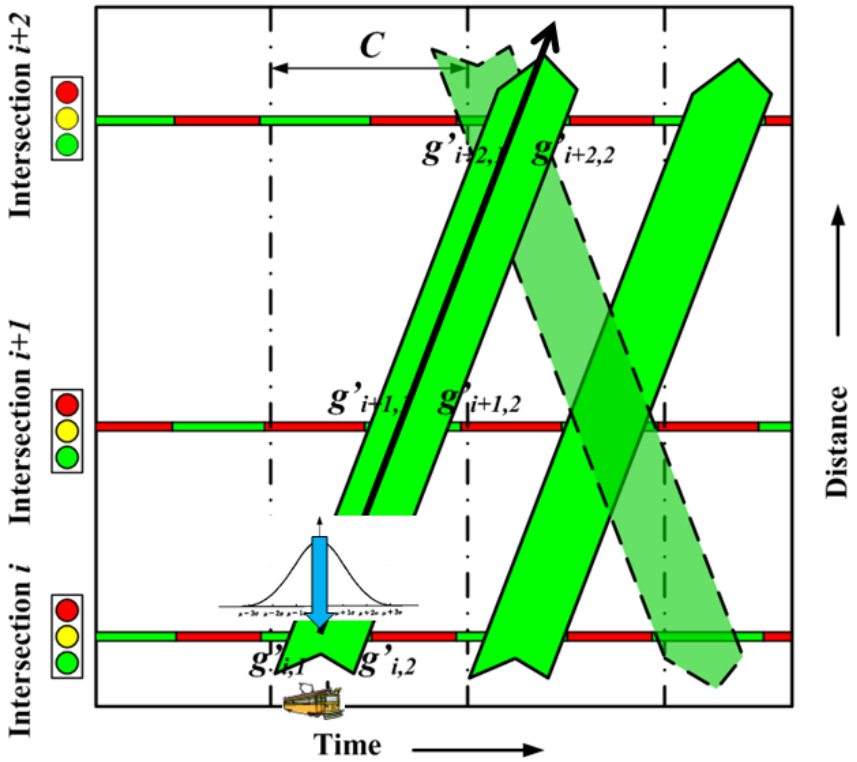

Figure 4.4: Illustration of adaptive signal control using the time-distance diagram

For the light rail transit (LRT) operation performance, signal delays along

multiple highway/railroad grade crossings are selected to better coordinate the movement of the light rail vehicle (LRV) and cross-street traffic operation. The green band or through band can be used to facilitate delay calculation along successive signalized intersections, which will be elaborated in the following. As shown in Figure 4.4, the slope of green band is the average travel speed of LRV, and its width is the amount of green available to the LRV through several intersections without stopping. Provided the movement prediction errors (shown in Figure 4.4) and uncertainties in the travel speed, a wider green band provides a better chance with which the LRV's trajectory will falls into the band. Figure 4.5 and Figure 4.6 present different signal timings with the same green splits on both phases. However, compared with Figure 4.5, Figure 4.6 shows better tuned signal timings because the green band is wider. In addition, for traffic signals under fixed-timing control, such green band repeats every cycle.

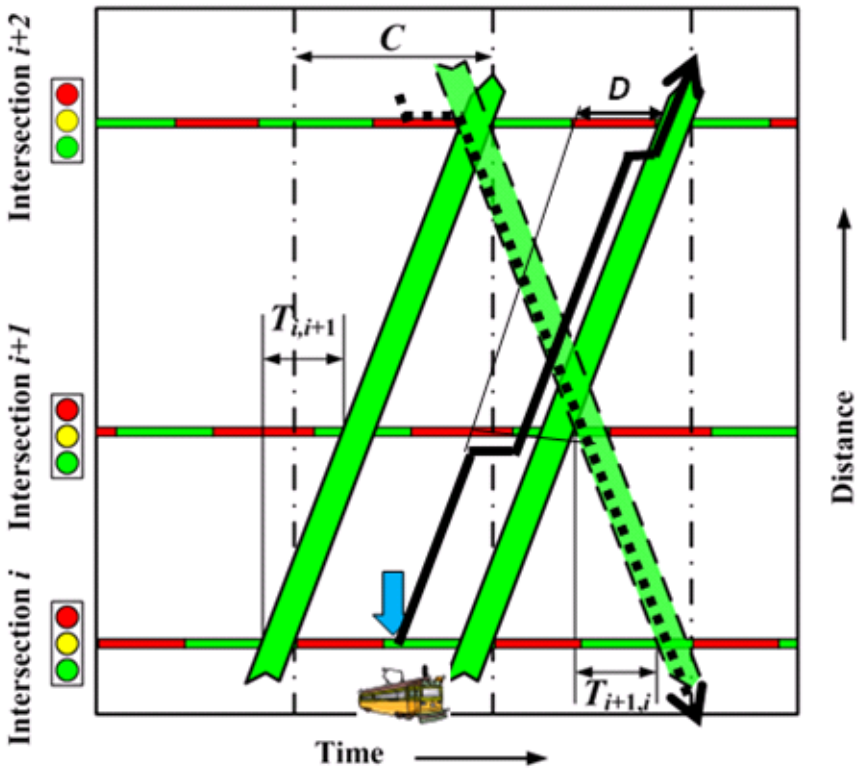

Figure 4.5: Illustration of worse-tuned traffic signals with time-distance diagram

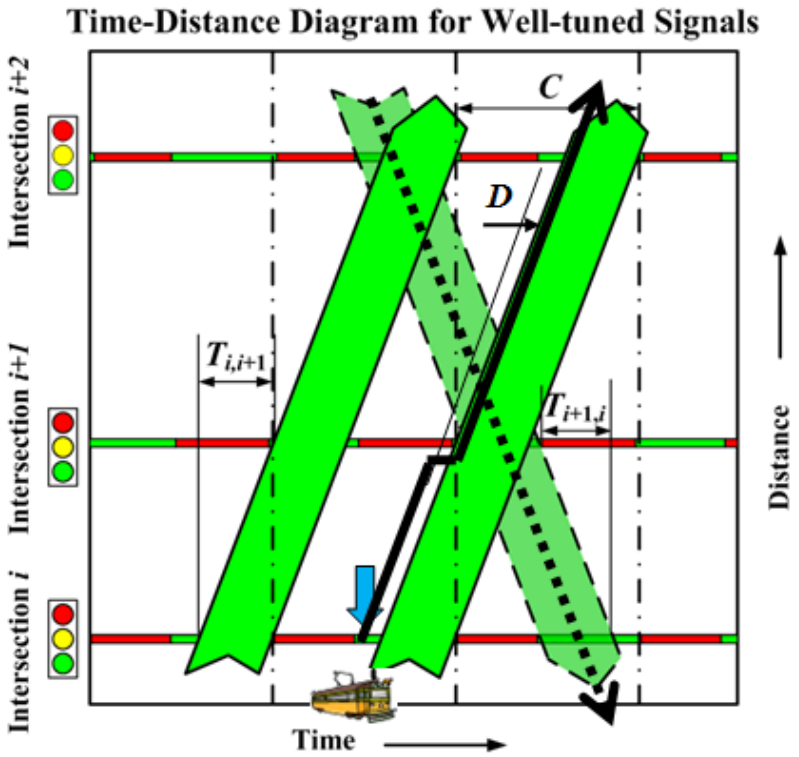

Figure 4.6: Illustration of better-tuned traffic signals with time-distance diagram

4.3 Problem Formulation

4.3.1 Decision Variables

Because the goal of the proposed adaptive signal control strategy is to determine the green splits for each phase of signals along the corridor, the primary decision variables are selected as the green start and end of each signals, $\boldsymbol{g_{i,1}}$ and $\boldsymbol{g_{i,2}}$. However, to quantify the width and location of green bands for both direction, the start and end points of green bands, $\boldsymbol{B_i^{1,S}}$, $\boldsymbol{B_i^{1,E}}$, $\boldsymbol{B_i^{2,S}}$ and $\boldsymbol{B_i^{2,E}}$, are also decision variables (called secondary ones), which depend on the primary decision variables. The relationship between green splits and start/end of green bands is illustrated in Figure 4.7.

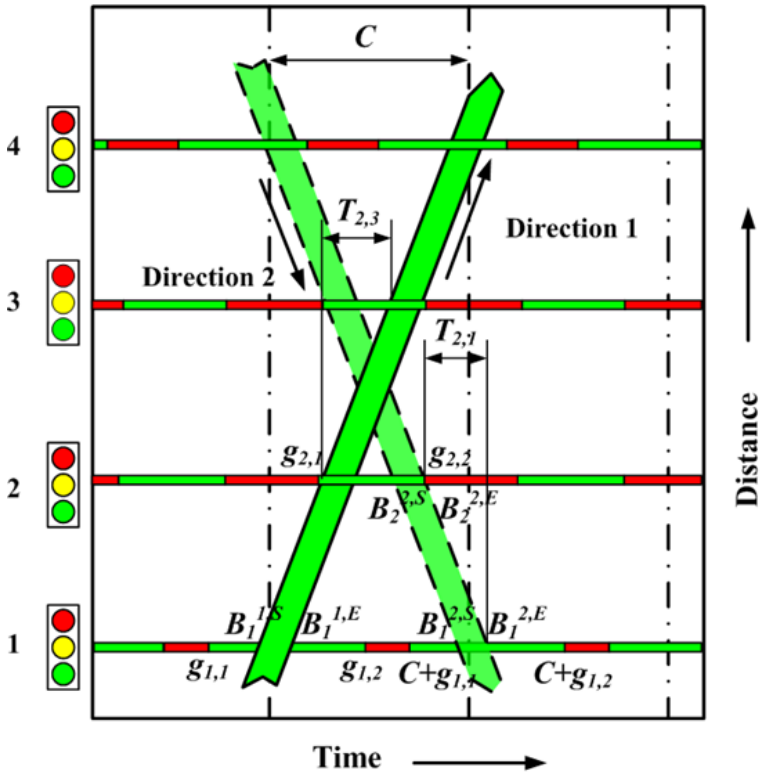

Figure 4.7: Illustration of the relationship among decision variables

4.3.2 Performance Index

4.3.2.1 Performance Index for LRV

According to the aforementioned, we need to minimize the intersection delays for both LRV and cross-street traffic, by carefully tuning the signal timings, or more specifically, adjusting the green splits of each traffic signal along multiple intersections. Therefore, it is natural to choose the start/end points of green intervals for every phase at each signalized intersections as primary decision variables. However, the decision on the green start for each phase will definitely affect the width of green bands for both directions and times when these green bands start and terminate in each cycle.

Assuming that the predicted arrival time of LRV at the first intersection, μ^{pred}, is available, and the prediction error follows a normal distribution with mean 0 and a known standard deviation (Figure 4.8), σ, i.e. $\varepsilon \sim N(0, \sigma^2)$, the actual arrival time at the

first intersection can be written as

$$\mu = \mu^{pred} + \varepsilon \sim N(\mu^{pred}, \sigma^2) \tag{4-1}$$

It is obvious that the delay of LRV travelling through multiple intersections is a function of μ, thus is also a random variable. Therefore, it makes more sense to calculate the expected delay for LRV along multiple intersections. However, it is critical to figure out a reasonable choice of time interval in integration to derive the closed form performance index for LRV.

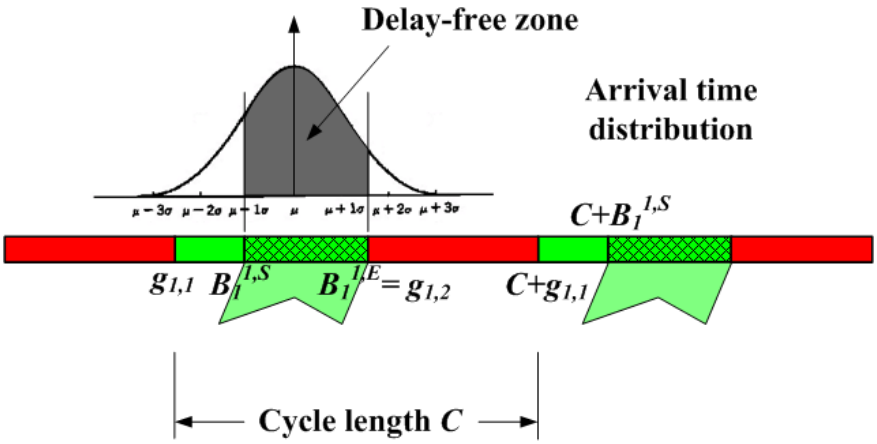

Figure 4.8: Illustration of the relationship between delay of LRV along multiple intersections and the actual arrival time at the first intersection

Since a normal distribution is assumed, we can obtain the expected delay for LRV by integrating from $-\infty$ to $+\infty$, i.e.

$$E[D^{LRV}(\mu)] = \int_{-\infty}^{+\infty} D^{LRV}(\mu) \cdot p_\mu \cdot d\mu \tag{4-2}$$

where $D^{LRV}(\mu)$ is the delay of LRV travelling through multiple intersections as a function of the actual arrival time at the first intersection, μ. p_μ is the probability density function of μ. However, due to the periodicity of traffic signal operation and green bands, it is desirable to choose a finite multiplicity of the cycle length, *C*, as the integration interval. Also, note that the cycle length is long enough to cover six times the standard deviation of prediction error, $6 \cdot \sigma$, in most cases in practice, we then select one cycle length, *C*, as the time interval for integration in the following part of this chapter.

As is shown in Figure 4.8, if we further force

$$B_1^{1,E} = g_{1,2} \tag{4-3}$$

at the first intersection, then the LRV's delay along multiple intersections is a piece-wise function.

$$D^{LRV}(\mu) = \begin{cases} B_1^{1,S} - \mu & \mu^{pred} - C/2 \le \mu \le B_1^{1,S} \\ 0 & B_1^{1,S} \le \mu \le B_1^{1,E} \\ B_1^{1,S} + C - \mu & B_1^{1,E} \le \mu \le \mu^{pred} + C/2 \end{cases} \tag{4-4}$$

where, $g_{i,1}$ and $g_{i,2}$ are the green starts of phases for LRV and for cross-street traffic at intersection *i*, respectively. $B_i^{1,S}$ and $B_i^{1,E}$ represent the start and end of the green band along the direction of interest at intersection *i*.

Then the expected delay of LRV can be calculated as

$$E[D^{LRV}(\mu)] = \int_{\mu^{pred}-C/2}^{\mu^{pred}+C/2} D^{LRV}(\mu) \cdot p_\mu \cdot d\mu \tag{4-5}$$

Furthermore, if the ridership information is available, then we can obtain the expected passengers' delay (pax*sec) of LRV by

$$D_{Pax}^{LRV}(\mu) = \omega_1 \cdot E[D^{LRV}(\mu)] = \omega_1 \cdot \int_{\mu^{pred}-C/2}^{\mu^{pred}+C/2} D^{LRV}(\mu) \cdot p_\mu \cdot d\mu \tag{4-6}$$

where ω_1 is a weighting factor representing the number of passengers on the LRV.

4.3.2.2 Performance Index for Cross-street Traffic

To simplify the problem, we assume that there is no or few other motor vehicles along the light rail, which is the case at most highway/railroad grade crossings, e.g. in San Diego downtown area. In this case, the delay caused by LRV to traffic is limited to the cross street only. It is reasonable to deal with each intersection as an isolated one when calculating the performance index, intersection delay, of cross-street traffic. Under the assumptions of the uniform arrival pattern and the under-saturated traffic condition, we use a deterministic model to estimate traffic delay at a signalized intersection, which is the shadowed area in Figure 4.9. At intersection *i*, the overall traffic delay (veh*sec) for

two-phased signal operation per cycle is

$$D_i^{Traffic} = \frac{a_i \cdot d_i}{(d_i - a_i)} \cdot \left[\frac{1}{2} \cdot \left(g_{i,2} - g_{i,1}\right)^2\right] \quad (4\text{-}7)$$

If the average number of passenger in each passenger vehicle, ω_2 is available, then the overall passengers' delay (pax*sec) per cycle at the *i*-th intersection can be written as

$$D_{Pax,i}^{Traffic} = \frac{\omega_2 \cdot a_i \cdot d_i}{(d_i - a_i)} \cdot \left[\frac{1}{2} \cdot \left(g_{i,2} - g_{i,1}\right)^2\right] \quad (4\text{-}8)$$

A commonly-used value for ω_2 is 1.2, i.e. the ridership in each passenger vehicle is 1.2 pax/veh on average.

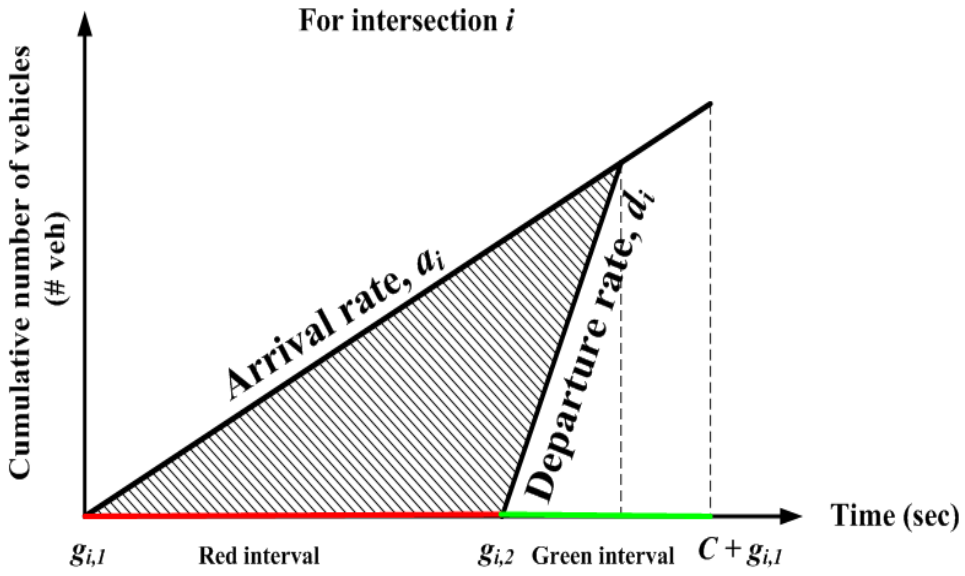

Figure 4.9: Illustration of delay calculation for cross-street traffic with deterministic model

4.3.3 Constraints

As to the constraints, there are three types in the proposed optimization model:

- Those related to the pedestrian safety, e.g. requirements on minimum green and maximum green for each phase.

- Those related to the formation and geometry of green bands, such as the time when the green bands start and terminate, etc.
- Boundary conditions for decision variables, $g_{i,1}$ and $g_{i,2}$

To be more specific, the constraint that relates to the pedestrian safety issue is

$$max\{G_{i,1}^{min}, C - G_{i,2}^{max}\} \leq g_{i,2} - g_{i,1} \leq min\{G_{i,1}^{max}, C - G_{i,2}^{min}\}$$
$$\forall\, i = 1, 2, \cdots, N \tag{4-9}$$

where C is the cycle length, $G_{i,1}^{min}$ and $G_{i,2}^{max}$ are the minimum green and maximum green for phase 1 and phase 2 at the i-th intersection. N is the number of successive intersections along the light rail.

To form green bands, we also require

$$B_j^{k,S} - B_i^{k,S} = B_j^{k,E} - B_i^{k,E} = T_{i,j}$$
$$\forall\, i, j = 1, 2, \cdots, N \text{ and } k = 1, 2 \tag{4-10}$$

where k represents the direction of trip, "1" for the outbound trip and "2" for the inbound trip. $B_i^{k,S}$ denotes the green band starting time at intersection i along the k-th direction. $B_j^{k,E}$ means the green band end time at intersection j along the k-th direction. $T_{i,j}$ is the historical or estimated travel time of LRT from intersection i to intersection j.

$$g_{i,1} + C \cdot n_i^k \leq B_i^{k,S}, B_i^{k,E} \leq g_{i,2} + C \cdot n_i^k$$
$$\forall\, i = 1, 2, \cdots, N \text{ and } k = 1, 2 \tag{4-11}$$

where n_i^k is a non-negative integer that may vary with different intersection and different travel direction of LRV.

$$B_i^{k,E} - B_i^{k,S} \geq B^{k,min} \tag{4-12}$$

where $B^{k,min}$ is a user-defined minimum width requirement on the width of green band along k-th direction.

$$B_1^{1,E} = g_{1,2} \tag{4-13}$$

$$0 \le g_{i,1}, g_{i,2} \le C \qquad \forall\, i = 1, 2, \cdots, N \tag{4-14}$$

Constraint (4-9) guarantees that in the optimized signal timings, the green length for each phase at each intersection cannot be greater than the maximum green requirement or smaller than the minimum one. Constraint (4-10) shows simple relationship between start/end points of green bands at each intersection and the average travel time of LRV between intersections. Constraint (4-11) means that green bands must fall into the green phases at each intersection for each bound. Constraint (4-12) reflects the consideration on minimum width of green band for both directions. Constraint (4-13) simplifies the delay calculation for LRV. In constraint (4-14), the green splits at each intersection are bounded by the cycle length.

4.3.4 Summary of Optimization Model

In summary, the proposed traffic signal optimization model can be cast into a nonlinear programming with linear constraints as follows

$$\min D_{Pax}^{LRV}(\mu) + \sum_{i=1}^{N} D_{Pax,i}^{Traffic} \tag{4-15}$$

or,

$$\min \ \omega_1 \cdot \int_{\mu^{pred}-C/2}^{\mu^{pred}+C/2} D^{LRV} \cdot p_\mu \cdot d\mu + \omega_2 \cdot \sum_{i=1}^{N} \frac{a_i \cdot d_i}{(d_i - a_i)} \left[\frac{1}{2} \cdot \left(g_{i,2} - g_{i,1}\right)^2\right] \tag{4-16}$$

subject to constraints (4-9) – (4-14). Numerical computation tool (MATLAB 7.0) is used to solve the nonlinear optimization problem above.

Before the validation of our proposed model, we note the following remarks.

- In the problem formulation, we do not require $g_{i,1}$ and $g_{i,2}$ to be integers for simplification of calculation. We can round them to the closest integers if they are fractional in the results and this will not make remarkable difference in practice.

- The choice of ω_1 and ω_2 may not necessarily be the average rider-ship, but reflects the weight that users place on different objectives. Obviously, the larger the ω_1 is, the longer the green interval in the optimal solution to favor LRV's direction.
- The value of $B^{1,min}$ may relate to the variance of prediction error on LRV's arrival time at the first intersection. On the other hand, $B^{2,min}$ depends on the consideration of LRV's performance along the other bound. The larger these two parameters are, the smaller the feasible region, and the worse the performance index in the optimal solution.
- To take into account the performance of on-time rate for LRV's operation, we need to have more constraints on the width and start point of green bands.
- In the proposed model, we can also choose n_i^k as decision variables. Then, the problem will be formulated as a *mixed-integer nonlinear programming* problem, which is much more complicated to solve.
- The numerical solution is sensitive to the initial point and the solution might not be globally optimal, which is in general the case for *nonlinear programming*.

4.4 Case Study and Sensitivity Analysis

4.4.1 Study Site and Model Parameters

To validate the proposed algorithm, we chose a section of C Street, between trolley stations Civic Center and Fifth Ave in San Diego downtown area, to conduct a case study, which involves sensitivity analysis on parameters: (a) user-defined minimum width of green bands along both directions, and (b) LRV's ridership and the standard deviation of prediction error. Below is a list of quantified parameters from the field.

- N = 3. There are totally three intersections within this studied section;
- C = 70 sec. During the period of 05:00 through 15:00 on a typical weekday, the cycle length is 70 sec at these three traffic signals;
- $G_{i,1}^{min} = G_{i,2}^{min} = 19$ sec, $G_{i,1}^{max} = G_{i,2}^{max} = 51$ sec, for i = 1, 2 and 3. During the same period the minimum green and maximum green are for these three traffic signals;
- a_{3rd} = 0.0889 veh/sec, a_{4th} = 0.2483 veh/sec, a_{5th} = 0.1525 veh/sec, d_{3rd} = 1.0139 veh/sec, d_{4th} = 1.5206 veh/sec, and d_{5th} = 1.5206 veh/sec. Based on

the historical survey data on traffic volumes, road characteristics of cross-streets, 3rd Ave, 4th Ave and 5th Ave and saturation flow rates suggested in [61], we can obtain the corresponding arrival rates and departure rates as listed above.

- $\sigma = 7.78$ sec. From the GPS data of LRVs, we calculated the average travel time among these three intersections for both bounds and predicted the arrival time with standard deviation of 7.78 sec [85];
- $\omega_1 = 84$. According to the ridership survey from *San Diego Transit Corporation* (SDTC) & *San Diego Trolley, Inc*. (SDTI), the average number of passengers on each trolley is 84;
- $B^{1,min} = 25 \approx 3.2 \cdot \sigma$sec and $B^{2,min} = 8 \approx \sigma$sec. In order to determine the minimum width of green bands, $B^{1,min}$ and $B^{2,min}$, we did sensitivity analysis on these user-defined parameters as shown in the following section.

4.4.2 Sensitivity Analysis

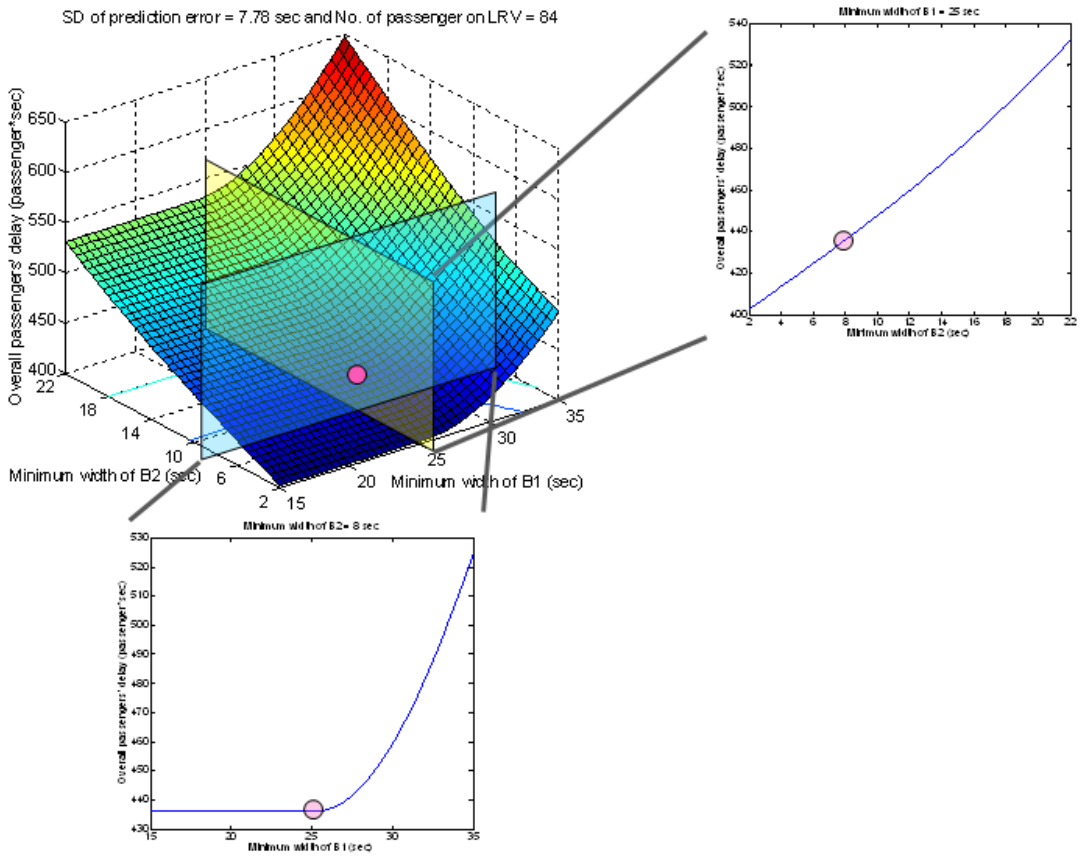

Figure 4.10: Sensitivity analysis on parameters – user-defined minimum width of green bands along both directions

As shown in Figure 4.10, if $\sigma = 7.78$ sec and $\omega_1 = 84$, then when $B^{1,min} > 25$, a sharp growth in the overall performance index is witnessed, and the overall passengers' delay increases linearly as $B^{2,min}$ is getting larger. Based on these observations, we decided $B^{1,min} = 25 \approx 3.2 \cdot \sigma$sec and $B^{2,min} = 8 \approx \sigma$sec;

Furthermore, to explore the impacts of ridership on LRV and the variance of prediction error on the performance index, we conducted another sensitivity analysis (see Figure 4.11). As shown in Figure 4.11, if $B^{1,\min} = 25$ sec and $B^{2,min} = 8$ sec, then the overall passengers' delay will grow noticeably as the standard deviation of prediction error increases. However, when the prediction involves little uncertainty, the number of passengers on LRV will have little impact on the overall performance index. In this case study, all n_i^k's are zeros, for i = 1, 2, 3 and k = 1, 2, due to the fact that the distances between intersections are not very long.

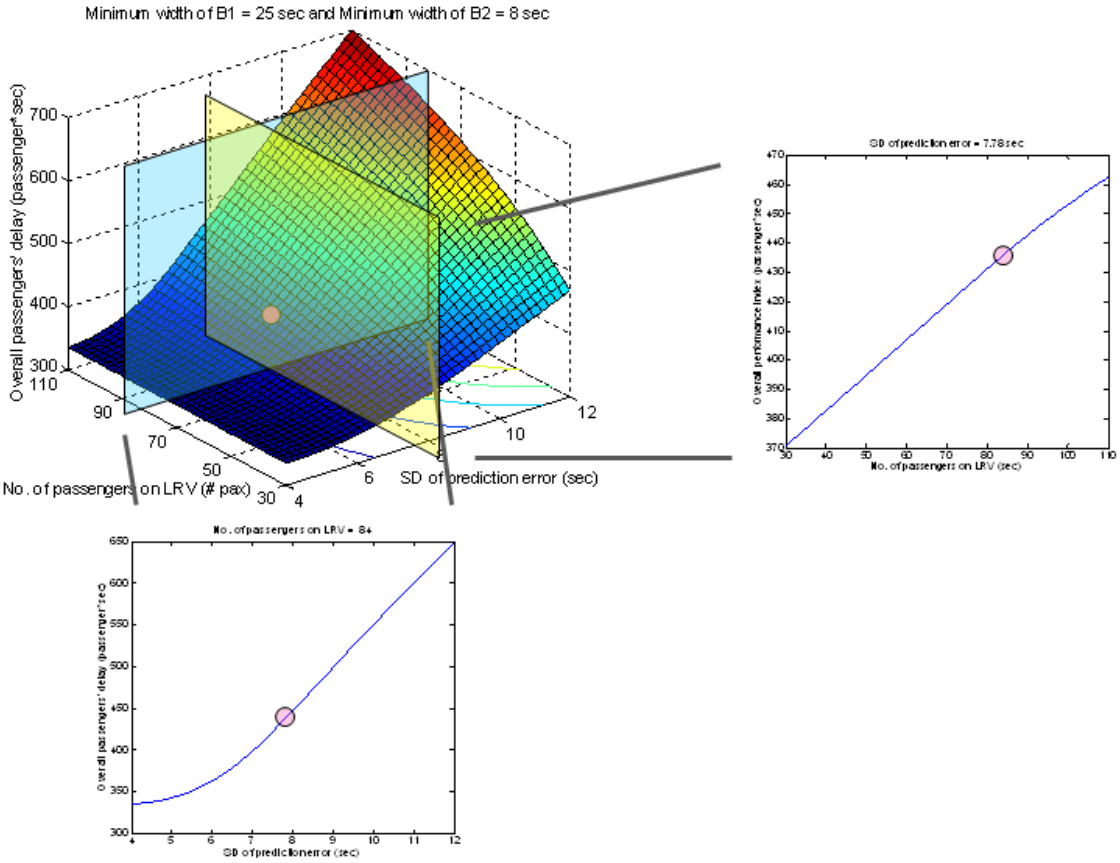

Figure 4.11: Sensitivity analysis on parameters – LRV's ridership and standard deviation of prediction error

4.5 Simulation Test

4.5.1 Simulation Setup

The adaptive signal control algorithm is simulated using a microscopic simulation model set up in PARAMICS (Figure 4.12). The model is calibrated with field data collected from 120 trolley trips under both current traffic signal timings (conventional scenario) and proposed traffic signal timings (optimal scenario), respectively. the proposed strategy is not applied to all 120 trips but to late trips which are randomly chosen about 10% (from SDTC) of total trips (5 outbound trips and 6 inbound ones). It needs to be pointed out that if the adaptive signal control algorithm is applied to all trips, then the results are not satisfactory because the frequent transitions of signal controllers may mess up the whole traffic system.

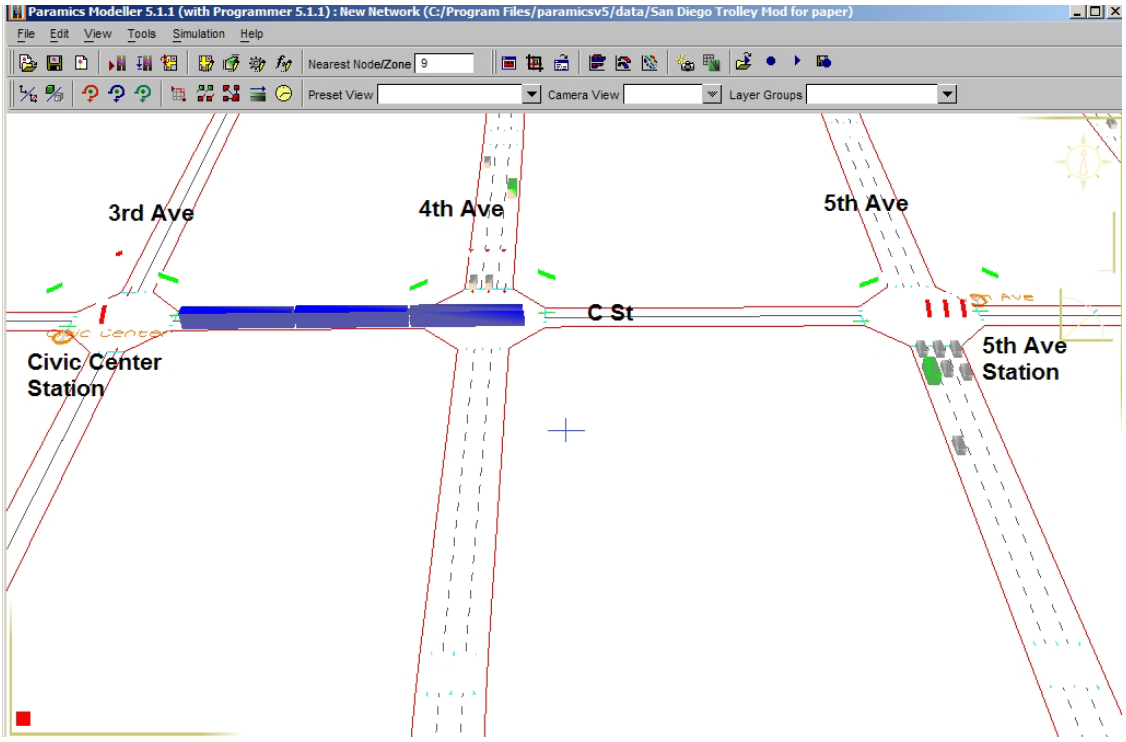

Figure 4.12: Snapshot of the simulation network at San Diego downtown area

4.5.2 Simulation Results

As is seen from Table 4.1, there is **no** stop for those late trips to which the algorithm has been applied and the average travel time between stations of these late trips can be shortened as much as **27.3%**. For other trips in the optimal scenario, there is no significant difference with those in the conventional scenario. On the other hand, for cross-street traffic, the total passengers' delays of these three intersections can be reduced **100.4** units per cycle, which is illustrated in Table 4.2. If the performance index is further investigated intersection by intersection, then it can be observed that there are negative impacts on 3rd Ave in the optimal scenario, because the traffic volume along 3rd Ave is relatively low compared with the other two intersections. However, based on what is defined in Table 4.3 [61], if the average delay per vehicle (Figure 4.13) is calculated and the level-of-service (LOS) is compared along these three intersections under both conventional scenario and optimal one, then promising results can be obtained as shown in Table 4.4. The LOS of 4th Ave and 5th Ave can be improved to A as opposed to B as in the conventional scenario.

Table 4.1: Simulation results for LRV's performance – average No. of stops between stations and average trip travel time

Measures of Effectiveness	**Conventional Scenario**	**Optimal Scenario**			
		Trips with ASP		Trips without ASP	
	Meas.	Meas.	Change	Meas.	Change
No. of stops	1.15	**0.0**	**-100.0%**	1.0	-13.0%
Trip time (sec)	45.2	**32.8**	**-27.3%**	43.9	-2.9%

Table 4.2: Simulation results for cross-street traffic passengers' delay

Scenarios		**Passengers' Delay Per Cycle (pax*sec)**			
		3rd Ave	4th Ave	5th Ave	Total
Conventional	Measurement	75.8	230.8	131.8	438.4
Optimal	Measurement	142.4	**113.4**	**82.0**	**337.8**
	Change	87.9%	**-50.9%**	**-37.8%**	**-23.0%**

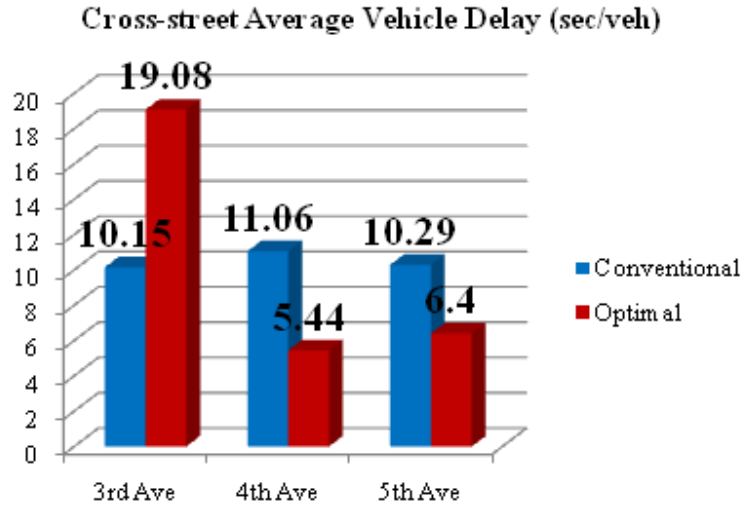

Figure 4.13: Simulation results on average vehicle delay for cross-street traffic at each intersection

Table 4.3: Definition of level of service (LOS) at signalized intersections

Level of Service (LOS)	Control Delay (sec/veh)
A	≤ 10
B	>10, and ≤20
C	>20, and ≤35
D	>35, and ≤55
E	>55, but ≤80
F	>80

Table 4.4: Comparison results on LOS between conventional scenario and optimal scenario at each intersection

Scenario	Level of Service (LOS)		
	3rd Ave	4th Ave	5th Ave
Conventional	B	B	B
Optimal	B	A	A

4.5.3 Remarks on OPD Model

The previous sections proposed an optimization algorithm for the online adaptive signal control at urban highway/railroad grade-crossings. Based on the detection

and prediction of LRT movements, the signal timings can be updated in real-time by running the proposed model to minimize overall passenger delays. A remarkable improvement on the operation of late trolleys can be witnessed in the case study of SDT system. At the same time, the level of service (LOS) of the cross-street can be noticeably enhanced. The simulation model coded in PARAMICS not only confirms such benefits obtained from the proposed control algorithm but also validates the practicality of the adaptive signal control system. Further simulation tests for larger system capacity, i.e. the percentage of trips that can trigger the proposed strategy without disruption of the traffic system, need to be performed.

4.6 Laboratory Testing

4.6.1 Testing Purpose

The laboratory testing is a step prior to the field operational testing for the proposed system in San Diego. The objective is to test and demonstrate the applicability of the proposed system, particularly the communication system and the traffic signal operation system in San Diego, i.e. the QuicNet/4 central control system in the traffic management center (TMC) and Type 170 controllers at roadside running McCain's Bitran 233 control software.

4.6.2 Testing Steps

There are two steps in the laboratory testing. The first step is to show the proposed system in an entirely closed laboratory environment. The second step is to move the testing one step closer to the field operational testing (FOT) and involve signal operation systems in the field and the actual communication system.

4.6.3 Laboratory Testing at PT^2L

The testing environment was jointly set up by McCain and PATH at Parsons Traffic and Transit Laboratory (PT^2L) at PATH. The testing platform consists of three Type 170 signal controllers with McCain's Bitran 233 program, a server computer with

McCain's QuicNet/4 software installed, the communication links between the three signal controllers and the QuicNet/4 server computer, a PATH control computer with all the adaptive signal control (ASC) software installed, and the communication link between the QuicNet/4 server and the PATH control computer.

The original configuration of signal controller settings in the testing platform at PT^2L is not identical with that at the San Diego Traffic Management Center (TMC). In particular, the "pre-timed" operation for phase 4 was enabled on the Bitrans 233 program. When McCain set up the controllers at PT^2L, the remote communication to SD's TMC had not been established yet. Thus McCain was not able to testify the settings with the field controllers. Under the incorrect settings at PT^2L, the force-off point of phase 4 is the time when the yellow of phase 4 starts. Under the field settings, phase 4 should be force-off at the beginning of its flash-don't-walk period. Under the help from the City of San Diego and McCain, such settings have been corrected. The control logic has been extensively examined. In addition, new constraints on force-off points of both phases as well as permissive end have also been tested in detail.

Because of the rectification of the signal controller settings, constraints of some parameters, e.g. the force-off point of phase 4, and the relationship among parameters, e.g. the gap between force-off point of phase 2 and phase 4, were modified accordingly. According to the results, the feasible region of the proposed optimization model is a bit smaller than that without the modification.

In the lab testing, if there is no disturbance on the predicted departure/arrival time at stations/signals, then all trips for both directions will experience zero-stop along all intersections between stations. However, most situations in the real world are far from being ideal and the predicted results cannot be guaranteed to be perfect at all. Therefore, sensitivity analysis on the prediction error is indispensable. The results are shown in Table 4.5 and Table 4.6.

Table 4.5: Sensitivity analysis for 3rd Ave and 4th Ave

	Sample Trips	**Delay at 3rd Ave**		**Delay at 4th Ave**	
		Mean	STD	Mean	STD
STD=0	29	0.17	0.38	0	0.00
STD=2	29	0.45	1.50	0.48	2.60
STD=5	28	6.89	16.92	5.11	15.18
STD=9	28	3.04	11.07	4.68	11.44
STD=14	27	5.48	10.79	13.59	17.09
STD=20	27	3.78	10.44	11.00	18.36

As can be observed from the results, system performance becomes worse as the standard deviation of the prediction error (unbiased prediction is assumed) gets larger. In other words, the overall delays of the simulated section, on average, keep increasing. At the same time, the variation of such delays becomes more and more noticeable.

Table 4.6: Sensitivity analysis for 5th Ave and the section

	Sample Trips	Delay at 5th Ave		Section Delay	
		Mean	STD	Mean	STD
STD=0	29	0	0	0.17	0.38
STD=2	29	2.28	11.11	3.21	11.51
STD=5	28	0.25	0.80	12.25	21.00
STD=9	28	3.86	10.34	11.57	21.68
STD=14	27	4.45	12.39	23.52	21.32
STD=20	27	4.59	13.24	19.37	23.29

4.6.4 Laboratory Testing at San Diego TMC

PATH worked with the City of San Diego and McCain and set up the testing environment at the San Diego TMC. The testing platform was quite similar with the one at PATH. It consisted of five Type 170 signal controllers with McCain's Bitran 233 programs, the TMC QuicNet/4 server computer with McCain's communication software installed, the communication links between the five signal controllers and the QuicNet/4 server computer, a PATH control computer with all the adaptive signal control (ASC) software installed, and the communication links between QuicNet/4 server and the PATH control computer and between the PATH control computer and the PATH server at PT^2L. PATH and the IT group at City of San Diego set up a reverse connection so that the PATH control computer can receive the trolley GPS data from the PATH server computer in Berkeley. All the hardware and communication links were tested at San Diego TMC. The five controllers were set up with identical settings as five field intersections at C Street: India Street, 3rd Avenue, 4th Avenue, 5th Avenue, and 6th Avenue.

Before using the trolley GPS data from the field to test our system, the lab testing was first conducted with simulated trolley runs on the TMC testing platform. Under this scenario, PATH-developed trolley simulation tool generated virtual trips and mimicked trolleys' movements. the study corridor with 13 signalized intersections was set up and one virtual trolley was sent out to travel back and forth. During the lab testing, five of the 13 traffic signals were controlled by real signal controllers as described above. The trolleys' historical movement data served as input parameters of the proposed optimization

algorithm. In addition, the dwelling times at the relevant stations, i.e. American Plaza, Civic Center, 5th Avenue and City College, came from both the historical operation data collected by the PATH automatic vehicle location (AVL) system and some latest field surveys conducted in June 2008. Since June 18th 2009, the lab testing had been run in the San Diego TMC continuously for four days. With simulated trolley runs, over 500 trolley runs were obtained with equal number of trips for both Southbound/Outbound and Northbound/Inbound directions. Given the perfect prediction of train movements and dwell times, all trolley runs under signal priority were able to travel through signalized intersections without any unnecessary stops (i.e. non-station stops), except for those trips released at around midnight. The cause of the stops is due to abnormal controller operation, which will be described in detail in the later section. To analyze the simulation data, some tools are developed using MATLAB to visualize the results and get further insight into the trolley and signal operations. Figure 4.14 shows one typical Southbound/Outbound trip in the lab testing. After detecting the incoming trolley, the PATH control computer generated signal priority requests based on the movements of trolleys and signal timings from the QuicNet/4 server, which then downloaded the signal timings onto the three controllers that were set up in the TMC. After the controllers implemented the new timings, the simulated trolley with priority was able to go through all three intersections without any stops. Note that the dwell times have been equivalently converted to travel times.

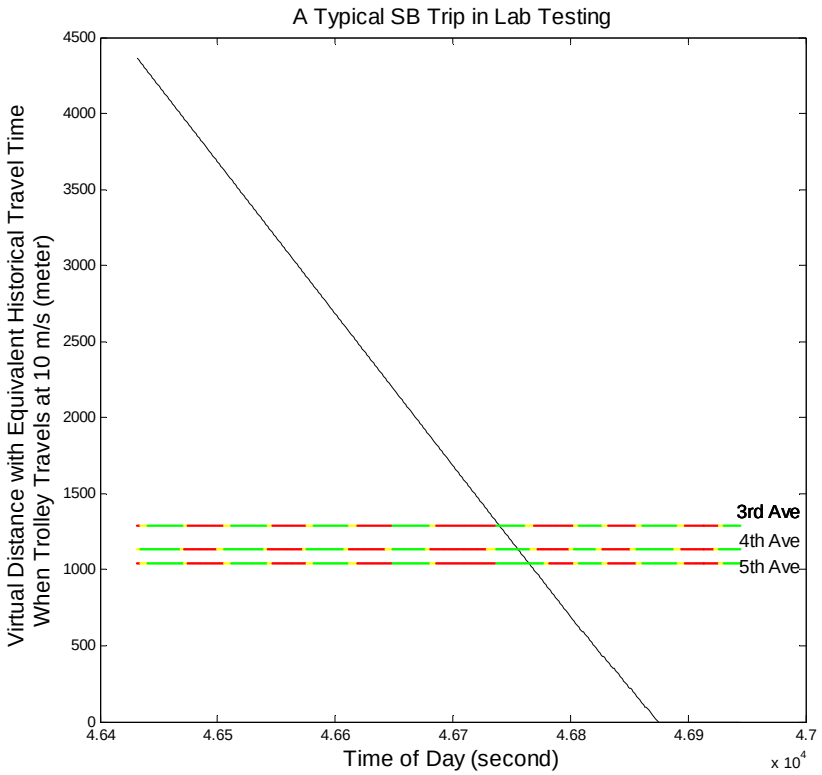

Figure 4.14: One typical southbound/outbound laboratory testing trip

Based on the observations and discussions with City of San Diego engineers, it is revealed that all signal controllers along the study corridor are reset at approximately midnight (00:00 A.M.) each day. During this time, all signal controllers are in transition for at least 150 seconds. This caused the trolley request to be dropped or not properly implemented. As a tentative solution, a predefined period (e.g. 10 minutes) can be blocked out around midnight when no signal priority requests will be processed.

Although the prediction tool is trying to filter out the GPS-related errors, bad GPS receptions sometimes will result in poor prediction. Subsequently, traffic signal timings can hardly be adjusted to adapt to trolleys' movements in the field. As mentioned before, there are two types of GPS problems: GPS reception errors and GPS signal losses. Both of these problems are partially due to "urban canyon" effects and the limitation of GPS devices. According to the testing results, the quality of GPS data is adequate for the field testing for the purpose of verifying the proposed system. However, for the large scale deployment of the system in the field, a more robust device will be needed.

The prediction of trolleys' dwelling times is very difficult particularly with the random arrivals of disabled people. This quantity is also a key parameter to the proposed system because signal controllers in pre-time mode require long lead-time to process timing change requests. Based on extensive tests in the simulation environment, the proposed algorithm will definitely work well if the prediction is good enough. In comparison with trolleys' travel times, dwelling times are less consistent and more unpredictable. For example, if a handicapped person needs to board the trolley, the dwelling time will get much longer than usual. According to the field data analysis, trolleys' waiting times (may include dwelling times and signal waiting times) at stations can range from approximately 30 seconds to 3 minutes. One possible way to increase the accuracy of the dwell time prediction is to build learning intelligence in the prediction software so that the prediction tool can improve the prediction by learning from the collected field data.

4.7 Preliminary Field Operational Testing

4.7.1 Testing Purpose

The objective of the preliminary field operational test (FOT) is to demonstrate the proof-of-concept of the proposed system in San Diego and evaluate the potential applicability of such a system in a large-scale implementation.

4.7.2 Testing Description

Based on discussions with City of San Diego and SANDAG, the selected testing bed is the 0.8-mile-long arterial segment of C Street in Downtown San Diego, as shown in Figure 4.15 with four trolley stations along this corridor: from the west to east, they are America Plaza, Civic Center, 5th Ave., and City College. The corridor consists of thirteen signalized intersections from India St. to 11th Ave. Two trolley lines (Blue and Orange) serve along this test bed with a regular headway of fifteen minutes. During the peak hours, the Blue Line runs more frequently with a short headway of seven minutes.

Figure 4.15: Map of testing site

There are two stages in data collection for the FOT. Stage 1 was for the "before" scenario in which trolleys did not experience any signal priority. Stage 1 was from October 30th, 2009 to November 8th, 2009. Stage 2 was "after" scenario in which selected trolleys were able to request transit signal priority (TSP) along the testing corridor. Stage 2 started on October 16th, 2009 and ended on October 26th, 2009. Table 4.7 presents the summary of sample trips in the FOT. Table 4.8 and Table 4.9 illustrate the detailed description of all trip samples for Stage 1 and Stage 2, respectively.

Table 4.7: Summary of trip samples

Stage	**Number of trips**	
	Outbound	Inbound
1 (Without ASC)	67	79
2 (With ASC)	109	123

Table 4.8: Detailed trip samples for Stage 1

Date	Trolley #1		Trolley #2		Trolley #6		Trolley #8		Summary	
	OB	IB	OB	IB	OB	IB	OB	IB	OB	IB
30th	0	0	0	0	1	2	6	8	7	10
31st	0	0	0	0	0	0	0	0	0	0
1st	0	0	0	0	0	0	6	7	6	7
2nd	0	0	0	0	3	4	6	7	9	11
3rd	1	1	0	0	2	3	2	4	5	8
4th	1	2	3	2	3	3	4	5	11	12
5th	1	2	0	1	3	4	7	8	11	15
6th	1	2	6	7	3	4	9	8	19	21
7th	0	0	0	0	0	0	5	6	5	6
8th	0	0	5	6	0	0	2	2	7	8
Sum.	4	7	14	16	15	20	47	55	81	98

Table 4.9: Detailed trip samples for Stage 2

Date (Oct.)	Trolley #1		Trolley #2		Trolley #6		Trolley #8		Summary	
	OB*	IB**	OB	IB	OB	IB	OB	IB	OB	IB
16th	0	0	5	5	1	2	3	3	9	10
17th	0	0	8	8	0	0	3	3	11	11
18th	0	0	0	0	0	0	5	4	5	4
19th	0	0	8	9	2	2	8	9	18	20
20th	0	0	7	8	2	2	1	1	10	11
21st	1	1	4	5	1	2	5	6	11	14
22nd	8	9	5	7	2	4	3	2	18	22
23rd	9	9	8	9	3	3	6	7	26	28
24th	7	7	2	1	0	0	3	3	12	11
25th	8	8	0	0	0	0	0	0	8	8
Sum.	33	34	47	52	11	15	37	38	128	139

* – Outbound trips include those operating along both Blue and Orange Lines within the study scope

** – Inbound trips include those operating along both Blue and Orange Lines within the study scope

The traffic signal timings serve as major inputs of the proposed adaptive signal control algorithm. Since the last data collection, engineers of San Diego have updated signal timings a few times. In order to prepare for the FOT, the most recent signal timing information has been collected from the City of San Diego. All timing parameters in the control software have been updated. In comparison with the previous version of traffic signal timings, changes include offsets, force-off points of phase 4, yellow intervals and all red clearances.

Due to the construction around San Diego City College, the City College trolley station was placed between 10th and 11th Avenues at C Street. Therefore, the original study corridor was from India Street @ C Street to 10th Avenue @ C Street. The whole corridor consisted of 12 signalized intersections. Upon the completion of the construction, the City College station was relocated between 11th Avenue @ C Street and Park Boulevard @ C Street. Now there are 13 signalized intersections along the study corridor: India Street, Front Street, 1st Avenue, 2nd Avenue, 3rd Avenue, 4th Avenue, 5th Avenue, 6th Avenue, 7th Avenue, 8th Avenue, 9th Avenue, 10th Avenue and 11th Avenue. For the additional intersection 11th Avenue @ C Street, the traffic signal timing information, geometry information, and traffic demand information have been collected and analyzed. 11th Avenue @ C Street is quite unique from a geometric perspective because it has a separate traffic phase, which parallels the trolley's movement. Therefore, a few changes have been made in the signal timing optimization software to generate the associated optimal signal timings.

In the previous work, signal timing Plan 2 was focused on during the study. Plan 2 covers the time of day between 03:00 and 15:00 and it is also consistent with the study period in the microscopic simulation model using PARAMICS. However, the trolley operational span is longer than the time window mentioned above. The optimal timing tables under Plan 4 are thus required and have been obtained by running the proposed optimization algorithm with corresponding parameters.

4.7.3 Analysis Results

4.7.3.1 Execution Rates for Requests

A successful implementation of the ASC system depends on whether the priority request can be properly generated, then communicated and finally deployed. Table 4.10

presents the execution rates for the priority requests at all intersections along the test corridor. It is observed that the majority of priority requests have been successfully executed. At most of the signals, over 98% of requests have been successfully generated, communicated, and executed at local signal controllers. At 11th Ave, there were five failure calls, which is 6% of all requests. According to the communication log file, communication issues between the QuicNet/4 server and the local signal controller (e.g. 11th Ave.) most likely caused the non-executions.

Table 4.10: Summary of execution rates for requests

Intersection	Total Number of Requests	Updated Calls	Effective Calls	Successful Calls	Failure Calls	Successful Rate
India St	175	70	105	103	2	98%
Front St	181	85	96	96	0	100%
1st Ave	179	79	100	100	0	100%
2nd Ave	178	82	96	96	0	100%
3rd Ave	148	62	86	86	0	100%
4th Ave	145	53	92	91	1	99%
5th Ave	154	63	91	90	1	99%
6th Ave	149	60	89	89	0	100%
7th Ave	148	61	87	87	0	100%
8th Ave	145	59	86	86	0	100%
9th Ave	152	58	94	93	1	99%
10th Ave	143	56	87	87	0	100%
11th Ave	141	56	85	80	5	94%

4.7.3.2 Impacts on Trolley Operation

As a part of the proof-of-concept for the proposed system, a real-world example was taken to evaluate the system performance. Figure 4.16 shows the trajectory of this trip from Civic Center to 5th Ave. As illustrated in the figure, there is no stop on red along the three signalized intersections of 3rd Ave, 4th Ave and 5th Ave between two stations, due to the successful execution of the priority request.

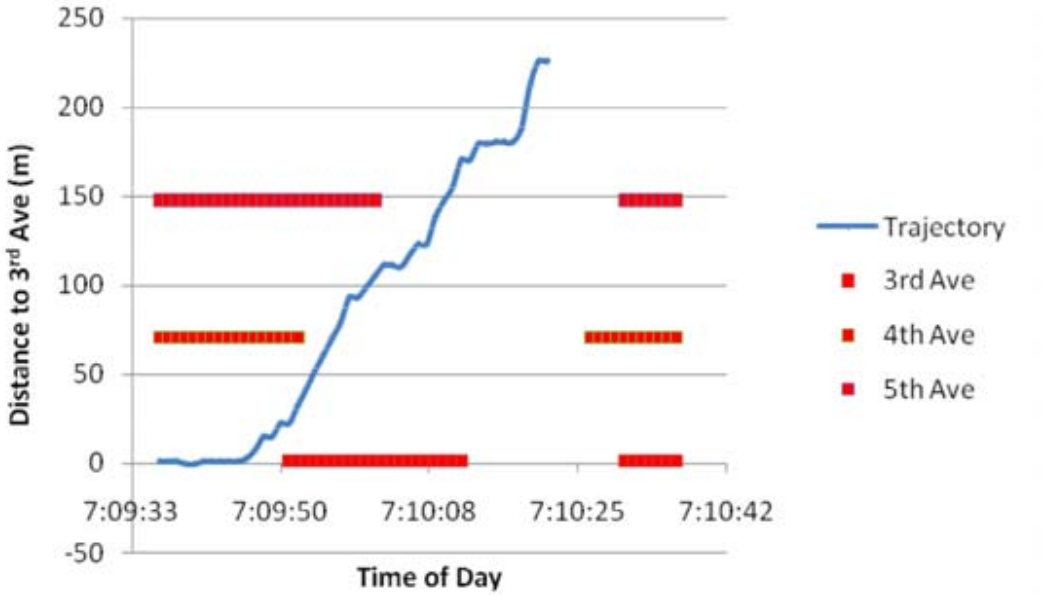

Figure 4.16: Trajectory of an example trip from Civic Center to 5th Ave

By carefully examining this trip, it can be observed that the actual departure time from Civic Center is 07:09:46 a.m., while the predicted departure time is 07:09:43 (only 3 seconds earlier). Based on such a good prediction, a priority request on the changes of signal timings is generated and executed. As a result, the differences between actual departure times and predicted times are trivial for the other two downstream intersections, i.e. 4th Ave and 5th Ave. The performance of this exemplar trip is illustrated in Table 4.11.

To further evaluate the benefits obtained from the proposed system, a hypothetical trip under original signal timings was constructed and its performance was compared with the scenario under the proposed signal timings. More than 16 seconds can be saved for this example trip at 3rd Ave (see Table 4.12). More specifically,

- If no priority request is available, the trolley would face the second half of red at 3rd Ave. However, this trolley passed through all three signals without any stop due to the successful execution of signal priority requests;
- A dedicated ‘green band’ (not too wide) along the trolley’s direction guaranteed such non-stop movement;
- At the same time, a wide ‘green band’ along the other direction made sure that the priority execution would not affect but favor trolleys’ movements from the opposite direction.

Table 4.11: Performance of an example trip from Civic Center to 5th Ave

	3rd Ave	4th Ave	5th Ave
Pred. Leave Time	07:09:43	07:09:59	07:10:08
Act. Leave Time	07:09:46	07:09:57	07:10:09
Pred. Error (sec)	-3	2	-1
Block Travel Time (sec)	11	12	

Table 4.12: Original and proposed timings for the example trip

	3rd Ave		4th Ave		5th Ave	
	FO 2 *	FO 4 **	FO 2	FO 4	FO 2	FO 4
Before Timings	0	34	0	34	0	34
After Timings	23	52	0	32	0	37
Expected Delay (sec)	>=16		0		0	

However, not all trips with priority request execution gain such satisfactory results and not all results under proposed signal timings are consistently better than those in the original scenario. The summary of all trips is presented below.

Table 4.13: Summary of number of stops at signals

Stage	Section I		Section II		Section III	
Inbound trips	Mean	STD	Mean	STD	Mean	STD
1 (Without ASC)	1.78	0.82	0.83	0.63	1.00	0.79
2 (with ASC)	1.61	0.81	0.83	0.64	1.33	0.96
Outbound trips	Mean	STD	Mean	STD	Mean	STD
1 (Without ASC)	1.29	0.86	0.95	0.61	2.38	0.78
2 (with ASC)	1.19	0.88	0.79	0.61	2.38	0.79

As is shown in Table 4.13, ASC successfully reduced the number of stops along Section I (between American Plaza and Civic Center) by about 10%. The standard deviations are comparable for the same section. Insignificant benefits can be obtained with applications of the proposed system for Section II, while minor negative impacts on

the number of stops along Section III are present. In the opposite direction, results are similar. ASC reduced the number of stops by about 10% along Section I and by another 15% along Section II. Along Section III, ASC was unable to significantly benefit trolleys' operations.

The impact of ASC on trolleys' travel times is similar with that on the number of stops as shown in Table 4.13. The benefits were insignificant for most of trips due to some external and internal issues, among which the inaccurate prediction of trolleys' departure times is the most important. Further detailed analysis will be presented in the following section.

At stage 2 with ASC, some of the priority requests may be blocked due to an earlier priority request execution for the other trolleys. To quantify the percentage of priority requests being not blocked, the priority request 'non-blockage' rate, δ, is defined at a section level (a section is defined as the segment between two consecutive stations). For Section *i*, 'non-blockage' rate of priority requests is

$$\delta_i = \frac{\#\ of\ trips\ with\ executed\ priority\ requests}{\#\ of\ trips}$$

Table 4.14 presents the results for different trip directions (outbound and inbound). As shown in the table, the priority request 'non-blockage' rate is greater than 0.9 in most cases, which means that over 90% of priority requests can be executed in the field operation testing. With a larger scale deployment, a smaller request 'non-blockage' rate may be expected. However, based on the schedule adherence, if only those late trolleys (around 10% of overall trips) send out priority requests, the priority request blockage rate will still fall into an acceptable range.

Table 4.14: Request non-blockage rates

Section	**Trolley #1**		**Trolley #2**		**Trolley #6**		**Trolley #8**	
	OB	IB	OB	IB	OB	IB	OB	IB
Sec. I	0.92	1.00	0.91	0.96	0.88	1.00	0.95	1.00
Sec. II	1.00	1.00	0.98	1.00	1.00	1.00	0.95	1.00
Sec. III	0.96	0.81	0.98	0.92	1.00	0.92	1.00	0.92

A priority request consists of a set of force-off points for the intersections between downstream and upstream trolley stations. With changes of force-off points, the starts/ends, and durations of signal phases may vary. Under priority, signal Phase 2 serving the trolley movement direction should be relocated and elongated to cover the

trolley's arrival time and the variation.

4.7.3.3 Impacts on Traffic Operation

The major concern for adaptive signal control under priority is the impact on general traffic due to the signal transition. Traffic engineers from City of San Diego worry about the incurred delay and number of stops for general traffic by providing adaptive transit signal priority. Table 4.15 summaries the changes on phase 4 for general traffic. Among all the intersections, the average change in duration of phase 4 is 4.9 seconds. The largest average change is 7.1 seconds at India Street, as shown in Figure 4.17. Although the average change in duration of phase 4 is around 20% that is significant within the two priority cycles, the impact over a whole day considering the number of impacted cycles per day is only 1.3%, which is negligible.

Table 4.15: Summary of changes on phase 4 (general traffic)

	Phase 4 Duration				**Phase 4 Force-Off (FO)**		
	Original duration (sec)	Average change by priority (sec)	Change for priority cycles (%)	Change over a day (%)	Original FO	Average change by priority (sec)	Change over a day (sec)
India St	18	7.10	39.5%	3.36%	34	9.35	0.80
Front St	30	5.01	16.7%	1.30%	35	7.18	0.56
1st Ave	31	3.27	10.6%	0.86%	36	5.45	0.44
2nd Ave	30	5.54	18.5%	1.44%	35	6.50	0.51
3rd Ave	29	3.16	10.9%	0.76%	34	4.78	0.33
4th Ave	29	3.10	10.7%	0.80%	34	5.62	0.42
5th Ave	29	4.76	16.4%	1.21%	34	6.82	0.50
6th Ave	29	4.67	16.1%	1.16%	34	6.52	0.47
7th Ave	29	4.31	14.9%	1.05%	34	9.16	0.65
8th Ave	37	6.31	17.1%	1.19%	42	6.08	0.42
9th Ave	24	7.03	29.3%	2.23%	29	8.37	0.64
10th Ave	28	3.97	14.2%	1.00%	33	5.10	0.36
11th Ave	33	5.22	15.8%	1.09%	34	6.03	0.42

Table 4.15 also presents the changes in phase 4 force-off (FO) points, which are an indicator of how much the priority requests shift signal timings from the original

settings. Across all the testing intersections, the average change of phase 4 force-off points is 6.7 seconds. The maximum average change is 9.35 seconds at India Street. Although the change is significant over the two priority cycles, the average change over a whole day is only 0.5 second, which is trivial and negligible. According to the testing log files, trolleys with extensive long dwelling times generated multiple requests. With more strict constraints on the number of requests for one trolley trip, the impact on other traffic can be further mitigated.

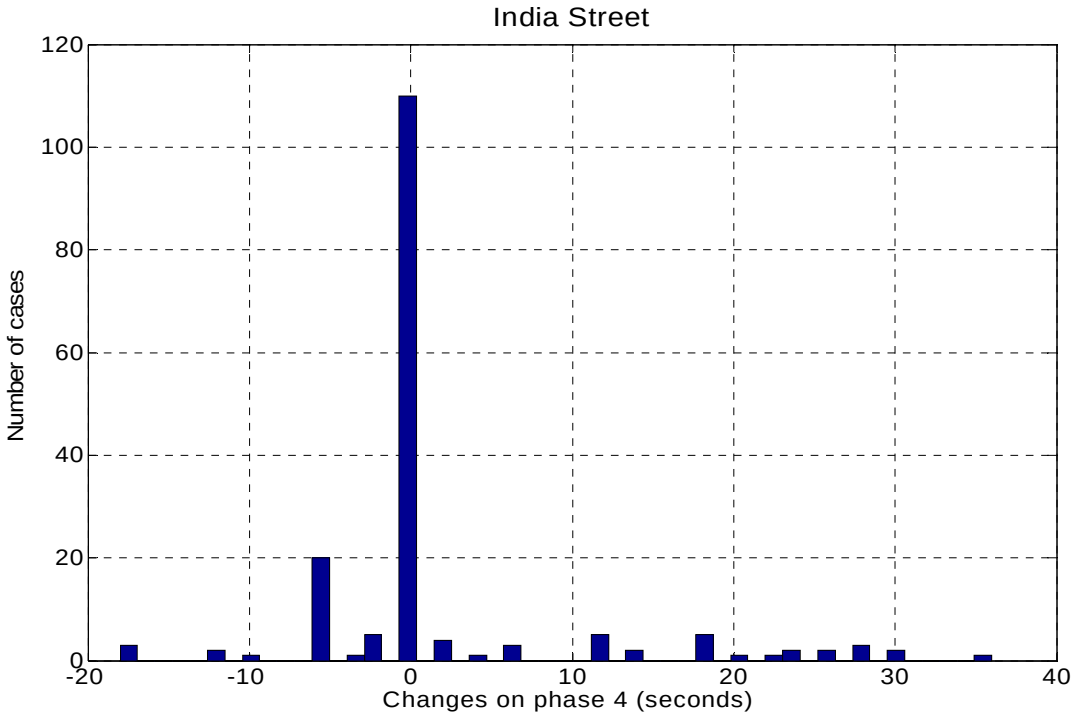

Figure 4.17: Changes on phase 4 at India Street

4.7.3.4 Prediction Analysis

The current algorithm was initially built for ‘short-term’ (i.e. the nearest signal) prediction. It aimed for applications with the capability of making instant changes on force-off points. A dynamic predicted arrival time to the nearest signal is calculated by combining both current trolley speed and historic trolley travel time. The predicted arrival time to the prioritized signal is the sum of the dynamic predicted arrival time to the nearest signal, the average ‘historic’ non-stop travel time between the nearest signal and the prioritized signal, and the dwelling time at stations in between. It is noted that the trolley is assumed to travel continuously between consecutive signals when no stations

are in place.

GPS Reception

In the FOT, the cell phone based AVL systems were installed on selected trolleys. Such systems failed to function as expected as shown in Figure 4.18 where both of the two outbound Orange Line trips deviate substantially from the tracks, particularly at the two corners of C Street, where America Plaza Station and City College Station are located. Figure 4.19 illustrates two Blue Line trajectories with similar and consistent reception issues.

Bad receptions are mainly due to two reasons: first, the cell phone-based AVL system does not have an external antenna for the GPS receiver and limits the capabilities to obtain good satellite signal. Second, the GPS receivers at the testing site in downtown San Diego experience the so-called “urban canyon” effect. An urban canyon is an artifact of the urban environment similar to a natural canyon. It is manifested by streets cutting through dense blocks of structures, especially skyscrapers. “Urban canyons” have impacts on the radio reception, particularly the reception of GPS signals. Moreover, the tracks around America Plaza have a glass roof, which also negatively affects the GPS reception.

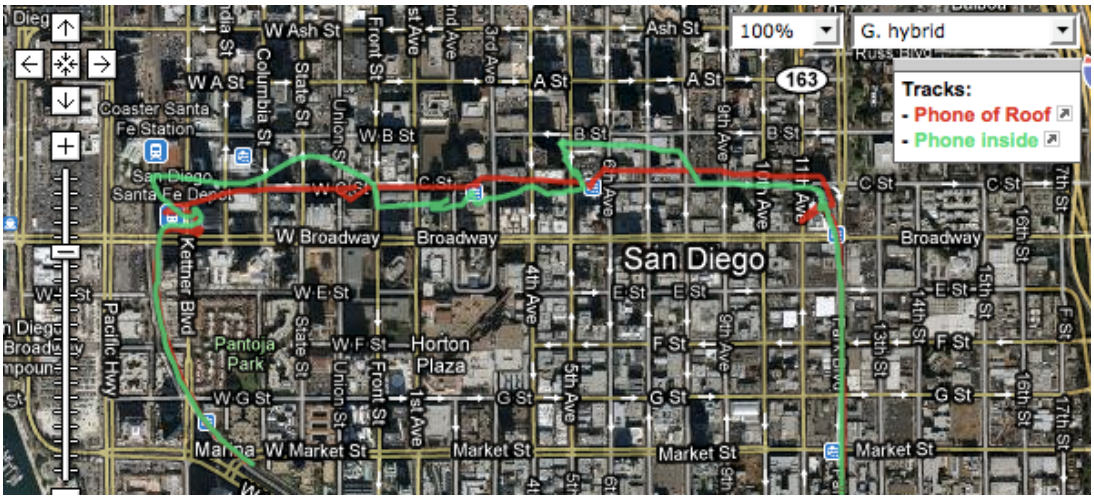

Figure 4.18: GPS trajectories for two Orange Line trips

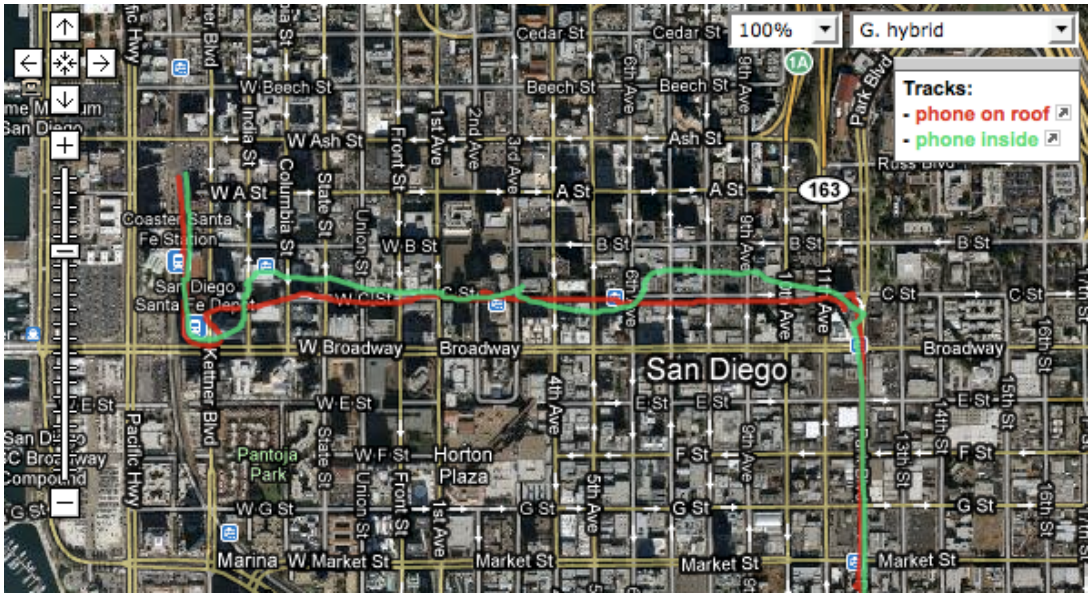

Figure 4.19: GPS trajectories for two Blue Line trips

Motion Prediction

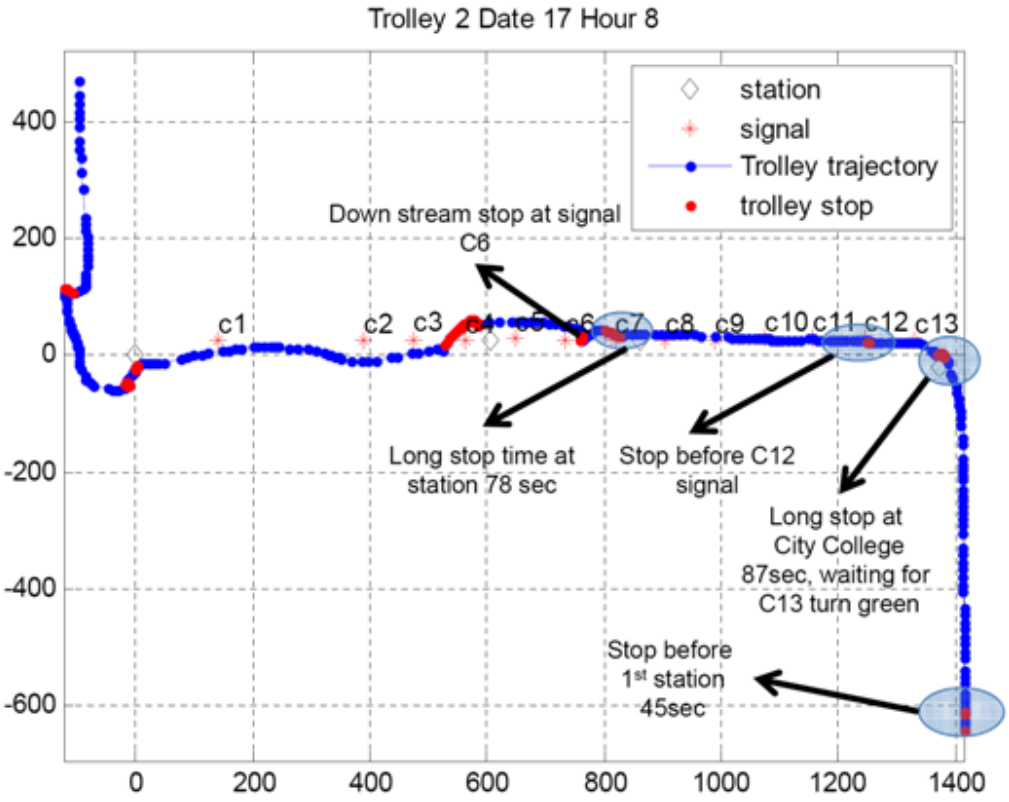

Figure 4.20: A typical trolley trajectory

Figure 4.20 shows a typical trolley trip (inbound trip). As shown in the figure, the trolley usually stops for a long time between the predicted starting point and the 1st test signal. This observation is quite different from the assumptions of prediction. As shown in the figure, the first test signal for the inbound trip is C St at 11th Ave (signal C13). The inbound trolley first stopped at Park & Market Station for about 45 seconds and then stopped at first station (City College) for 87 seconds. Such discrepancies between reality and assumption create large prediction errors for the predicted arrival times at the first test signal, which may result in a "chain reaction" along downstream signals. For example, the trolley also stopped before signal C12 (C St at 10th Ave), due to a large prediction error of the arrival time.

Figure 4.21 and Figure 4.22 show the histogram of prediction errors. When the assumption of prediction is met, i.e. no stop in between stations, the prediction is very accurate. Otherwise, large prediction errors dominate.

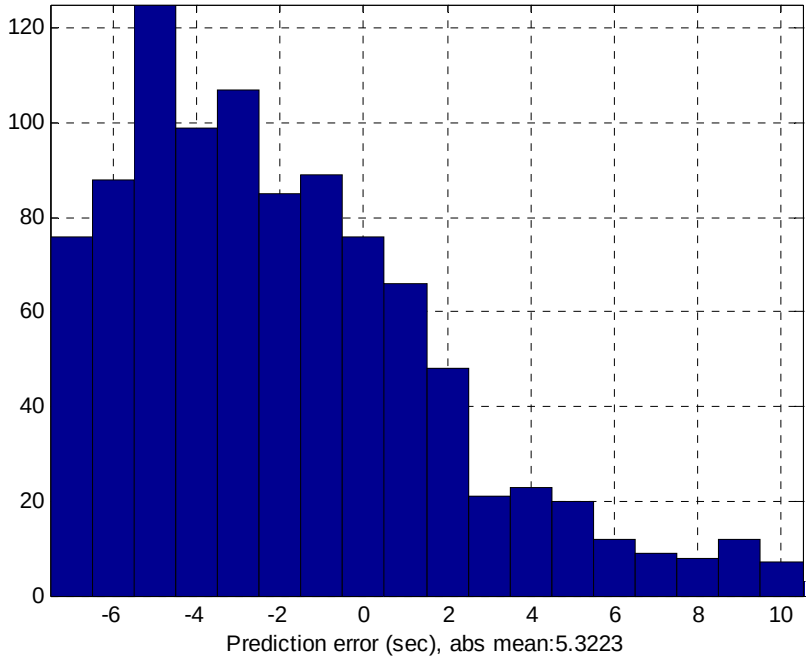

Figure 4.21: Distribution of prediction errors without stopping time at stations

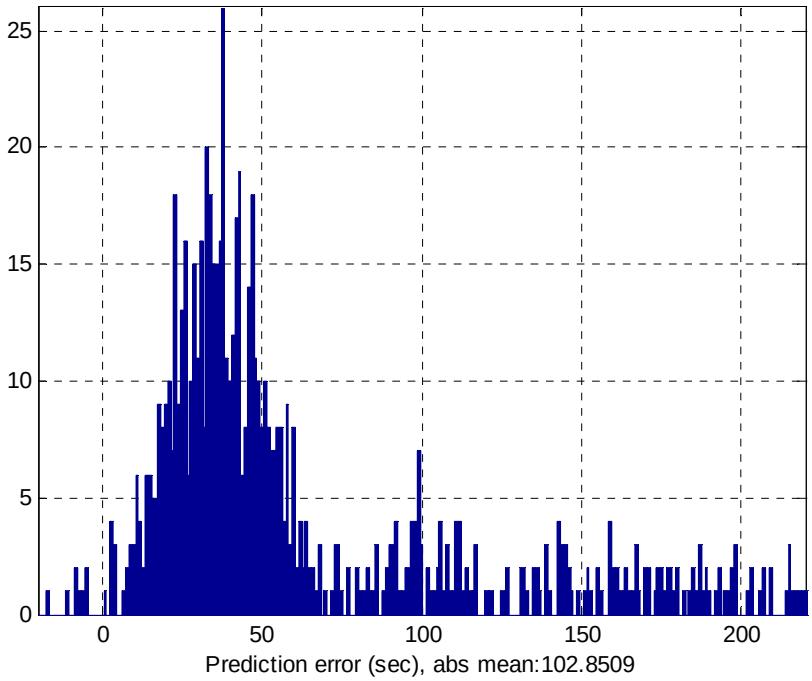

Figure 4.22: Distribution of prediction errors with stopping time at stations

Dwelling Time Prediction

The prediction of dwelling time is very challenging. Because all the trolley stations in downtown San Diego are near-side stations, the trolley dwelling time is the sum of the passenger loading time, the door open/close time, and the signal waiting time. As discussed in earlier documents [84, 86], the passenger loading time is highly random due to unpredictable passenger arrivals and passenger activities. In spite of fixed-timing control, the signal waiting time at stations is also random because the trolley's arrival time and passenger loading time are random.

Some observations can be made together with conclusions from the data analysis. The distribution of dwelling times at trolley stations do not have obvious time-of-day patterns, as shown in Figure 4.23 and Figure 4.24 for America Plaza and 5th Avenue, respectively. The dwelling times at some stations exhibit "dual-layer" phenomena, as shown in Figure 4.24. The average time difference of these two "layers" is around 70 seconds, which is exactly a full signal cycle. Such phenomenon means that trolleys' arrival times at 5th Avenue normally locate at a similar location on the local clock of the signal controller for the downstream intersection. The departure time would be either the next start of green or the following green if the trolley cannot finish loading passengers by the beginning of the current green. Operators actually follow the rule of departing stations only within a small window of the green start. It is noted that such phenomenon

normally happens when ASC is not activated.

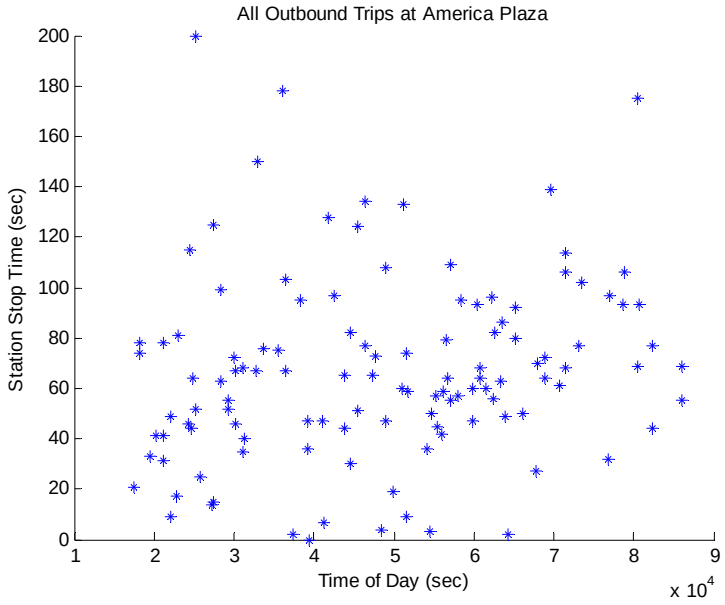

Figure 4.23: Distribution of dwelling times of outbound trips at America Plaza

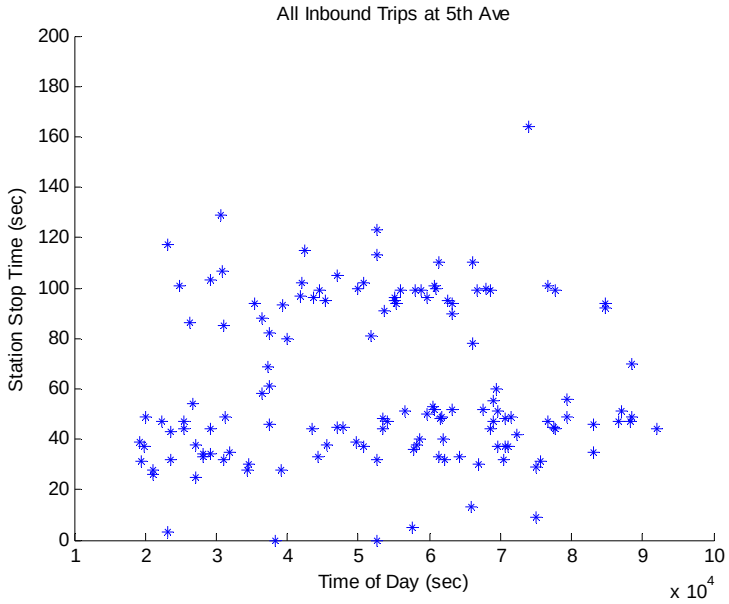

Figure 4.24: Distribution of dwelling times of inbound trips at 5th Ave

Prediction Errors

The prediction errors are mainly contributed by four factors: passengers'

activities, operators' behaviors, equipment accuracy, and traffic signal operations. Although detailed GPS trajectory data and traffic operation data are collected, the prediction error cannot be directly measured because the exact time when a trolley is ready to depart from a station is unknown. Here we analyzed the prediction errors by the following two randomly selected sample trolley trajectories.

The first chosen trip was an outbound train entering the testing site at 06:59:54 on October 16th, 2009. The first predicted time-to-arrival (TTA) to India Street started at 78 seconds. From 07:01:09 to 07:06:54 for 345 seconds, the train's GPS location almost did not move at all. It is totally different from the historical dwelling time at America Plaza. The predicted TTA stayed at about 18 seconds from 07:01:09 to 07:04:27 and jumped to 34 seconds at 07:07:20. The reason for the failure prediction is the extensive long dwelling time and possible bad GPS reception under the glass roof at America Plaza.

The second selected trip was an inbound trip started at 09:30:14 on October 16th, 2009. The first predicted TTA to 11th Ave started at 69.5 seconds. The trolley did not stop at signals before 11th Ave. and departed at 11th Ave station at 09:32:26. Given the historical dwelling time of 31 second at City College and 21.6 seconds at Market Street, the prediction error is only 10 seconds and within 10%. The trolley left 11th Ave at the beginning of the green cycle. Because of the predicted 10 seconds early, the train stopped for about 5 seconds at 7th Ave and went through all other intersections without any stops.

It is noted that the success of trolley arrival prediction would normally lead to a successful ASC implementation, as illustrated by the second selected trip. However, many cases have significant issues in predicting the departure times at those near-side stations. Based on the field operational testing result, the following can be observed:

- Long dwelling times at stations (a limited number of observations in the field underestimate dwelling times in most cases);
- A GPS reception issue at America Plaza due to the glass roof;
- An outbound trolley may stop at grade crossings before arriving at America Plaza;
- An inbound Trolley may stop at signals before arriving at City College.

4.7.4 Recommendations and Future Steps

The preliminary FOT has been completed. According to the data analysis, there are still many issues before a large deployment of the proposed system can be conducted. This section summarizes the issues and recommendations in order to further improve the system towards the next step.

4.7.4.1 Signal Transition

As described in a previous report [84], the proposed adaptive signal control strategy (Scheme I) is used for those late trips, which account for about 10% of total trips. If the system capacity is required to be increased, say, there are 80% of trips which are late or require adaptive signal control, then the strategy shown in the previous section will fail to work. The major restriction results from the logic of signal controllers, in particular, signal transition logic.

In many cases, an additional cycle is required for signal controllers to complete the transition from one set of signal timings to another. Therefore, if the frequency of a priority request increases, then such a transition period becomes longer, which will have more negative impacts on the overall traffic system, e.g. unrequested trolleys and cross-street traffic.

In addition, due to the signal transition logic, the solution of the proposed adaptive signal control algorithm may not be implementable in the field. For implementation, the signal timings in the current cycles may highly relate to the signal timings in the previous cycle.

There are at least two remedies to take into account the signal transition logic:

- Set up another model to obtain the signal timings for the transition cycle, such that the signal timings from the proposed adaptive signal control algorithm are guaranteed to be implemented in the cycle after the transition;
- Put more constraints on the adaptive signal control model mentioned above, such that the signal timings from the modified adaptive signal control strategy are to be implemented in the cycle right after the one with base-line timings.

4.7.4.2 Signal Progression

The original signal progression design also affects the performance and design of the proposed adaptive signal control system. A better progression design in the original scenario requires less timing changes to redesign the progression for approaching trolleys given the real-time trolleys' movement information. According to the field data, some segments actually suffer from the existing signal progression design. As shown in Figure

4.25 and Figure 4.26, many trips have to stop at intersections between stations due to the inappropriate progression design. Therefore, it is also important to redesign the signal progression before the large-scale implementation of the proposed system.

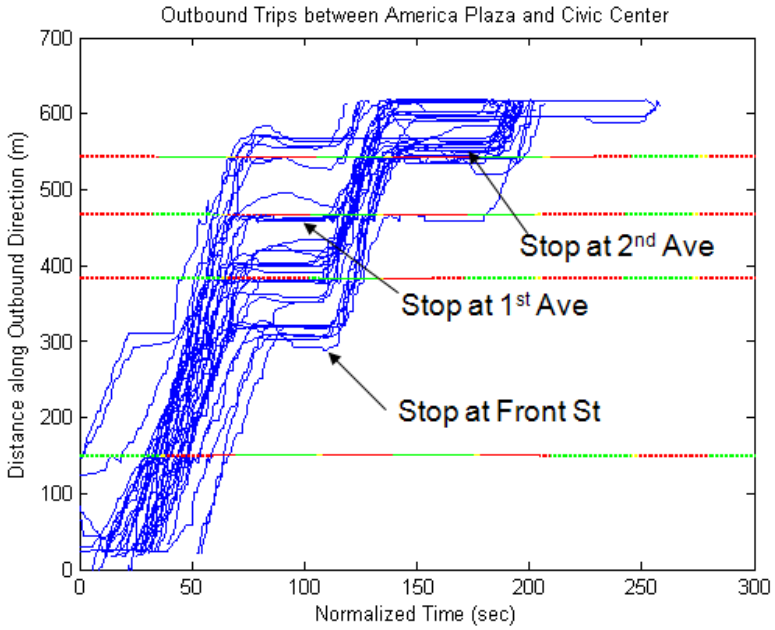

Figure 4.25: Outbound trajectories between America Plaza and Civic Center (Stage 1)

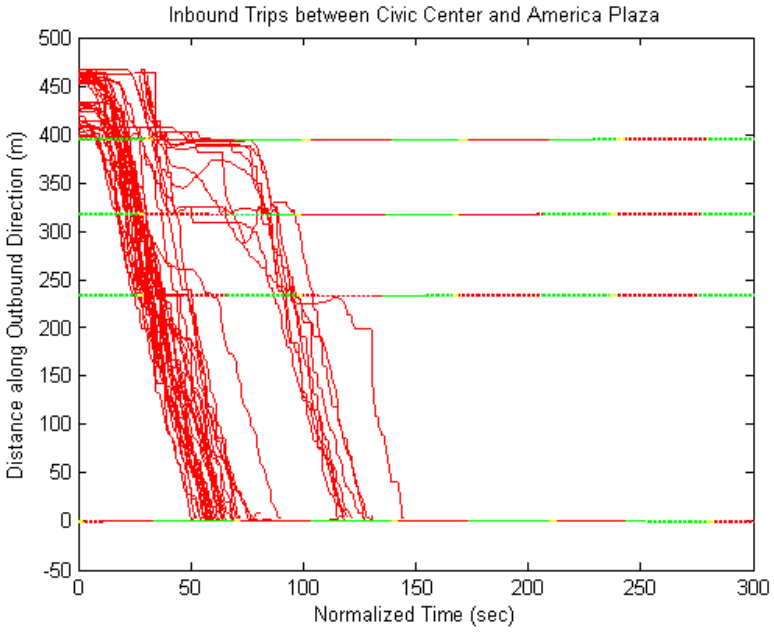

Figure 4.26: Inbound trajectories between Civic Center and America Plaza (Stage 1)

4.7.4.3 Dwelling Time Prediction

The proposed adaptive signal control algorithm takes the trolley's predicted arrival time as one of the inputs. The effectiveness of the proposed strategy largely depends on the accuracy of the arrival time prediction. Unfortunately, few studies have been conducted on the prediction of station dwelling time because there are so many uncertainties which make it impossible to obtain an accurate prediction. For example, if a handicapped person needs to board the trolley, the dwelling time may be much longer (e.g. 2 or 3 more minutes) than usual. In addition, the downstream signal status also contributes to the dwell time of nearside stations.

However, a simple linear regression model based on limited observed field data is applied to predict the dwelling time at each station. More data from the field are required to obtain more knowledge on the dwelling time. Furthermore, the prediction of dwelling time statistics, e.g. 95% percentile, is more tractable and pragmatic than the prediction of exact dwelling time or the mean of dwelling time. Due to the interaction between the trolley dwelling time and the downstream signal status, it is more appropriate to optimize signal timings by integrating them with dwelling time prediction.

4.7.4.4 Arrival Time Prediction at Station

As presented in the previous section, benefits of the ASC system on trolleys' operations, in particular on reducing trolleys' travel times, are not as many as expected. Under the existing ASC system, the optimization algorithm takes trolleys' predicted departure times at stations, current signal statuses at downstream intersections and signal timing constraints as inputs to design a desired trolley green band. In order to to execute the trolley green band timings, the request decision needs to be sent out 2 minutes ahead of the start time of the designed green band. Due to the variations of a trolley's intersection delay and dwelling times at a station, a trolley often misses the designed green band.

The predicted departure time at a station consists of two components: the predicted arrival time at a station and the predicted dwelling time at a station. The trolley's intersection delay was not considered when providing the first component - the predicted arrival time at a station and a predetermined constant was used as the second component – the predicted dwelling time at a station. The inability of the prediction algorithm to deal with variations of trolleys' intersection delays and dwelling times is the major cause for a trolley missing the designed green band.

Real-time signal status needs to be incorporated into the prediction algorithm to gain the ability to estimate a trolley's intersection delay. Because the trolley hardly share the road with other motor vehicles, it is reasonable to believe that incorporating signal status will achieve a more accurate prediction.

4.7.4.5 Automatic Vehicle Location (AVL) System

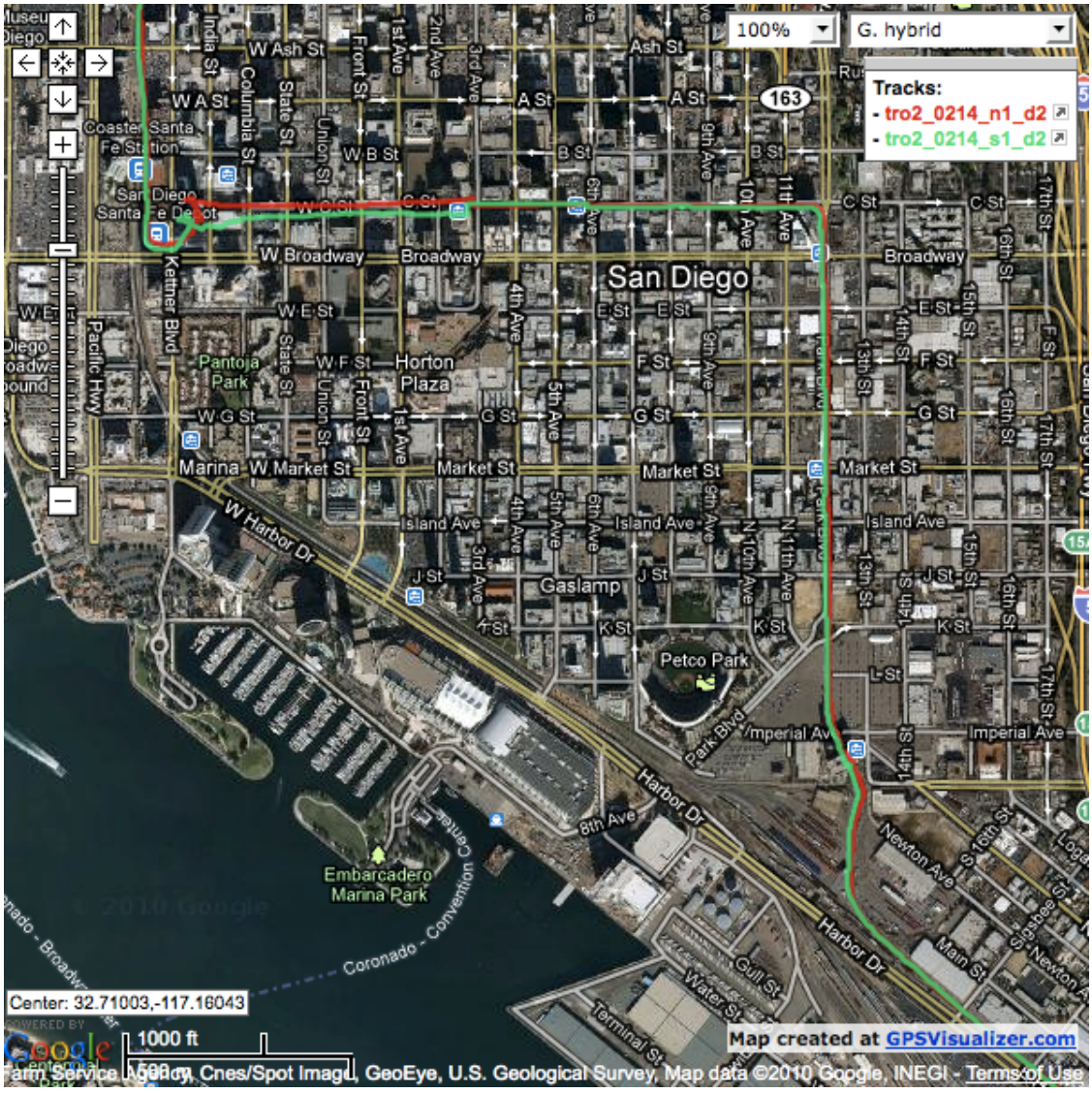

Figure 4.27: GPS receptions with GPS external antenna

The cell phone based cost-effective AVL system in the preliminary FOT is not

successful due to the serious “urban canyon” effect. A better solution should be proposed and tested. At the beginning of the project, another type of AVL system based on a GPRS modem and GPS receiver with external antenna was tested. As shown in Figure 4.27, the trolley trajectories are more stable and closer to the geometry street map when compared with the results from the cell phone based system (Figure 4.18 and Figure 4.19). Such a system with an external GPS antenna can be a potential solution for future testing. However, more tests are still needed before the next FOT, particularly at the area around America Plaza where the existing system performed the worst.

Chapter 5

5. Conclusion and Future Work

5.1 Conclusion

The major contributions of this dissertation are three-folds:

- ***Development of the AVL-based adaptive signal control system***

By integrating the information on locations and movements of transit vehicles continuously obtained from the equipped automatic vehicle location (AVL) system, and information on other traffic condition, such as traffic volumes and turning counts at signalized intersections, a new traffic signal control system, adaptive signal control (ASC) system is developed, which can gracefully balance the performance measures of the instrumented transit vehicles and the negative impacts on other motor vehicles.

- ***Modeling of the traffic signal timing optimizer, which is the most important component of the proposed system***

Based on the un-intermitted location information sent by the PATH-developed cellular GPS trackers, movements of transit vehicles are predicted by combining linear regression model and Kalman filtering. At the same time, the measurements of effectiveness (MOEs) of the other traffic can be estimated by applying the well-accepted model with appropriate modifications to those available traffic condition data. Accompanied by the real-time or pre-set traffic signal timings data from the field, both the second-by-second location data and movement prediction of equipped transit vehicles, and the most updated traffic condition and prediction are fed into the database and the traffic signal timings optimizer. With the user-defined performance index for the traffic system of interest, the constraints related to the mechanism of traffic signal controllers and other needs, and the parameters determined by the configuration of studied intersection, a set of optimal signal timings are obtained by the proposed optimization model. Such set of traffic signal timings, i.e. the outputs from the mathematical model, are then sent to the signal timings request server. The field master and local controllers execute the commands from the signal timings request server to implement the desired traffic operation strategy in the field.

- ***Applications of the proposed system, in particular the adaptive signal control strategy, to two real world cases and attractive results available for further research***.

The proposed AVL-based adaptive signal control system has been applied to two real world studies. One is to relieve the traffic congestion and/or queue accumulation at the isolated signal around the grade crossing operated under preemption of SPRINTER rail transit. The other is to improve the schedule adherence, reduce the intersection delay and enhance the trip reliability for San Diego trolleys travelling along a signalized corridor in the downtown area under the priority operation. The negative impacts (e.g. delay increase) on other traffic are minimized simultaneously. Both numerical analysis and simulation tests verify the validities of the proposed system for different types of rail transit operations: preemption and priority, and different setups of studied sites: isolated signalized intersection and signalized corridor. The results present a promising future for further field operational testing.

Some remarks related to these contributions follow.

- Although the examples presented in this dissertation are related to the rail transit operation, the proposed AVL-based adaptive signal control system is far from being restricted to rail service application. The same strategy also can be readily applied to other public transits, such as buses, demand responsive transit (DRT), which are highly related to the road surface traffic system. Furthermore, emergency vehicles and/or other high priority vehicles equipped with AVL system can use such signal control strategy to improve their service without having too much negative impacts on the efficiency of the overall traffic system.
- The traffic signal controls are pre-timed in both applications: SPRINTER rail transit and San Diego trolley. However, the proposed system can be readily extended to handle the semi-/fully-actuated traffic signal control and conventional adaptive signal control, although the system may become much more complex than what is presented in this dissertation.
- The proposed AVL-based adaptive signal control system, which can also be categorized as a type of traffic responsive control, is different from the conventional adaptive traffic signal control, such as RHODES. The conventional adaptive signal control system is the counterpart of pre-timed signal control and semi-/fully-actuated traffic signal control. Its major data source is traffic information from inductive loop detectors (ILDs), i.e. point detection means, for the decision making. The proposed system demonstrates another possibility to fuse data from different types of detection means, e.g. continuous detection from AVL system and point detection from ILDs, which may provide more benefits to the overall traffic

system.

- In addition, the proposed AVL-based adaptive signal control system can be considered as a more generalized development than the adaptive transit signal priority (ATSP) system. The proposed system can not only offer priority for the transit vehicle based on its movement information, but also provide benefits for the overall traffic system at a higher level, as is shown in SPRINTER's application, by using the real-time location data of the transit vehicle.

5.2 Future Work

5.2.1 SPRINTER Rail Transit

In the application to SPRINTER rail transit service so far, the proposed AVL-based adaptive signal control strategy is only targeting at the traffic signal optimization right after the preemption based on the information of when the SPRINTER rail transit vehicle approaches the grade crossing and how long the preemption lasts. Due to these constraints, the extent to which the traffic congestion at the signalized intersection around the grade crossing can be relieved by the signal timing optimization is very limited. If the predictions of grade crossing approaching time and departure time are available, based on either rough estimation from the departure time at the upstream grade crossing or more reliable estimation from continuous detection by AVL system, then the traffic signal timings can be adjusted before the initiation of preemption such that the overall traffic is less congested when the transit vehicle is approaching.

The dissertation mainly focuses on the system efficiency issue for SPRINTER rail transit application. Nevertheless, safety is another important issue for traffic operation, in particular at grade crossings. If the movement of SPRINTER rail transit can be well predicted, a more advanced traffic signal optimization strategy or other intelligent transportation systems (e.g. changeable message sign, etc.) can be developed to reduce the number of vehicles and/or probability of individual vehicle trapped at the grade crossing when the transit vehicle arrives at the intersection.

5.2.2 San Diego Trolley System

Since the goal set for the San Diego trolley system is to deploy the proposed

AVL-based adaptive signal control system in the field, one critical question is how often a request on traffic signal adjustment can be processed by the proposed system. In other word, what is the capacity of system to handle the signal timing change request triggered by trolleys?

Due to the operation mechanism and the logic coded in traffic signal controllers, it always takes a certain amount of time for signal controllers to transition from an old set of timings to a new one and keep the timings. As the frequency of requests gets higher, the disruption to the other traffic caused by such signal transitions becomes worse. If the frequency or intensity of requests gets high enough, then some of the requests may be blocked by the previous ones and may not be able to process in time. If such situation happens in the field, then the *first come first served* (FCFS) rule is applied.

Based on the simulation results shown in Chapter 4, if there are around 10% of trolleys sending out the requests and these requests are almost uniformly distributed (or no request is blocked by others), then the system can perfectly handle all the requests and ensure the trolley travels along the corridor without any stops. However, when the penetration rate reaches as much as 25%, some of the requests will be blocked and the associated trolleys cannot get benefits due to the failure of signal timing change. A potential way to quantitatively investigate the capacity of the proposed system is the Scenario-based Optimization (SBO) method [87].

Another concerns for field deployment is the variation of traffic condition. A real-time version of the proposed system and/or robust optimization model for the application of San Diego trolley system can be the potential option(s) to remedy such problem.

5.2.3 AVL-based ASC System

It should be noted that AVL-based ASC system by itself is a real-time optimization strategy. Traffic condition in the real world varies from time to time, and there are a lot of disturbances and noises introduced into the traffic system. The robust optimization method should be used to account for the uncertainties of parameters as well as system inputs. For example, the distribution of measurement errors in traffic volumes can be assumed to obtain a set of robustly optimal signal timings for the studied intersection(s).

As mentioned in previous chapters, more involved traffic arrival pattern(s) can be assumed to quantify the intersection delays and set up the stochastic optimization

problem. Or based on users' needs, other performance index can be selected to optimize. For example, pollutant emissions receive more and more attention due to the public concerns on the energy consumption and environmental protection. However, there is a trade-off between the choice of performance index and the computational tractability.

As the urbanization advances, pedestrians play a more and more important role in the operation of traffic system. The interaction among vehicles, pedestrians and traffic signals is getting stronger and stronger. To optimize the overall traffic system, it is undoubtedly required to take into consideration pedestrian-related performance index. Furthermore, there is a strong relationship between pedestrians and safety at a signalized intersection.

One of the difficulties confronted by the proposed AVL-based adaptive signal control system in field implementation is that it is always hard to predict the dwelling time for public transit vehicles. The dwelling times at stations sometimes, e.g. arrival and boarding of the handicapped, may vary a lot or is almost impossible to predict. Compared with the rail transit, the dwelling times for buses are much less consistent and more difficult to estimate. More real-world data need to be analyzed and more reliable prediction method should be developed for the field operational test.

Reference

[1] U. S. Census Bureau, International Data Base (IDB). Accessed as of April 5th, 2010. http://www.census.gov/ipc/www/idb/worldpopinfo.html.

[2] U. S. Department of Transportation (USDOT), Federal Highway Administration (FHWA). *Highway Statistics 2007*. Accessed as of December 20th, 2010. http://www.fhwa.dot.gov/policyinformation/statistics/2007/.

[3] Bandivadekar, A., et al. *On the Road in 2035: Reducing Transportation's Petroleum and Consumption and GHG Emissions*. Massachusetts Institute of Technology, July 2008.

[4] Davis, S. and S. Diegel. *Transportation Energy Data Book: Edition 26th*. Oak Ridge National Laboratory, ORNL-6978, 2007.

[5] The U.S. Environmental Protection Agency (EPA). *Toxic air pollutants*, 2009. http://www.epa.gov/oar/toxicair/newtoxics.html.

[6] American Public Transit Association (APTA). *2009 Annual Report*, 2009. http://www.apta.com/about/governance/Documents/annual_report_09.pdf.

[7] Federal Transit Administration (FTA). Accessed as of April 2nd, 2010. http://www.fta.dot.gov/assistance/technology/research_4240.html

[8] Walters, C. H., S. P. Venglar, D. B. Fambro, and J. R. Daniel. *Development of Analytical Tools for Evaluating Operations of Light-Rail At-grade within an Urban Signal System*. Texas Transportation Institute, March 1993.

[9] Celniker, S. and Terry, E. W.. *Trolley Priority on Signalized Arterials in Downtown San Diego*. Paper prepared for presentation at the National Light Rail Transportation Conference, May 1991.

[10] Taylor, P. C., Lee, L. K., and Tighe, W. A.. *Operational Enhancements: Making the Most of the Light Rail, Light Rail Transit: New System Success at Affordable Prices, TRB Special Report 221*. Transportation Research Board National Research Council, Washington D.C., 1982, pp.578-592.

[11] Wilson, N. H. M.. *Improving Service on the MBTA Green Line through Better Operations Control*. Transportation Research Record, No. 1361, pp. 296-304, 1993.

[12] Walshaw, J. R.. *LRT On-Street Operations: The Calgary Experience, Light Rail Transit: System Design for Cost-effectiveness, State-of-the-art Report 2.* Transportation Research Board National Research Council, Washington, D.C., 1985, pp. 221-226.

[13] Fox, G.. *Light Rail/Traffic Interface in Portland, -- The First Five Years*. Paper presented at the 1992 TRB Light Rail Conference, Calgary, Canada, May 1992, pp. 1-17.

[14] Tighe, W. A. and Patterson, L. A.. *Integrating LRT into Flexible Traffic Control Systems, TRB State-of-the-art Report 2*. Transportation Research Board National Research Council, Washington, D.C., pp. 213-219.

[15] Banks, J. H.. *Introduction to Transportation Engineering, 2nd Ed.* McGraw-Hill, San Francisco, 2002.
[16] Roess, R. P., McShane, R. W. and Prass, S. E.. *Traffic Engineering, 2nd Ed.* Prentice Hall, Upper Saddle River, New Jersey, 1998.
[17] U. S. Department of Transportation (USDOT), Federal Highway Administration (FHWA). *Traffic Signal Timing Manual*. Publication No. FHWA-HOP-08-024. 2008.
[18] National Electrical Manufacturers Association (NEMA). Accessed as of April 3rd, 2010. http://www.nema.org/stds.
[19] United States General Accounting Office. *Transportation Infrastructure*. Report No. GAO/RCED-94-105, 1994.
[20] Skabadonis, A.. *Evaluation of the Fuel Efficient Traffic Signal Management (FETSIM) Program: 1983 – 1993*. Research Report UCB-ITS-RR-94-11, University of California, Berkeley, 1994.
[21] Hunt, P. B., Robertson D. I., Bretherton, R. D., and Royle, M. C.. *The SCOOT On-line Traffic Signal Optimisation Technique*. Traffic Engineering and Control, Vol. 23, 1982, pp. 190-192.
[22] Lowrie, P. R.. *SCATS: The Sydney Coordinated Adaptive Traffic System – Principles, Methodology, Algorithms*. In Proc. IEE Int. Conf. Road Traffic Signaling, London, UK, 1982, pp. 67-70.
[23] Gartner, N. H.. *OPAC: A Demand-responsive Strategy for Traffic Signal Control*. Transportation Research Record. No. 906, 1983, pp. 75-81
[24] Farges, J.L., Henry, J.J. and Tufal, J.. *The PRODYN Real-time Traffic Algorithm*. In Proc. 4th IFAC Symp. Transport. Systems, Baden-Baden, Germany, 1983, pp. 307-312
[25] Mirchandani, P. and Head, L.. *RHODES --- A Real-time Traffic Signal Control System: Architecture, Algorithms, and Analysis*. In TRISTAN III (Triennial Symp. Transport. Analysis) Vol. 2, San Juan, Puerto Rico, Jun 17-23, 1998.
[26] Smith, B. L., Scherer, W. T., Hauser, T. A., and Park, B. B.. *Data-driven Methodology for Signal Timing Plan Development: A Computational Approach*. Computer-Aided Civil and Infrastructure Engineering, Vol. 17, No. 6, 2002, pp. 387-395.
[27] Allsop, R.E.. SIGSET: *A Computer Program for Calculating Traffic Signal Settings*. Traffic Engineering and Control, Vol. 13, No. 2, 1971, pp. 58-60.
[28] Little, J. D. C., Kelson, M. D. and Gartner, N.H.. *MAXBAND: A Program for Setting Signals on Arteries and Triangular Networks*. Transportation Research Record, No. 795, 1981, pp. 40-46.
[29] Texas Transportation Institute (TTI). *PASSER II-90 Microcomputer User's Guide*. Texas A&M University, College Station, Texas, 1991.
[30] Stamatiadis, C. and Gartner, N. H.. *MULTIBAND-96: A Program for Variable Bandwidth Progression Optimization of Multiarterial Traffic Networks.*

Transportation Research Record, No 1554, 1996, pp. 9-17.
[31] Robertson, D. I.. *'TRANSIT' Method for Area Traffic Control*. Traffic Engineering and Control, Vol. 10, 1969, pp. 276-281.
[32] Wallace, C. E., Courage, K. G., Hadi, M. A., and Gan A. G.. *TRANSIT-7F User's Guide*. University of Florida, Gainesville, FL, 1998.
[33] Trafficware. *Synchro 6 User's Guide*. Trafficware, Albany, CA, 2003.
[34] Lee, J., Abdulhai, B., Shalaby, A., and Chung, E-H.. *Real-time optimization for adaptive traffic signal control using genetic algorithms*. Journal of Intelligent Transportation Systems. Vol 9. No. 3, 2005, pp. 111-122
[35] Stevanovic, A., Martin, P.T., and Stevanovic, J.. *VISSIM-based genetic algorithm optimization of signal timings*. Transportation Research Record, No. 2035, 2007, pp. 59-68
[36] Lo, H.K.. *A novel traffic signal control formulation*. Transportation Research Part A. Vol. 33, 1999, pp. 433-448
[37] Lin, W-H, and Wang, C.. *An enhanced 0-1 mixed-integer LP formulation for traffic signal control*. IEEE. Transactions on Intelligent Transportation Systems, Vol. 5, No. 4, 2004, pp. 238-245
[38] Daganzo, C.. *The Cell Transmission Model. Part I: A Simple Dynamic Representation of Highway Traffic.* Research Reports, PATH, 1992.
[39] Daganzo, C.. *The Cell Transmission Model. Part II: Network Traffic*. Working Papers, PATH, 1994.
[40] California Center for Innovative Transportation (CCIT). *Automatic Vehicle Location*. On-line Report at UC Berkeley. Accessed as of November. 15th, 2008. http://www.calccit.org/itsdecision/serv_and_tech/Automatic_vehicle_location/avl.html.
[41] Volpe National Transportation Systems Center for the Federal Transit Administration. *Advanced Public Transportation Systems Deployment in the United States*. FTA-MA-26-7007-99-1, DOT-VNTSC-FTA-99-1; EDL number 8165. January 1999.
[42] Mahdavifar, S. A., Sotudeh, G. R., and Heydari, K.. *Automatic Vehicle Location Systems*. World Academy of Science, Engineering and Technology, No. 54, 2009.
[43] Baek, T. K., Shin, Y. E.. *Development of Automatic Vehicle Location System*. Reports of the Faculty of Science and Engineering, Saga University, Vol. 30, No. 2, 2001, pp. 51-56.
[44] Mckay, K. M.. *Integrated Automatic Vehicle Location Systems*. IEEE AES Systems Magazine, March, 1997, pp. 18-22.
[45] Wikipedia (on-line). *Automatic Vehicle Location*. Accessed as of April 4th, 2010. http://en.wikipedia.org/wiki/Automatic_vehicle_location.
[46] Li, M., Song, M. K., and Wu, G.. *An On-line Performance Measurement Method Based on Arterial Infrastructure Data*. 87th Transportation Research Board Annual Meeting, Washington D. C., January, 2009.

[47] Li, M., Zhang, L. Song, M. K., and Wu, G. et al.. *Improving Performance of Coordinated Signal Control Systems Using Signal and Loop Data*. UC Berkeley, PATH Research Report, UCB-ITS-PRR-2010-07, 2010.

[48] Wu, G., Zhang, W-B, and Li, M. et al.. *Traffic Emission Reduction at Signalized Intersection: A Simulation Study of Benefits of Advanced Driver Information*. 15th World Congress on Intelligent Transportation Systems, Nov. 16-20, 2008.

[49] Li, M., Boriboonsomsin, K., Wu, G., Zhang, W-B, and Barth, M. J.. *Traffic Energy and Emission Reductions at Signalized Intersections: A Study of the Benefits of Advanced Driver Information*. International Journal of ITS Research, Vol. 7, No. 1, June, 2009, pp 49-58.

[50] Wu, G., Boriboonsomsin, K., Zhang, W-B, Li, M., and Barth, M. J.. *Energy and Emission Benefit Comparison between Stationary and In-vehicle Advanced Driving Alert Systems*. Transportation Research Record, Transportation Research Board, Washington D.C., 2010 (In press).

[51] Smith, H. R., Hemily, B., and Ivanovic, M.. *Transit Signal Priority (TSP): A Planning and Implementation Handbook*. May, 2005.

[52] Gifford, J., Pelletiere, D. and Collura, J.. *Stakeholder Requirements for Traffic Signal Preemption and Priority in the Washington D. C. Region*. 80th Transportation Research Board Annual Meeting, Washington D. C. January, 2001.

[53] U. S. Department of Transportation (USDOT), Federal Highway Administration (FHWA). *Manual on Uniform Traffic Control Devices (MUTCD) – for Streets and Highways, 2003 Edition, including Revision 1 and 2, 2007*.

[54] Tan, C. W. et al.. *Prediction of Transit Vehicle Arrival Times at Signalised Intersection for Signal Priority Control*. Proceedings of the IEEE ITSC, 2006.

[55] Zhou, K. et al.. *Development of Adaptive Transit Signal Priority Systems*. UC Berkeley, PATH Research Report, UCB-ITS-PRR-2004, 2004

[56] Shalaby, A. and Farhan, A.. *Bus Travel Time Prediction Model for Dynamic Operations Control and Passenger Information Systems*. 82nd Transportation Research Board Annual Meeting, Washington D. C., January, 2003.

[57] Chien, S. I., Ding, Y. and Wei, C.. *Dynamic Bus Arrival Time Prediction with Artificial Neural Networks*. Journal of Transportation Engineering, Vol. 128, No. 5, pp. 429-438.

[58] Jeong, R. H. and Rilett, L. R.. *Prediction Model of Bus Arrival Time for Real-Time Applications*. Transportation Research Record. No. 1927, 2005, pp. 195-204.

[59] Jeong, R. H.. *The Prediction of Bus Arrival Time Using Automatic Vehicle Location System Data*. Ph. D dissertation, Texas A&M University, December 2004.

[60] Rajbhandari, R.. *Bus Arrival Time Prediction Using Stochastic Time Series and Markov Chains*. Ph. D dissertation, New Jersey Institute of Technology, January, 2005.

[61] Transportation Research Board. *HCM 2000: Highway Capacity Manual 2000.* Washington D. C., 2000.

[62] Papageorgiou, M. et al.. *Review of Road Traffic Control Strategies*. Proceedings of the IEEE, Vol. 91, No. 12, 2003.
[63] Zhang, L.. *Optimizing Traffic Network Signals around Railroad Crossings*. Ph. D Thesis, Virginia Polytechnic Institute and State University. May 2000.
[64] LINDO System. *LINDO API 6.0*. Accessed as of January 28th, 2010. http://www.lindo.com/.
[65] IBM. *ILOG CPLEX – High-performance mathematical programming engine*. http://www-01.ibm.com/software/integration/optimization/cplex/.
[66] Webster, F. V.. *Traffic Signal Settings*. Her Majesty's Stationery Office, Technical Report, Road Research Technical Paper, No. 39, 1958.
[67] Khalil, H. K.. *Nonlinear Systems, 3rd Edition*. Prentice Hall, New Jersey, 2002.
[68] Bazaraa, M. S., Sherali, H. D. and Shetty, C. M.. *Nonlinear Programming – Theory and Algorithms, 3rd Edition*. John Wiley & Sons, Inc. 2006.
[69] Yin, Y.. *Robust Optimal Traffic Signal Timing*. Transportation Research, Part B, 42, pp. 911-924, 2008.
[70] Li, J-Q, Wu, G., and Zhou, N.. *The Model and Algorithm for Investigating the Impacts of Signal Timings of Vehicle Emissions*. Submitted to IEEE Trans. on Intelligent Transportation System, 2010.
[71] Li, M., Wu, G., Li, Y., Bu, F. and Zhang, W-B. *Active Signal Priority for Light Rail Transit at Grade Crossings*. Transportation Research Record 2035, TRB, National Research Council, Washington, D. C., 2007, pp.141 – 149.
[72] American Railway Engineering & Maintenance-of-Way Association, *2000 AREMA Communications & Signals Manual*, 2000.
[73] Boillot, F., Blosseville, J. M., and Lesort, J. B. et al.. *Optimal signal control of urban traffic networks.* Road Traffic Monitoring, 1992.
[74] Skabardonis, A., Bertini, R. L., and Gallagher, B. R.. *Development and Application of Control Strategies for Signalized Intersections in Coordinated Systems*. Transportation Research Record 1634, TRB, National Research Council, Washington, D. C., 1998, pp. 110-117.
[75] Cho, H. and Rilett, L. R.. *Improved Transitional Preemption Strategy for Traffic Signals at Intersections Near Highway-Railway Grade Crossings*. 83rd Transportation Research Board Annual Meeting, Washington D. C., 2004.
[76] Jacobson, M., Venglar, S. and Webb, J.. *Advanced Intersection Controller Response to Railroad Preemption – Stage I-IV Report*, Texas Transportation Institute, Texas A&M University, College Station, Tex., May 1999-February 2000.
[77] Ho, C. H. and Hwang, T. L.. *Modeling real-time dynamic queue length for urban traffic control systems.* Proceedings of the Intelligent Vehicles '94 Symposium, 1994, pp. 438 - 442
[78] Mystkowski, C. and Khan, S.. *Estimating Queue Lengths Using SIGNAL94, SYNCHRO3, TRANSYT-7F, PASSER II-90, and CORSIM.* Proceedings of the 78th Transportation Research Board Annual Meeting, Washington, D.C., January, 1998.

[79] Kang, Y-S. *Delay, Stop and Queue Estimation for Uniform and Random Traffic Arrivals at Fixed-time Signalized Intersections*. Ph. D Dissertation, Virginia Poly -technic Institute and State University, 2000.

[80] Geroliminis, N. and Skabardonis, A.. *Prediction of arrival profiles and queue lengths along signalized arterials by using a Markov decision process*. Transportation Research Record, No. 1934, 2005, pp. 116-124.

[81] Comert, G. and Cetin, M.. *Queue Length Estimation from Probe Vehicle Location: Undersaturated Conditions.* 86th Transportation Research Board Annual Meeting, Washington, D.C., January, 2007.

[82] Dion, F., Rakha, H. and Kang, Y-S. *Comparison of Delay Estimates at Under-saturated and Over-saturated Pre-timed Signalized Intersections.* Transportation Research Part B, Elsevier, 2003.

[83] Wu, G., Li, Y., Zhang, W-B et al.. *SPRINTER Rail: Grade Crossing/Traffic Signal Optimization Study*. UC Berkeley, PATH Research Report, UCB-ITS-PRR-2009-21, 2009.

[84] Li, M., Wu, G., Johnston, S., and Zhang, W-B. *Analysis toward Mitigation of Congestion and Conflicts at Light Rail Grade Crossings and Intersections*. UC Berkeley, PATH Research Report, UCB-ITS-PRR-2009-09, 2009.

[85] Li, Y., Bu, F., Li, M., Wu, G., Zhang, W-B. and Zhou, K.. *Application of Advanced Detection Data in the Development of an Active Signal Priority System*. 86th Transportation Research Board Annual Meeting, Washington D.C., January, 2007.

[86] Wu, G. Tomizuka, M., Zhang, L., Li, M. and Zhang, W-B. *System Performance Optimization at Urban Rail-Highway Grade Crossings Using Online Adaptive Priority Strategy*. 88th Transportation Research Board Annual Meeting, Washington D.C., January 11-15, 2009.

[87] Mars, J. and Hundt, R.. *Scenario Based Optimization: A Framework for Statically Enabling Online Optimization*. IEEE International Symposium on Code Generation and Optimization, 2009.